PHOSPHO-DEPENDENT MODULATION OF POTASSIUM CHLORIDE CO-TRANSPORTER KCC2

HING CHEONG LEE

A thesis submitted to UCL for the degree of Doctor of Philosophy

October 2008

Department of Neuroscience, Physiology and Pharmacology

UCL

To my parents

Abstract

The neuronal-specific potassium chloride co-transporter 2, KCC2, is a major chloride extruder in brain. The expression of KCC2 during neuronal development is fundamental to the switch of GABAergic response from excitatory to inhibitory. Malfunction of KCC2 can cause impairment of chloride homeostasis in neurons and is implicated in neurological disorders such as epilepsy.

To date the role of protein phosphorylation in the regulation of KCC2 remains elusive. In this thesis, direct phosphorylation of KCC2 by PKC and Src tyrosine kinase was shown *in vitro* and in cultured neurons using the radioactive isotope ^{32}P. Single mutation of serine residue at position 940 in the intracellular domain of KCC2 (Ser^{940}) to alanine (S940A) blocked the phosphorylation of KCC2 under PKC activation. However, tyrosine phosphorylation of KCC2 was shown to not affect Tyr^{1087}, the putative tyrosine kinase phosphorylation site. To better understand phosphorylation of KCC2 at Ser^{940}, a phospho-specific antibody against this residue - namely p-S940 - was developed. Interestingly, agents inhibiting PKC and phosphatases altered signal of p-S940, indicating involvement of PKC, phosphatase-1 (PP1) and phosphatase-2A (PP2A) in the regulation of Ser^{940} phosphorylation. In an *in vitro* method using p-S940, it was shown that PP1 and PP2A dephosphorylated KCC2.

To examine the functional effect of phospho-dependent modulation of KCC2, cell surface stability of KCC2 and its co-transport activity were determined. Notably, PKC activation increased cell surface expression of KCC2 by reducing its endocytosis, an effect blocked by S940A mutation. PKC activation also increased furosemide-sensitive [$^{86}Rb^{+}$] uptake in HEK-293 cells, indicating that PKC mediates KCC2 co-transport activity. Concomitantly, S940A mutation blocked the effect of PKC activation on its co-transport activity, while its basal activity remained intact. Together, this thesis describes direct phosphorylation of KCC2 and the functional detail of such phosphorylation in the regulation of KCC2 cell surface expression and co-transport activity.

Acknowledgements

Since I arrived Philadelphia in 2003 and started working in the Moss lab, my horizon has expanded so much that I think my life will never be the same. The experience working in a great lab is valuable to me. Here I would like to thank everyone whom I met in the past 5 years.

This work would never be possible without the support and guidance of my supervisor, Professor Stephen Moss. I thank him for having me as his student and providing me an excellent environment to learn in great freedom. I also thank several postdocs in Moss's lab, including Nobu, Richard, Guido, Verena, Tija, Yury, Raquel, Jay, Rachel and Miho, for their scientific discussion and technical guidance. Special thanks are given to J.P. Miho, I.P. Mansi and Boy-Borat Matt for their caring in lab and sharing of great food outside of the lab. I would also like to thank Josh for his excellent technical support of my work. I am also indebted to Yolande, our beloved lab-mum a.k.a. Bormann or B, for her patience in proofreading my writing for grant applications and my thesis. Also, I want to express my sincere appreciation to Professor Edward Cooper at UPenn and Professor Philip Haydon at Tufts University for their help in different aspects during my study. In addition, I would like to thank Professor John Payne and his lab at UC Davis for their collaboration and discussion of the KCC2 project.

I would also like to take this opportunity to thank my friends who shaped this unforgettable journey for me. Firstly I thank Tsz Ki from Hong Kong who has

been very encouraging to me. I also thank my roommates in I-house Philadelphia, Jonathan and Pak, for all the good times. Significantly, I have to express my sincere gratitude to my ‘family’ in Philadelphia including Ingrid, Catherine, Connie, Terrance, Kelvin, Gordon, Alice and Liza, for their accompaniment and the endless excitement they brought to me. I also thank them for their help during my move from Philadelphia to Boston.

I would like to thank my parents in Hong Kong for their unconditional love and support during my study; none of this would have been possible without them. I also thank my brother Patrick and sister Crystal. I am delighted to see them graduate from university and steadily develop their careers.

I also thank you, the reader of my thesis. I hope you find something interesting (or entertaining) and helpful in it.

Contents

List of tables and figures

Abbreviations

aa	Amino acid
Amp	Ampicillin
AP2	Adaptor protein 2
APS	Ammonium persulphate
ATP	Adenosine triphosphate
BDNF	Brain-derived neurotrophic factor
BSA	Bovine serum albumin
CalC	Calphostin C
CCC	Cation chloride co-transporter
CKB	Brain type creatine kinase
$[Cl^-]_i$	Intracellular chloride concentration
CMV	Cytomegalo virus
CO_2	Carbon dioxide
CPM	Specific count per minute
CR2	Intracellular domain of $GABA_B$ receptor R2-subunit
CsA	Cyclosporin A
DAG	Diacylglycerol
DMEM	Dulbecco's modified eagle medium
DMSO	Dimethyl sulphoxide
DNA	Deoxyribonucleic acid
dNTP	Deoxyribonucleoside triphosphate
DTT	Dithiothreitol
E_{Cl}	Equilibrium potential for Cl^-
EDTA	Ethyleneadiaminetetraacetic acid
EGFR	Epidermal growth factor receptor
EGTA	Ethylene glycol tetraacetic acid
Egr4	Early growth factor 4
FBS	Fetal bovine serum
FITC	Fluorescein isothiocyanate
GABA	γ-amino butyric acid
GFP	Green fluorescence protein
GFX	GF109203X
GST	Glutathione S-transferase

HCl	Hydrochloric acid
HEK	Human embryonic kidney
HEPES	4-(2-hydroxyethyl)-1-piperazineethanesulfonic acid
HRP	Horseradish peroxidase
IB	Immunoblotting
IC_{50}	Half of maximal inhibitory concentration
IP	Immunoprecipitation
IPTG	Isopropyl β-D-1-thiogalactopyranoside
IgG	Immunoglobulin G
KCC2	Potassium chloride co-transporter 2
KCC2-FL	Expression construct of cDNA encoding full length KCC2
kDa	Kilodalton
λ-PPase	λ-phosphatase
mL	Milliliter
mM	Millimolar
$NaPO_4$	Sodium phosphate
Na_3VO_4	Sodium pervanadate
NEM	N-ethylmaleimide
NH_4HCO_3	Ammonium hydrogen carbonate
NKCC	Sodium potassium co-transporter
NRSE	Neuronal restrictive silencing element
OA	Okadaic acid
OD	Optical density
PAGE	Polyacrylamide gel electrophoresis
PBS	Phosphate-buffered saline
PBS-CM	Phosphate-buffered saline with 1mM Ca^{2+} and 0.5mM Mg^{2+}
PCR	Polymerase chain reaction
PDBu	Phorbol 12, 13-dibutyrate
pep-S940	Non-phospho-peptide of KCC2 at Ser^{940}
PKA	cAMP-dependent protein kinase, Protein kinase A
PKC	Ca^{2+}/phospholipid-dependent protein kinase, Protein kinase C
PMA	Phorbol 12-myristate-13-acetate
PP1	Protein phosphatase 1
P-pep-S940	Phospho-peptide of KCC2 at Ser^{940}

p-S940	Phospho-specific antibody to residue Ser^{940} of KCC2
P-Y	Anti-phospho-tyrosine antibody
PS	Phospho-serine
PT	Phospho-threonine
PTK	Protein tyrosine kinase
PY	Phospho-tyrosine
Rb^+	Rubidium ion
RTKs	Receptor tyrosine kinases
SDS	Sodium dodecyl sulphate
SEM	Standard error of the mean
SH2	Src homology 2
TBS-T	Tris-buffered saline with 0.1% Tween
TEMED	N, N, N', N'-tetramethylethylenediamine
TLC	Thin layer chromatography
TM	Transmembrane
TRITC	Tetramethyl rhodamine isothiocyanate
µL	Microliter
µM	Micromolar
WNK3	With no lysine kinase isoform 3
WT	Wild-type

Chapter 1 Introduction

1.1 Classification of K^+-Cl^- co-transporters

K^+-Cl^- co-transporters (KCC) belong to the superfamily cation chloride co-transporters (CCC) that transport cation and chloride ions in the same direction across the cell membrane (Payne, 1997). Ion co-transporters exist throughout the whole body. They are important in many physiological processes such as cell volume regulation, excretion and neuronal communication (Gamba, 2005). KCCs exist in a wide range of organisms in the animal kingdom so their functions are evolutionarily conserved (Adragna et al., 2004). To date four members of the KCC family have been identified: KCC1, KCC2, KCC3 and KCC4. These transporters differ in their expression pattern and their molecular weight (Table 1). All KCC members are capable of transporting potassium and chloride ions across the cell membrane in a 1:1 stoichiometric ratio in the same direction; hence they are electroneutral (i.e. their activities do not alter membrane potential) (Gamba, 2005). Although KCCs are capable of transporting ions into or out of the cell, thermodynamically a net removal of ions is favored due to a concentration gradient driving potassium ions out; thus they are highly associated with regulatory cell volume control (Russell, 2000). Among different members of the KCC family, KCC2 is unique due to its neuronal-specific expression (Payne et al., 1996). Subsequently a single neuronal restrictive silencing element (NRSE) responsible for its neuronal specific expression has been identified within the KCC2 gene in human and mouse (Karadsheh and Delpire, 2001) (See also section 1.6). Physiologically

Table 1 Members and characteristics of the KCC family.

	KCC1	**KCC2**	**KCC3**	**KCC4**
Gene name	*SLC12A4*	*SLC12A5*	*SLC12A6*	*SLC12A7*
Expression	Ubiquitously expressed	Brain	Brain, heart, kidney	Ubiquitously expressed
Deduced molecular weight (kDa)	120	123	127	120
Activation by N-ethylmaleimide (NEM)	Yes	Yes	Yes	Yes
Response to change in osmolarity	Yes	Yes	Yes	Yes
Sensitivity to furosemide (IC_{50})	~200μM	~20μM	~200μM	~1mM
Major physiological function	Cell volume regulation, cell cycle control	Cl^- equilibrium potential in neurons, determining GABA reversal potential	Arterial pressure regulation, development of inner ear, cell volume regulation	K^+ re-absorption in neurons, acid-base metabolism
Phenotype of knock-out animal	(Not applicable)	Postnatal death due to respiratory failure	Hypertension, progressive hearing loss	Deafness
Associated disorders	Cervical cancer	Epilepsy, neuropathic pain	Anderman syndrome, hypertension, cervical cancer	Cervical cancer

expression of KCC2 is related to the emergence of inhibition mediated by γ-amino butyric acid type A receptor ($GABA_A$ receptor) during neuronal development (Rivera et al., 1999; Ben-Ari, 2002). The role of KCC2 in setting and maintaining Cl^- equilibrium potential in neurons and directly determining fast GABAergic inhibition has been confirmed by measuring the driving force of $GABA_A$ response in hippocampal slices after exposing to phosphorothionated oligodeoxynucleotides which knocked down KCC2 gene expression (Rivera et al., 1999) (Table 2).

Similar to other KCC members, KCC2 is activated by the sulfhydryl agent N-ethylmaleimide (NEM) and inhibited by loop diuretics such as furosemide and bumetanide (Payne, 1997). To date the detailed mechanisms of how these agents activate or inhibit KCC2 activities are not known but the region between TM2 and TM3 domains of KCC2, which shares high homology with other CCC members, is speculated to play a significant role (Gamba, 2005) (See also section 1.4).

1.2 Molecular structure of KCC2

KCC2 has been cloned in different species including rat, mouse and human (Gillen et al., 1996; Payne et al., 1996; Song et al., 2002). In rat, the KCC2 gene is found in chromosome 3 with a locus position 3q42 (GenBank accession number Slc12a5). In mouse the gene is found in chromosome 8, and in humans it is found in chromosome 20. The *SLC12A5* gene spans over 30kb in size and consists of 24 exons (Sallinen et al., 2001). A splice variant that encodes

Table 2 Expression of KCC2 in rat hippocampus and polarity of $GABA_A$ receptor mediated responses. *Adapted from Rivera et al., 1999.*

Preparations (P, postnatal)	**KCC2 expression**	**$GABA_A$ receptor responses**
P0-P4	Low	Depolarizing
P>12	High	Hyperpolarizing
P>12, exposed to KCC2 antisense oligonucleotides	Low	~0
P>12, exposed to KCC2 sense oligonucleotides	High	Hyperpolarizing

different 40 amino acid residues at its N-terminus was also identified recently; however it contributes only to 5-10% of total KCC2 mRNA in mature mice cortex (Uvarov et al., 2007). The complete coding sequence of rat KCC2 can be found in GenBank by accession number U55816. KCC2 molecules from rat are made of 1116 amino acids with a predicted molecular weight of approximately 123.6kDa (Payne, 1997) (Fig. 1.1). It has been proposed that KCC2 molecules consist of two major intracellular domains on both the N-tail (amino acid 1-102) and the C-tail (amino acid 635-1116), which are linked by 12 transmembrane domains (Payne, 1997) (Fig. 1.2). Sequence comparison shows that KCC2 shares 67% identity with KCC1 and 25% identity with sodium potassium chloride co-transporters (NKCC) (Russell, 2000; Gamba, 2005).

Intracellular N-tail and C-tail

The intracellular N-tail and C-tail of KCC2 are hydrophilic and account for 50% of the molecular mass of this protein (Williams et al., 1999). These intracellular regions are believed to harbor regulatory sites for the co-transporter; for example, putative sites for PKC phosphorylation (Thr^{34}, Ser^{728}, Thr^{787}, Ser^{940} and Ser^{1034}) and that for tyrosine kinase phosphorylation (Tyr^{1087}) have been documented (Payne et al., 1996; Strange et al., 2000) (Fig. 1.2). Interestingly, Ser^{940} is found in a region unique to KCC2 among all other KCC family members due to an insertion of an extra exon in the *SLC12A5* gene, while Tyr^{1087} is highly conserved among them (Payne et al., 1996) (Fig. 1.3). Within this unique region of KCC2 protein, a stretch of 15 amino acids, an

MLNNLTDCEDGDGGANPGDGNPKESSPFINSTDTEKGREYDGRNMALFEEEMDT
SPMVSSLLSGLANYTNLPQGSKEHEEAENNEGGKKKPVQAPRMGTFMGVYLPCL
QNIFGVILFLRLTWVVGIAGIM**ESFCMVFICCSCTMLTAISM**SAIATNGVVPAGGSYYM
ISRSLGPEFGG**AVGLCFYLGTTFAGAMYIL**GTIEILLAYLFPAMAIFKAEDASGEAAAM
LNNM**RVYGTCVLTCMATVVFVGV**KYVNK**FALVFLGCVILSILAIYAGV**IKSAFDPPNF
PICLLGNRTLSRHGFDVCAKLAWEGNETVTTRLWGLFCSSRLLNATCDEYFTRNNVTE
IQGIPGAASGLIKENLWSSYLTKGVIVERRGMPSVGLADGTPVDMDHPYVFSDMTSYF
TLLVGIYFPSVTGIMAGSNRSGDLRDAQKSIPTG**TILAIATTSAVYISSVVLFG**ACIEGVV
LRDKFGEAVNGNLVVGTLAWPS**PWVIVIGSFFSTCGAGLQSLT**GAPRLLQAISRDGIVP
FLQVFGHGKANGEPTW**ALLLTACICEIGILIASLDE**VAPI**LSMFFLMCYMFVNLACAVQ**
TLLRTPNWRPRF**RYYHWTLSFLGMSLCLALMF**ICS**WYYALVAMLIAGLIYKYIEY**RG
AEKEWGDGIRGLSLSAARYALLRLEEGPPHTKNWRPQLLVLVRVDQDQNVVHP
QLLSLTSQLKAGKGLTIVGSVLEGTFLDNHPQAQRAEESIRRLMEAEKVKGFCQV
VISSNLRDGVSHLIQSGGLGGLQHNTVLVGWPRNWRQKEDHQTWRNFIELVRET
TAGHLALLVTKNVSMFPGNPERFSEGSIDVWWIVHDGGMLMLLPFLLRHHKVW
RKCKMRIFTVAQMDDNSIQMKKDLTTFLYHLRITAEVEVVEMHESDISAYTYEKT
LVMEQRSQILKQMHLTKNEREREIQSITDESRGSIRRKNPANTRLRLNVPEETACD
NEEKPEEEVQLIHDQSAPSCPSSSPSPGEEPEGEGETDPEKVHLTWTKDKSAAQKN
KGPSPVSSEGIKDFFSMKPEWENLNQSNVRRMHTAVRLNEVIVNKSRDAKLVLLN
MPGPPRNRNGDENYMEFLEVLTEQLDRVMLVRGGGREVITIYS**

Fig. 1.1 Amino acid sequence of rat KCC2. Sequence is obtained from GenBank accession number U55816. The 2 major intracellular domains (N-tail, amino acid 1-102, and C-tail, amino acid 635-1116) are in **bold face**, 12 transmembrane domains are underlined, sites predicted to be phosphorylated by PKC are highlighted in **red** (Thr^{34}, Ser^{728}, Thr^{787}, Ser^{940} and Ser^{1034}) while the site putatively phosphorylated by tyrosine kinase is denoted in **blue** (Tyr^{1087}).

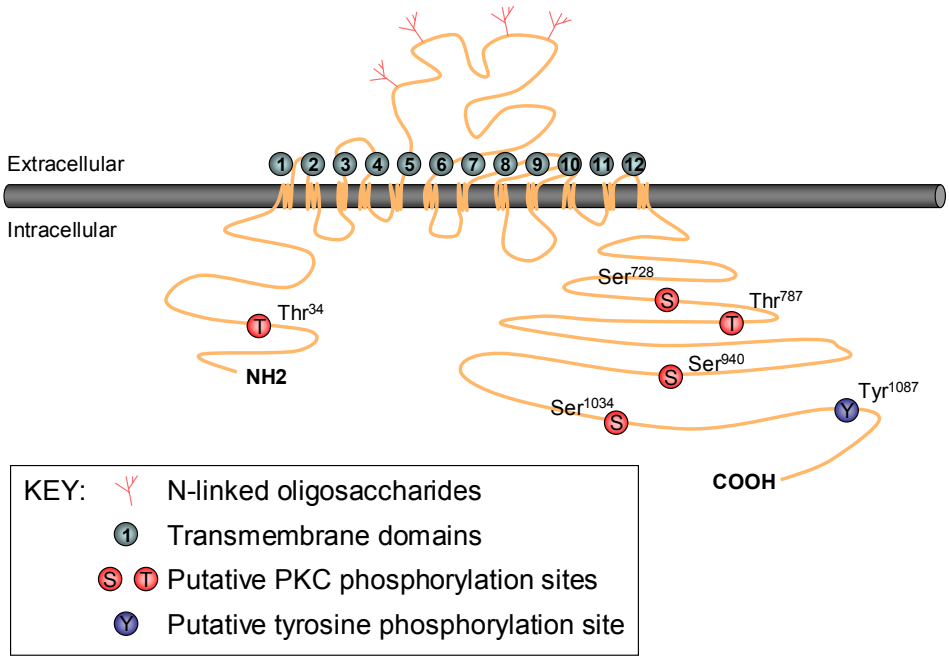

Fig. 1.2 Molecular organization of KCC2. Membrane-bound KCC2 molecules consist of two major intracellular domains at N-tail (amino acid 1-105) and C-tail (amino acid 635-1116) in which putative phosphorylation sites by PKC and tyrosine kinase can be found. There are twelve transmembrane domains and a major N-linked glycosylated extracellular domain between TM5 and TM6.

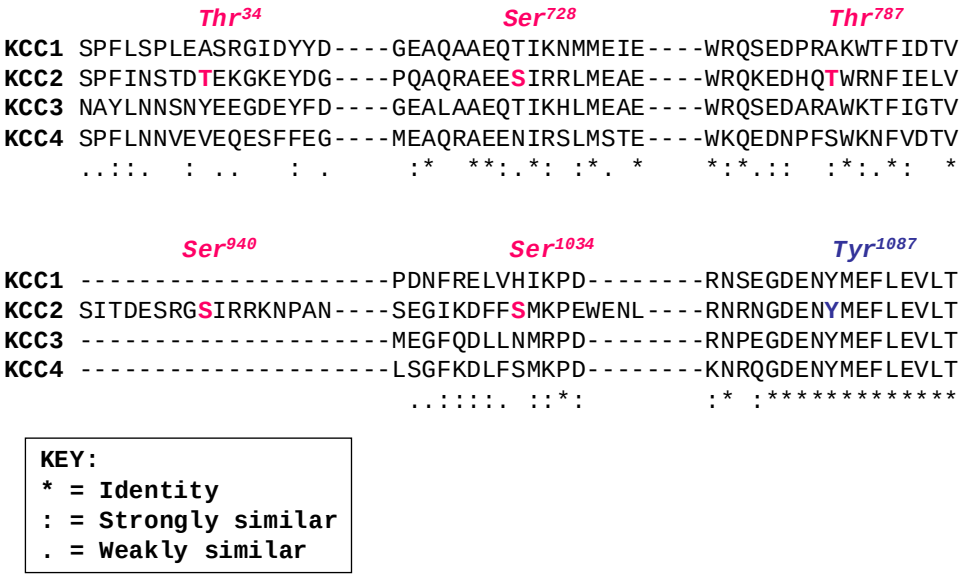

Fig. 1.3 Sequence alignments of KCC family members at putative phosphorylation sites of KCC2. Eight amino acids before and after the phosphorylation sites on KCC2 (colored red for PKC phosphorylation sites and blue for tyrosine kinase phosphorylation site) are shown. Sequence homology among KCC1 to KCC4 are indicated as identity (*), strongly similar (:) and weakly similar (.).

"ISO segment", was identified as responsible for its constitutive activity in isotonic conditions (Mercado et al., 2006). In addition, regions in the C-tail have been identified as interacting with potential regulatory effectors (Bergeron et al., 2006) and cytoskeleton-associated proteins (Li et al., 2007). The C-tail of KCC2 is thus believed to play important roles in regulation of co-transport function by cell signaling molecules such as kinases and maintenance of structural integrity of neuronal dendrites (Li et al., 2007) (See also section 1.5).

Transmembrane domains

There are 12 putative transmembrane (TM) domains in KCC2 molecules (Williams et al., 1999). These regions display the highest identity (>90%) between KCC1 and KCC2. In particular, TM2 and TM3 are highly conserved among CCC family members (Payne et al., 1996). These regions may also be involved in determining ion affinity and bumetanide binding of KCC2 as demonstrated by other CCC family members (Russell, 2000).

Extracellular loop

There is a prominent extracellular loop between TM5 and TM6 of KCC2 which is glycosylated at four positions as predicted (Payne et al., 1996; Williams et al., 1999) (Fig. 1.2). The exact function of glycosylation is unknown, but it may be involved in the modification of co-transport activities. The glycosylation increases apparent molecular weight of KCC2 from 123kDa to around 145kDa in the expression systems (Williams et al., 1999). This

molecular weight can be reduced in size by N-glycosidase (Williams et al., 1999).

1.3 Expression of KCC2

KCC2 can be found in different parts of the central nervous system. A range of experimental techniques have been used to demonstrate the expression of KCC2. For example, protein expression of KCC2 has been detected with techniques such as western blotting and immunohistochemistry in cortex (Bayatti et al., 2007; Molinaro et al., 2007), retina (Vardi et al., 2000; Vu et al., 2000) and cochlear nucleus (Vale et al., 2005); KCC2 protein expression with electron microscopy in hypothalamus (Belenky et al., 2008); KCC2 mRNA with *in situ* hybridization in temporal lobe (Huberfeld et al., 2007) and spinal cord (Vinay and Jean-Xavier, 2008). Interestingly, KCC2 is found to express heavily in the inferior colliculus (Reid et al., 2001) and dentate gyrus (Pathak et al., 2007), brain regions that are highly associated with epileptic seizures. This suggests a correlation between KCC2 and epilepsy. Furthermore, KCC2 has been found to express in the hypothalamic suprachiasmatic nucleus, the primary circadian clock in mammals which regulates rhythmic behavior and physiology (Belenky et al., 2008).

KCC2 is neuronal specific and its expression is central to the inhibitory function of $GABA_A$ receptors (Rivera et al., 1999). An NRSE has been identified within the intron 1 of mouse KCC2 gene (Karadsheh and Delpire, 2001). More recently, a 1.4kb promoter region directly upstream of KCC2 gene

has been identified in mouse to be sufficient for neuronal-specific expression (Uvarov et al., 2005). The role of KCC2 in Cl^- efflux has also been demonstrated using recombinant expression (Payne et al., 1996; Strange et al., 2000; Bergeron et al., 2006). Significantly, measurement of the reversal potential of GABA has demonstrated that expression of KCC2 is essential to the inhibitory action of $GABA_A$ receptors (Rivera et al., 1999). It has now been established that KCC2 is the major Cl^- extruder in the central nervous system and that it is directly related to the transition in response to GABA from depolarization in the prenatal stage (when $[Cl^-]_i$ is above its electrochemical potential equilibrium) to hyperpolarization in the postnatal period (when $[Cl^-]_i$ is below this equilibrium) (Rivera et al., 1999).

Expression of KCC2 under the regulation of neuronal transmission had been investigated but remained elusive. It has been shown that expression of KCC2 is not affected by blocking either glutamatergic transmission or action potential (Ganguly et al., 2001; Ludwig et al., 2003). However, there is contradictory evidence both to support (Ganguly et al., 2001) and deny (Ludwig et al., 2003) the notion that GABAergic transmission regulates KCC2 expression during neuronal development. Despite this conflicting evidence, brain-derived neurotrophic factor (BDNF) may play a role in regulating postsynaptic transmission by down-regulating KCC2 expression (Rivera et al., 2002; Wardle and Poo, 2003). A positive shift in the reversal potential for Cl^- and a less inhibitory GABAergic current was observed when BDNF was applied during hippocampal slice recordings (Rivera et al., 2002).

1.4 Pharmacology of KCC2

KCC2 can be activated by 1mM NEM, possibly through a sulfhydryl modification of the co-transporter or an associated protein, although the binding site for NEM has not been identified on KCC2 molecules (Lauf, 1985; Gamba, 2005). On the other hand, KCC2 can be inhibited by loop diuretics and is more sensitive to furosemide (20μM) than to bumetanide (55 μM); however, to date there is no selective inhibitor of KCC2 (Payne, 1997). Inhibition of KCC2 by loop diuretics is possibly controlled by a region close to TM2 and TM3 domains of KCC2, which shares the highest homology among different CCC members and is known to be responsible for cation binding in NKCC2 (Gagnon et al., 2004). To date the ability of NEM or loop diuretics to cross the blood-brain barrier is not known. There is also no known pharmacological agent to modify KCC2 activities *in vivo*. Unlike other KCC members, KCC2 exhibits constitutive activity in isotonic conditions, and does not require activation by cell swelling (Payne, 1997).

1.5 Functional significance of KCC2

Cellular homeostasis

The activity of KCC2 is defined as secondary active transport, since its activity derives from the intracellular concentration of K^+, $[K^+]_i$, but not from the availability of adenosine triphosphate (ATP) (Payne, 1997). This is particularly important since KCC2 is energy independent; ionic balance controlled by this

co-transporter can be carried out even when energy is not readily available. Activity of KCC2 is also electroneutral, since both K^+ and Cl^- are transported in a 1:1 stoichiometry. This enables KCC2 to carry out its function without affecting the electrical property of neurons. When ions are transported across the neuronal membrane, water molecules are also moved due to osmotic action. KCC2 thus plays a role in the homeostasis of neurons by controlling water movement during ion transport (Gamba, 2005).

K^+ buffering

The high affinity of KCC2 for extracellular K^+ can be reflected by its Km value (5.2mM) compared to that of KCC1 (25mM). KCC2 is therefore able to respond to subtle changes in extracellular concentration of K^+ ($[K^+]_o$) which indicates that KCC2 is a strong K^+ buffer for neuronal transmission (Payne, 1997). During neuronal transmission, outward K^+ movement from neurons leads to a fall in intracellular concentration of K^+ ($[K^+]_i$). To prevent depletion of $[K^+]_i$ there are several mechanisms to return K^+ back into neurons including Na^+-K^+-ATPase and glial spatial buffering (Walz, 1989). Since KCC2 has a high affinity for an extracellular concentration of K^+ ($[K^+]_o$), a subtle increase in $[K^+]_o$ after neuronal depolarization results in a shift of equilibrium of K^+ and Cl^- and a net influx of both ions is favored (Payne, 1997) (Fig. 1.4). This serves as a mechanism for neurons to respond to depletion of $[K^+]_i$.

Maintenance of Cl^- equilibrium potential, E_{Cl}

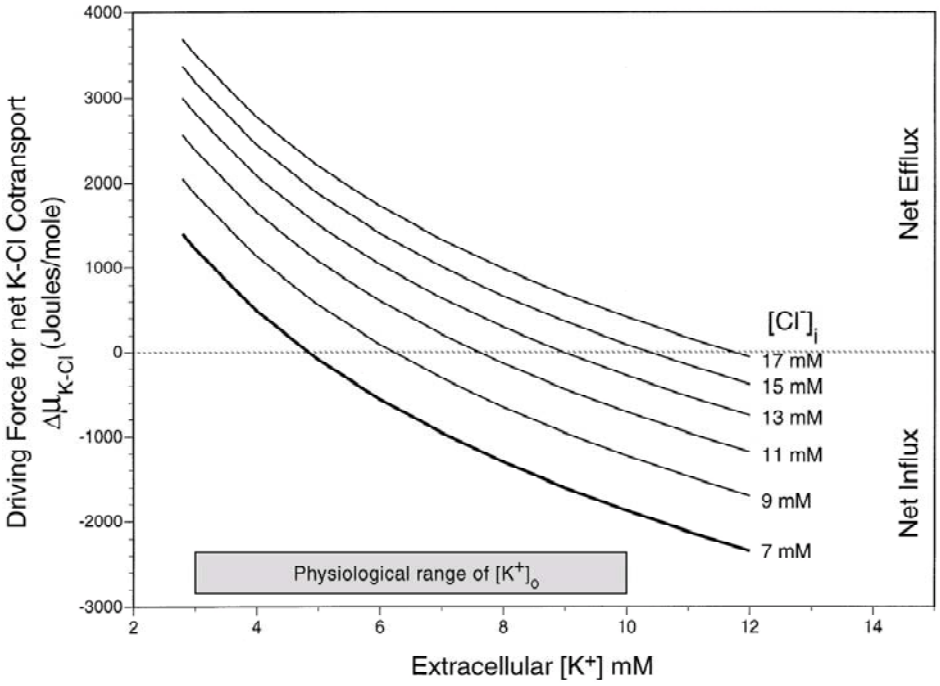

Fig. 1.4 Thermodynamic driving force of KCC2 (J/mol) as a function of $[K^+]_o$ at various $[Cl^-]_i$ values. ***Adapted from Payne, 1997.*** At a physiological concentration of $[Cl^-]_i$ such as 7mM, a change of $[K^+]_o$ from a low value (<5mM) to a high value (>5mM) will induce net influx of ions.

Co-localization of KCC2 and $GABA_A$ receptor β2/β3 subunits shown by immunofluorescence microscopy suggests that KCC2 is highly associated with GABAergic functions (Williams et al., 1999). Concentration of Cl^- in neurons is maintained by ion co-transporter systems including NKCC1 and KCC2 (Gamba et al., 1994; Haas and Forbush, 1998; Mount et al., 1998; Russell, 2000). The former is an ion importer while the latter is an exporter. The relative activities of these co-transporters determine the Cl^- gradient across the neuronal membrane, which contributes to E_{Cl}. In particular, during neuronal development protein expression of NKCC1 is lowered at the postnatal stage and that of KCC2 is increased approximately 10 days after birth (Li et al., 2002; Wang et al., 2002; Delpy et al., 2008). These changes in expression of co-transporters reduce $[Cl^-]_i$ in adult animal and lower E_{Cl}, which in turn renders GABA inhibitory (Owens et al., 1996; Ehrlich et al., 1999; Rivera et al., 1999). In the brain differential expression of KCC2 gives rise to altered E_{Cl} and thus to an altered GABAergic response; for example, $GABA_A$ reversal potential is less negative and less hyperpolarizing in dopaminergic neurons than in GABAergic neurons due to lower KCC2 expression in the former type of neuron (Gulacsi et al., 2003).

Neuronal development

It is now accepted that KCC2 plays an important role in neuronal development, functioning as a molecular switch to alter fast synaptic signaling (Rivera et al., 2005). As described above, GABA transmission is mainly excitatory prenatally. It has been speculated that Ca^{2+} signaling during the excitatory response of the

$GABA_A$ receptor in the early developmental stage is important in establishing the neuronal network. Studies show that protein expression of KCC2 is important for establishing the GABAergic synapse (Chudotvorova et al., 2005). The GABAergic network is thought to be constructed and stimulated by the lowering of $[Cl^-]_i$ by the functional expression of KCC2. Recently KCC2 has been found to interact with the spine cytoskeleton 4.1N through which synaptic spine maturation is promoted (Li et al., 2007). Interestingly, expression of the non-chloride-extruding form of KCC2 lacking its N-terminal intracellular domain is able to restore the formation of spine and functional synapse in KCC2-deficient mice (Li et al., 2007). The development of spine is thus independent of its co-transport function and KCC2 is important for neuronal transmission, development and survival of neurons.

Cell volume regulation and survival of neurons

Cell volume change is one of the hallmarks of cell progression to apoptosis or proliferation. For example, KCC1, KCC3 and KCC4 are involved in erythropoiesis (De Franceschi et al., 2007). KCC1 is also known to play an important role in cell volume regulation due to its ubiquitous expression (Gamba, 2005). In brain, KCC2 is found to play a classical role in cell volume regulation. It has been shown that dendritic swelling caused by neuronal excitation is opposed by KCC2 activity (Gulyas et al., 2001). The fact that KCC2 is more sensitive to osmolarity than are other members in its family and is more sensitive to $[Cl^-]_i$ indicates that a tight control over the hyperpolarizing

effects of GABA is important for neurons (Bergeron et al., 2006). A schematic diagram showing different functions of KCC2 can be found in Fig. 1.5.

1.6 Regulation of KCC2

Since KCCs play important roles in a number of different physiological processes, their regulation inside cells is important; for example, maintenance of activity of KCC2 is essential in keeping the transmembrane Cl^- gradient in neurons. To date, the regulation of KCC2 in neurons is not well understood. Studies on KCC2 have focused on transcriptional regulation and post-translational modification.

Transcriptional regulation

KCC2 is unique among all other KCC members in being neuronal-specific. To identify elements in the KCC2 gene that confer its neuronal-specific expression, an NRSE has been identified within intron 1 of the KCC2 gene (Karadsheh and Delpire, 2001). This unique element of KCC2 has been shown to silence reporter gene activity in non-neuronal cells. Furthermore, a 21-base pair region of this NRSE was found to share 80% homology with the consensus binding sequence of neuronal restrictive silencing factor and to bind to extracted nuclear proteins from mouse neural progenitor cell line C17. The early growth factor 4 (Egr4) binding element has been identified in this promoter region and it binds to Egr4 proteins in a mobility shift assay (Uvarov et al., 2006). It has been shown that antisense knockdown of Egr4 or expression of dominant

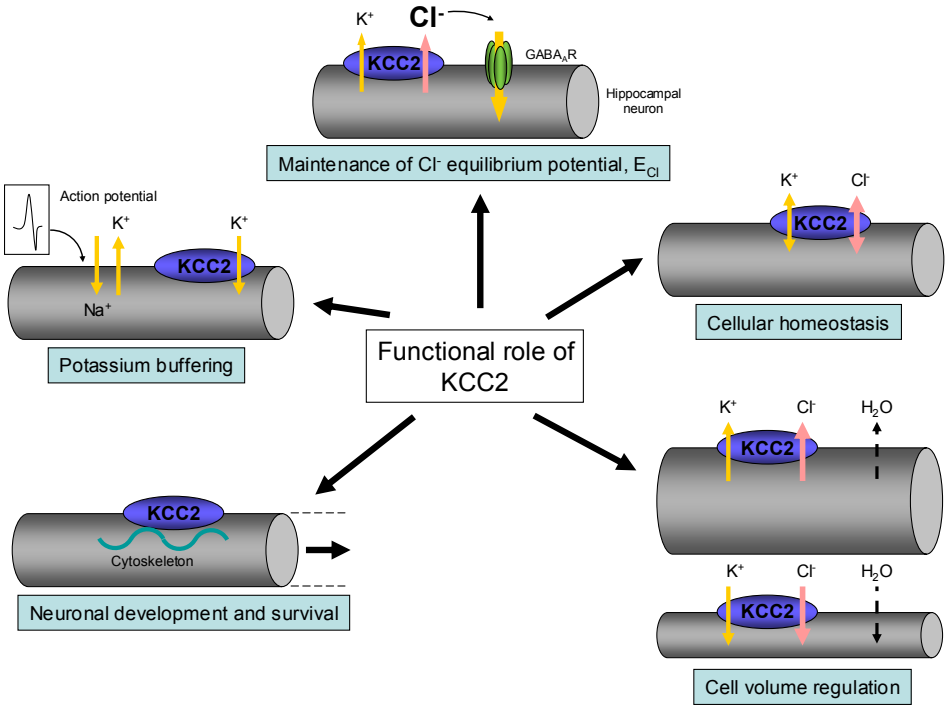

Fig. 1.5 Functional significance of KCC2. Schematic diagram summarizing different functional aspects of KCC2 in neurons. Capable of transporting K^+ and Cl^- across neuronal membrane, KCC2 is responsible for establishment and maintenance of the Cl^- equilibrium potential (E_{Cl}) that renders GABA inhibitory, ionic homeostasis, K^+ buffering during neuronal transmission, neuronal development and survival and cell volume regulation.

negative form of Egr4 down-regulates KCC2 protein expression in neurons. This indicates an important role for this factor in developmental up-regulation of KCC2 gene expression.

Post-translational modification

A few studies show that KCC2 is regulated by phosphorylation. Brain type creatine kinase (CKB) has been reported to interact with KCC2 (Inoue et al., 2004) and activate KCC2 function in HEK-293 cells (Inoue et al., 2006). CKB is an ATP-generating enzyme and plays critical role in energy support in cells (Mahajan et al., 2000). Interestingly, lowered CKB activity has been linked to neurological disorders such as Alzheimer's disease and schizophrenia (Smith et al., 1991; Burbaeva et al., 2003). KCC2 may thus play a role in these CKB-mediated diseases. In addition, tyrosine phosphorylation of KCC2 has been linked to the regulation of KCC2 cell surface stability and activity during neuronal stress (Wake et al., 2007). A loss of tyrosine phosphorylation of KCC2 reduces its cell surface stability and co-transport function. Furthermore, activity of WNK3 kinase, a member of the WNK family of serine/threonine kinases, is shown to down-regulate KCC2 (Kahle et al., 2005). In addition, mutation studies of KCC2 have revealed that the region around Ser^{940} of the C-tail intracellular domain of KCC2 is responsible for regulation by effector proteins that are mediated by PKC activation (Bergeron et al., 2006).However, in these studies direct phosphorylation of KCC2 mediated by WNK3 or PKC was not shown. The role of phosphorylation in regulation of KCC2 cells surface stability and activity thus remains elusive.

Phosphorylation is an ubiquitous mode of post-translational modification that regulates protein-protein interactions, protein activities and intracellular trafficking (Brandon et al., 2000; Kuramoto et al., 2007); for example, regulation of $GABA_A$ and $GABA_B$ receptors by phosphorylation has been investigated extensively (Fairfax et al., 2004; Jovanovic et al., 2004; Houston et al., 2007). It has been shown that phosphorylation increases the efficacy of GABA (Kanematsu et al., 2006), channel opening frequency of $GABA_A$ receptors (Porter et al., 1990), and receptor interaction with proteins such as clathrin adaptor protein complex AP2 (Kittler et al., 2008). Since KCC2 controls transmembrane Cl^- potential, which in turn determines the polarity of GABA currents, regulation of KCC2 function is likely to have a profound effect on GABAergic transmission. The effect of phosphorylation on KCC2 molecules is thus of particular interest in regards to the regulation of inhibitory transmission in the brain.

1.7 Role of protein kinase C (PKC) in the regulation of neuronal inhibition

PKC is abundantly expressed in brain and its activity is highly associated with neuronal function including excitation (Sheng et al., 1998; Belousov et al., 2002), inhibition (Staley, 1994; Brandon et al., 2002) and long term potentiation (Madison et al., 1991). PKC regulates both pre-synaptic (Shuntoh et al., 1989; Macek et al., 1999) and post-synaptic (Malinow et al., 1989) processes and therefore exerts tight regulation on neuronal transmission.

In the central nervous system fast synaptic inhibition is carried out mainly through the activation of $GABA_A$ receptors, leading to the influx of Cl^- due to its negative equilibrium potential. PKC is involved extensively in such GABA-mediated neuronal inhibition. Pre-synaptically PKC affects release of GABA into the synaptic cleft (Taniyama et al., 1990) and its re-uptake into the pre-synaptic compartment (Cupello et al., 1993). GABA transporter GAT1 is also regulated by PKC in recombinant system (Sato et al., 1995). Furthermore, interaction between GABA transporter and syntaxin 1A is regulated by PKC activity (Beckman et al., 1998). Post-synaptically activation of PKC increases Cl^- permeation (Rapallino et al., 1993). PKC has also been found in different studies to regulate $GABA_A$ receptors (Brandon et al., 1999; Brandon et al., 2000; Jovanovic et al., 2004). PKC thus plays an important role in the regulation of neuronal inhibition.

To date, the role of PKC in the regulation of neuronal inhibition mediated through $GABA_A$ receptors has been investigated extensively. It has been shown that $GABA_A$ receptors are directly associated and phosphorylated by PKC *in vitro* and in neurons (Brandon et al., 1999; Brandon et al., 2000). Several residues of β and γ subunits of $GABA_A$ receptors have been identified as PKC substrates. β1 subunit of $GABA_A$ receptor has been found to be phosphorylated by PKC at its residue Ser^{409} (Moss et al., 1992). Subsequently Ser^{410} of β2 and Ser^{408}, Ser^{409} of β3 subunits have been shown to be PKC substrates (McDonald and Moss, 1997). In addition, Ser^{327} of γ2 subunit has been shown to be phosphorylated by PKC (Moss et al., 1992). Phosphorylation of these residues

results in modifications of receptor trafficking, channel opening properties and interactions of their associated binding proteins (Brandon et al., 1999; Brandon et al., 2000; Brandon et al., 2002; Jovanovic et al., 2004; Kittler et al., 2005). It has been established that binding of AP2 complex to β3 subunit of $GABA_A$ receptors occurs in a motif in which PKC phosphorylation site is found (Kittler et al., 2005). Phosphorylation at this site inhibits binding of AP2 and thus slows down endocytosis and enhances the efficacy of GABAergic transmission (Kittler et al., 2005).

Studies have suggested that phosphorylation may play a role in regulating KCC2 functions. Putative PKC phosphorylation sites are found within the intracellular domains of KCC2 (Fig. 1.1, 1.2). Intriguingly, mutation studies showed that the phosphorylation site at position Ser^{940} is involved in co-transport activity in isotonic condition (Bergeron et al., 2006). PKC is thus a candidate to regulate KCC2 function by directly phosphorylating this co-transporter.

1.8 Endocytosis is a process modulating cell surface protein stability

Cell surface protein expression is affected by the rate of endocytosis, degradation and re-cycling. To date, the mechanism of endocytosis mediated through the clathrin-coated vesicle is well characterized (Le Roy and Wrana, 2005). It is a major pathway for the internalization of cell surface proteins.

Clathrin-mediated endocytosis is a process through which proteins at the cell surface are transported to the intracellular domain for subsequent degradation or recycling. A crucial step in this process is the recruitment of clathrin protein to plasma membrane by the interaction between clathrin and AP2 complex. There are four identified adaptor protein complexes (AP1-4) and they all play roles in the regulation of protein trafficking; however, AP2 is unique in that it plays a role in the formation of clathrin-coated vesicles from cell surface (Owen et al., 2004). AP2 is hetero-tetrameric, consisting of α, β2, μ2 and σ subunits. Among these subunits β2 has been shown to interact directly with clathrin proteins while μ2 is responsible for the interaction of specific amino acid sequence motifs within the cytoplasmic domain of membrane proteins (Collins et al., 2002). Identification of sequence motifs in membrane proteins for AP2 binding is thus important in hypothesizing whether a protein is likely undergoing clathrin-mediated endocytosis.

There are several identified consensus sequence motifs for the endocytosis of cell surface proteins. A classical example is the NPXY motif (Asparagine-Proline-X-Tyrosine where X represents any amino acid residue) which was identified as the signal for internalization of LDL receptor, integrins and the β-amyloid precursor protein (Bonifacino and Traub, 2003). In addition, the YXXØ motif (Tyrosine-X-X-Ø where Ø represents any bulky hydrophobic amino acid) was also identified as an important internalization signal of membrane proteins including the transferrin receptor. In the sequence of KCC2, the YXXØ motif is found from amino acid 1087 to 1090 (YMEF) which

contains the putative tyrosine phosphorylation site Tyr^{1087}. It is thus important to investigate whether this site is involved in internalization of KCC2.

1.9 KCC2 and neurological disorders

Since KCC2 plays an important role in homeostasis and neuronal transmission, impaired expression of KCC2 during development or malfunction of KCC2 in mature neurons has been related to various neurological disorders.

Epilepsy

The role for KCC2 in epileptogenesis has been inferred due to its function as the major Cl^- extrusion mechanism in mature neurons. Compromised GABAergic synaptic transmission and excess excitability is often observed in both humans and in animal models of epilepsy (Treiman et al., 1990; Lowenstein and Alldredge, 1998; Coulter, 2001). This pathophysiology may be due to a reduced functional expression of KCC2 such that a normal E_{Cl} is not maintained (Fig. 1.6). Consistent with this reduced KCC2 mRNA levels, impaired Cl^- extrusion have been observed in various seizure models (Reid et al., 2001; Rivera et al., 2002; Rivera et al., 2004; Jin et al., 2005). Jin et al. has been able to show, using a gramicidin-perforated patch clamp technique, that chronically injured cortex is less effective in maintaining low $[Cl^-]_i$ during repetitive activation of $GABA_A$ receptor due to impaired KCC2 expression. In addition, disruption of the KCC2 gene leads to hyperexcitability in mice (Woo et al., 2002). Agents that modulate KCC2 activity have also been shown to

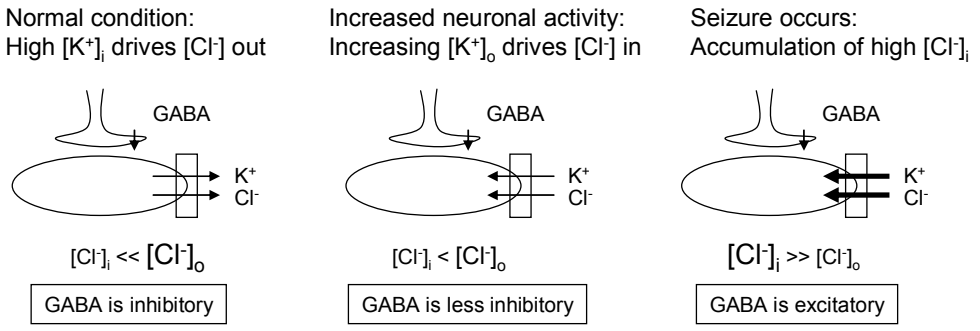

Fig. 1.6 Compromised KCC2 activity and epilepsy. In mature neurons, KCC2 maintains low $[Cl^-]_i$ by transporting Cl^- out of intracellular domains. This action produces a negative E_{Cl} such that activation of $GABA_A$ receptors results in an influx of Cl^- and a subsequent inhibitory synaptic response. Increased neuronal activities increase $[K^+]_o$ level and decrease outward flux of K^+ and Cl^- directed by KCC2 activity such that E_{Cl} is shifted towards positive. In epilepsy, a loss of KCC2 function is observed that promotes an accumulation of intracellular Cl^- and E_{Cl} becomes positive. Activation of $GABA_A$ receptor results in an outflux of Cl^- and an excitatory response.

decrease seizure activity in rats (Reid et al., 2000). In addition BDNF, which is shown to be related to the developmental up-regulation of KCC2 and modulation of the GABAergic response (Aguado et al., 2003; Wardle and Poo, 2003), is implicated in epileptogenesis (Binder et al., 2001). An *in vivo* knock-in study of TrkB receptor, which is activated by BDNF, showed that activation of this receptor may play opposite roles in regulating KCC2 expression mediated through Shc (increased KCC2 expression) and CREB (decreased KCC2 expression) (Rivera et al., 2004). Together these studies show that there is a linkage between epilepsy and malfunction of KCC2.

Neuropathic pain

Diabetes-induced neuropathic pain has been associated with hyperexcitability and spontaneous hyperactivity in spinal cord neurons. It has been shown that, in a streptozotocin-induced diabetes rat model in which insulin-producing pancreatic beta-cells are damaged, expression of KCC2 is significantly reduced but expression of GABA is elevated in the dorsal horn laminae (Morgado et al., 2008). This combined effect is likely to exaggerate the depolarization response of GABA. Such a loss of GABA-mediated inhibitory tone at the spinal cord may result in neuronal hyperexcitability and spontaneous hyperactivity in diabetes. Furthermore, local blockade of KCC2 using [(dihydroindenyl)oxy]alkanoic acid, DIOA, or knock-down of spinal KCC2 using antisense oligodeoxynucleotides, also reduces the nociceptive threshold in rats (Coull et al., 2003). Using thermal and mechanical stimuli, investigators were able to show that knock-down of KCC2 decreases the latency for rats to

withdraw their paws, indicating increased pain sensation. Together these suggest that malfunction of KCC2 leading to an abnormal Cl^- gradient and subsequent GABA-mediated depolarization is the underlying mechanism of abnormal excitability in the pathophysiology of neuropathic pain. Novel therapeutic strategies to restore normal KCC2 function can be valuable to ameliorate this disorder.

1.10 Aims of this study

Whilst it has been suggested that phosphorylation modulates KCC2 activity, regulation of KCC2 by direct phosphorylation remained elusive. There is no evidence showing that KCC2 is directly phosphorylated (Strange et al., 2000; Adragna et al., 2004; Bergeron et al., 2006; Wake et al., 2007). Based on the current understanding of regulation of KCC2, it is hypothesized that KCC2 is phosphorylated by kinases and that this action affects its co-transport activity. A possible mechanism affecting KCC2 activity is the modulation of its cell surface stability and expression. In this thesis, experiments were carried out to investigate how direct phosphorylation of KCC2 modulates its cell surface stability and co-transport function. Specifically, the aims of this study are:

1) To demonstrate that KCC2 is phosphorylated on specific residue(s) and identify the kinase(s) activities responsible for this phosphorylation.
2) To develop a phospho-specific antibody as a molecular tool to examine KCC2 phosphorylation.

3) To examine whether phosphorylation of KCC2 modulates its cell surface stability and membrane trafficking.

4) To examine whether phosphorylation of KCC2 modulates its co-transport activities.

Chapter 2 Methods and Materials

Molecular biology

2.1 Polymerase chain reaction (PCR)

PCR was set up according to manufacturer specifications (Stratagene). Typically, reaction mixture in a 50μL reaction contains 5μL 10x PCR reaction buffer, 4μL 10mM deoxyribonucleoside triphosphate (dNTP) (Roche, Cat# 1969064), 2μL each of 10μM sense and anti-sense primers, 5μL plasmid DNA template (10ng/μL), 4μL of *Pfu* turbo polymerase (Stratagene, Cat# 600250-52) and 26μL of deionized water. The ingredients were mixed well in a thin-walled 200μL polypropylene tube and transferred to a thermocycler machine. The conditions of thermo cycles depend on application, but are typically:

95^{o}C for 3min

95^{o}C for 30s, 55^{o}C for 30s and 68^{o}C for 10min (15-30 cycles)

68^{o}C for 5min

The reaction was stopped by reducing the temperature to 4^{o}C.

2.2 Bacterial strains

BL21 [F^-, *ompT*, *hsd*S_B($r_B^-m_B^-$), *gal*, *dcm*] was used in fusion protein induction and expression.

JM109 [*end*A1, *rec*A1, *gyr*A96, *thi*, *hsd*R17($r_K^-m_K^+$), *rel*A1, *sup*E44, Δ(*lac-pro*AB)] was used in plasmid carriage and propagation.

2.3 Preparation of competent cells

Competent cells for electroporation method were prepared according to Sambrook and Russell, 2001. First, 50mL of bacteria was inoculated in LB broth with appropriate antibiotic which was grown for 16h at 37°C to 1L LB broth with antibiotic. The culture was grown in a shaker for 2h until OD_{600} achieved 0.5 and then put in an ice bath for 15min. The bacteria were spun down by centrifugation at 1000x *g* for 15min at 4°C. The pellet was washed with 1L ice-cold deionized H_2O followed by 0.5L ice-cold 10% (v/v) glycerol and 20mL ice-cold 10% (v/v) glycerol. Finally, the bacteria were spun down and resuspended in 10mL GYT medium. The competent cells were kept at -70°C in 40μL aliquots.

2.4 Transformation of bacteria with plasmid DNA

Transformation of bacteria (heat shock method) was carried out according to Sambrook and Russell, 2001. First, 10μL of transforming materials was mixed with 100μL competent cells in a 1.5mL Eppendorf tube for 30min. The tube was transferred to a water bath at 42°C for 45s then quickly transferred to an ice bath for 3min. 1mL of LB broth was added to the transformed bacteria and the whole tube was transferred to a water bath at 37°C for 1h. The bacteria were then spun down briefly using a benchtop centrifuge, resuspended in

100μL of LB broth and spread evenly on an LB agar plate with appropriate antibiotic. The LB agar plate was then incubated at 37^{o}C for 16h or until bacterial colonies appeared.

Transformation by electroporation was carried out by first mixing 2μL of transforming materials with 100μL electrocompetent cells in a 1.5mL Eppendorf tube. The mixture was transferred to a pre-chilled Gene Pulser electroporation cuvette (Bio-Rad, Cat# 1652086) and electroporated under the transformation protocol provided by the manufacturer. 1mL of LB broth was quickly added to the bacteria and transferred to a 1.5mL Eppendorf tube. The tube was transferred to a water bath at 37^{o}C for 1h and spread onto an LB agar plate as described above.

2.5 Growth media

LB broth was made by dissolving 10g of LB broth powder (Sigma, Cat# L3022) in 500mL deionized water in a conical glass flask. The dissolved medium was autoclaved under 15psi at 121^{o}C for 30min for sterilization. The LB agar plate was made by dissolving 1 package of EZMix LB agar powder (Sigma, Cat# L7533) in 500mL deionized water in a glass bottle. The dissolved medium was autoclaved similarly and then incubated in a water bath at 55^{o}C until the temperature equilibrated. Appropriate antibiotic was added to the medium, mixed well and 20mL aliquots each dispensed into a 100mm diameter Petri dish. The plates were allowed to dry, solidified at room temperature, and stored at 4^{o}C.

2.6 Agarose gel electrophoresis of DNA

A 0.9% w/v agarose gel was made by first mixing 0.45g ultrapure grade agarose (Invitrogen, Cat# 15510-027) in 50mL 1x TAE buffer. The mixture was boiled in a microwave oven at high power intensity for 2.5min, allowed to cool to around 50^{o}C and 2.5μL ethidium bromide (10mg/mL) added. The mixture was poured into a Mini-Sub Cell GT electrophoresis system (Bio-Rad, Cat# 170-4406) to set for 30min before use. To perform gel electrophoresis of DNA, samples were added with 6x DNA sample buffer and applied to the wells of the agarose gel which was placed inside the electrophoresis tank. Electrophoresis was carried out by passing 100V across the gel.

2.7 Restriction digestion of plasmid DNA

Restriction digestion reactions were set up according to manufacturer's instruction (New England Biolabs). Typically, a restriction digestion reaction (50μL) was set up by first mixing 5μL 10x reaction buffer (corresponding to a particular enzyme), 2μg of plasmid DNA, 5μL restriction enzyme, 0.5μL BSA (10mg/mL) and 37.5μL deionized water in a 1.5mL Eppendorf tube. The reaction mixture was incubated in a water bath at 37^{o}C for 1h. The reaction was stopped by placing the tube in an ice bath.

2.8 Purification of restriction digested plasmid DNA

After performing a restriction digestion, the reaction product was analyzed by agarose gel electrophoresis. The DNA was visualized under UV light and the desired DNA band was cut out with a scalpel. The agarose gel containing DNA under purification was weighed and purified using a QIAquick gel purification kit (Qiagen, Cat# 28706).

2.9 Ligation

Ligation reactions were set up according to manufacturer's instruction (Invitrogen). Typically, a ligation reaction (10μL) was set up by first mixing 2μL 5x ligation reaction buffer, 2μL purified, restriction enzyme-digested vector, 5μL purified, restriction enzyme-digested DNA inserts and 1μL ligase (Invitrogen, Cat# 15224-041) in a thin wall polypropylene tube. The reaction mixture was incubated at 16^{o}C for 12h. The reaction was stopped by placing the tube in a -20^{o}C freezer.

2.10 Site-directed mutagenesis

Site-directed mutagenesis was carried out first by performing PCR with the mutation situated at the primer as described in the QuikChange Site-directed mutagenesis kit (Stratagene). After PCR the reaction product was analyzed by agarose gel electrophoresis. The amplified DNA product was visualized under UV light and cut out with a scalpel. The DNA was purified and digested by DpnI restriction enzyme. The product was purified again and ligation was performed. The ligation product was then transformed into bacteria by heat-

shock or electroporation. Bacterial colonies from transformation were analyzed by extracting plasmid DNA from them and sequencing the DNA.

2.11 List of oligonucleotides

Primer name	Primer sequence
GST-N-S	CCAGAATTCAGATGCTCAACAACCTGACGGACTGC
GST-N-AS	CCACTCGAGTCAGCCCATGAAGGTGCCCATGCG
GST-C-S	CCAGAATTCAGCGGGGGGCAGAGAAGGAGTG
GST-C-AS	CCACTCGAGTCAGTTCAAGTTTTCCCACTCCGGCTTC
His-N-S	CCAGGATCCAGATGCTCAACAACCTGACGGACTGC
His-N-AS	CCACTCGAGTCGCCCATGAAGGTGCCCATGCG
His-C-S	CCAGGATCCGAGCGGGGGGCAGAGAAGGAGTG
His-C-AS	CCACTCGAGTCAGTTCAAGTTTTCCCACTCCGGCTTC
His-112-S	CCAGGATCCGATCCGAGGCCTGTCTCTCAGTGCAGC
His-112-AS	CCACTCGAGTCAGGAGTAGATGGTGATGACCTCTCG
His-C-Δ-S	TCGGAGGGGATCAAGGACTTCTTCAG
His-C-Δ-AS	CTGGATCTCCCGTTCCCGCTCGTTCT
S728A-S	GAGGCTATCCGGCGCCT GATGGAGGC
S728A-AS	CTCTGCCCGCTGAGCCTGAGG
T787A-S	AGGAACTTCATCGAACTCGTCCGGGAAACTAC
T787A-AS	CCAAGCCTGATGATCCTCCTTCTGTCGCCAGTTGC
S940A-S	GAATCTCGGGGCGCTATTCGGAGGAAGAATCCAGC
S940A-AS	ATCTGTGATGCTCTGGATCTCCCGTTCC

S1034A-S	GAAAACTTGAACCAGTCCAACGTGCG
S1034A-AS	CTTCATAGCGAAGAAGTCCTTGATCCCCTCCGAG
Y1087F-S	AACTTCATGGAATTCCTGGAG
Y1087F-AS	TTCATCTCCATTGCGGTTG
Y1087D-S	AACGATATGGAATTCCTGGAG
Y1087D-AS	TTCATCTCCATTGCGGTTG

2.12 DNA constructs

KCC2-FL: mammalian expression construct of KCC2 in pRK5 vector. The KCC2 coding sequence (3351 bp) was obtained from a restriction digestion of 5E14 clone provided by John Payne using XbaI and HindIII. The DNA insert was purified and ligated with pRK5 vector digested with the same enzymes for unidirectional cloning (Fig. 2.1).

GST-N: bacterial expression construct of KCC2 N-tail intracellular domain (aa 1 to aa 102) in pGEX4T-2 vector (Fig. 2.2).

GST-C: bacterial expression construct of KCC2 C-tail intracellular domain (aa 645 to aa 1116) in pGEX4T-2 vector (Fig. 2.2).

His-N: bacterial expression construct of KCC2 N-tail intracellular domain (aa 1 to aa 102) in pTrcHis2C vector (Fig. 2.2).

His-C: bacterial expression construct of KCC2 C-tail intracellular domain (aa 645 to aa 1116) in pTrcHis2C vector (Fig. 2.2).

His-112: bacterial expression construct of KCC2 intracellular domain (aa 932 to aa 1043) in pTrcHis2C vector (Fig. 2.2).

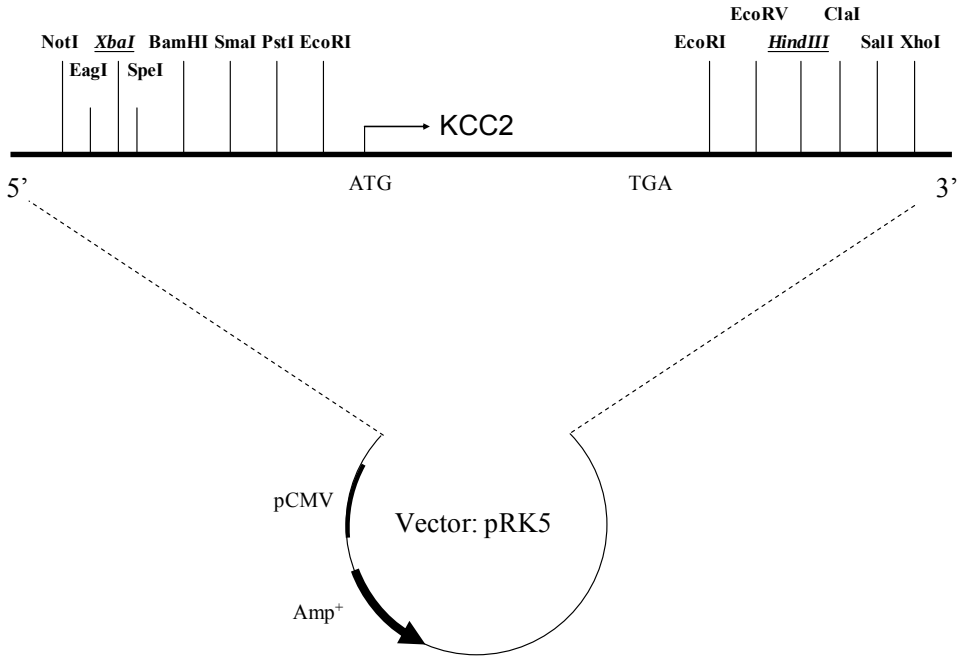

Fig. 2.1 Cloning map of KCC2-FL. Coding DNA sequence of KCC2 (3351 bp) is subcloned into pRK5 vector through XbaI and HindIII restriction sites. Expression of KCC2 is driven under mammalian cytomegalo virus promoter pCMV. pRK5 vector contains an ampicillin-resistant gene (Amp^+) for selection of plasmid after transformation into bacteria.

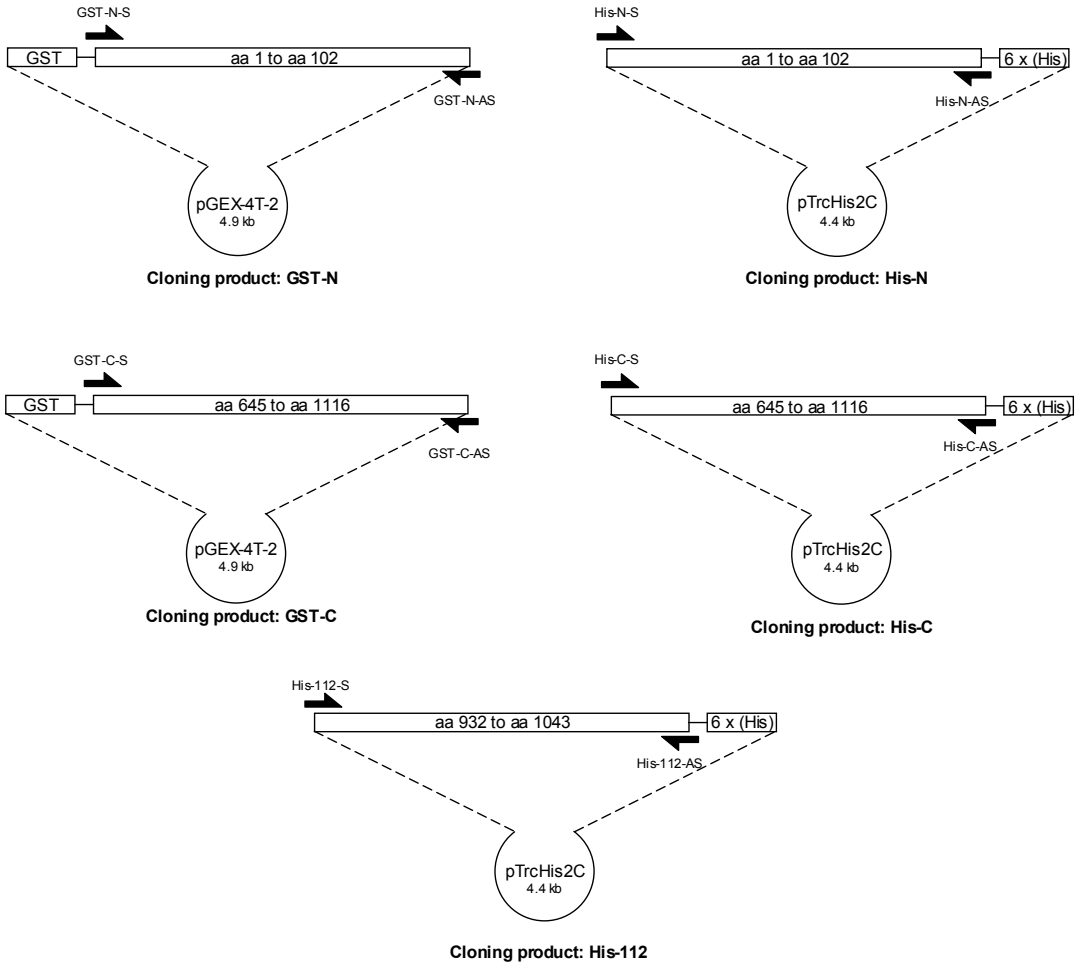

Fig. 2.2 Cloning maps of GST-N, GST-C, His-N, His-C and His-112. Coding DNA sequences of KCC2 were amplified by corresponding primers using PCR and subcloned into pGEX-4T-2 vector to form GST-tagged constructs or pTrcHis2C vector to form His-tagged constructs.

His-C-Δ: bacterial expression construct of KCC2 C-tail intracellular domain with a deletion of aa 932 to aa 1043 in pTrcHis2C vector (Fig. 2.3).

2.13 Small-scale preparation of plasmid DNA from bacteria (mini-prep)

Mini-prep was carried out according to Sambrook and Russell, 2001. Briefly, the bacterial colony on an LB agar plate was picked up using a pipette tip and transferred to 3mL LB broth with appropriate antibiotic in a 15mL polypropylene tube. The culture was grown in a shaker at 200rpm at 37^{o}C for 16h. The bacteria were then spun down in a benchtop centrifuge at top speed. Extraction of plasmid DNA was performed by first resuspending bacteria in a 1.5mL Eppendorf tube in 100μL of solution containing 50mM glucose, 25mM Tris-Cl and 10mM EDTA (pH8) (Solution I). To the resuspension, 200μL of solution containing 0.2N NaOH and 1% w/v sodium dodecyl sulphate (SDS) (Solution II) was added and the mixture was inverted 5 times until it became sticky. Next, 150μL of solution containing 3M potassium acetate and 11.5% glacial acetic acid (Solution III) was added and mixed quickly. The mixture was then placed in an ice bath for 3min and spun down in a benchtop centrifuge at top speed for 5min at 4^{o}C. Supernatant after centrifugation was collected in a new 1.5mL Eppendorf tube and 450μL of phenol/chloroform mixture (1:1 v/v) was added and mixed well. The mixture was separated by centrifuge at top speed for 2min at 4^{o}C, and the upper layer transferred to a new 1.5mL tube. To the solution in the new tube, 900μL of 95% ethanol was added, mixed and allowed to stand for 2min at room temperature. Plasmid DNA was then collected as a pellet by centrifugation at top speed for 5min at

Sense primer (His-C-Δ-S):

TCG GAG GGG ATC AAG GAC TTC TTC AG

Antisense primer (His-C-Δ-AS):

CTG GAT CTC CCG TTC CCG CTC GTT CT

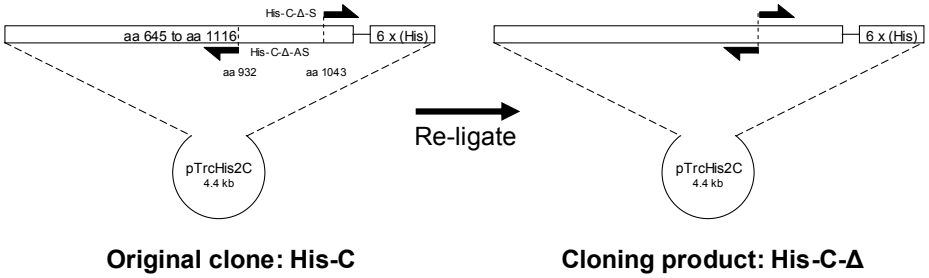

Original clone: His-C **Cloning product: His-C-Δ**

Fig. 2.3 Cloning of His-C-Δ. Polymerase chain reaction was performed on the original template His-C with primers His-C-Δ-S and His-C-Δ-AS. The product was re-ligated to form a plasmid that expresses C-tail of KCC2 with a deletion from aa 932 to aa 1043.

4°C. The DNA pellet was then washed using 1mL of 70% ethanol, dried and resuspended in 50μL deionized water.

2.14 Large-scale preparation of plasmid DNA from bacteria (maxi-prep) by caesium chloride

Maxi-prep was carried out according to Sambrook and Russell, 2001. A 250mL bacterial culture in LB broth in appropriate antibiotic was first grown for 16h. Bacteria were then spun down by centrifuge at 1000x *g* for 15min. After removal of supernatant, bacteria were resuspended in 10mL of Solution I. To the resuspension, 20mL of Solution II was added and the mixture inverted 5 times until it became sticky. The mixture was then put in an ice bath for 5min. After that, 15mL of Solution III was added and mixed quickly. The mixture was then put in an ice bath again for 5min. The debris was removed by centrifugation at 3000x *g* for 20min, while the supernatant was added to an equal volume of isopropanol and mixed well. Centrifugation at 3000x *g* was performed and a DNA pellet was obtained. The pellet was then dissolved in 10mL of deionized water. DNA was precipitated again by adding 1mL of 5M ammonium acetate and 25mL of 95% ethanol. The precipitated DNA was collected by centrifugation at 3000x *g* for 10min. The DNA pellet was then dissolved again by deionized water. Caesium chloride was added to the solution such that caesium chloride concentration was 1g/mL. To this resuspension, 100μL ethidium bromide solution (10mg/mL) was added. The solution was then dispensed into Quick-seal polyallomer tubes (Beckman, Cat# 358980) and subject to ultracentrifugation at 100,000rpm at 22°C for 16h. After

centrifugation, 2 bands of DNA stained with red ethidium bromide were visible as they appeared at the middle of the height of the centrifuge tube. These bands were removed using a needle and syringe puncturing the side of the tube. Typically 2mL of DNA solution stained with ethidium bromide was extracted. To purify, 4mL of water-saturated butanol was mixed with the DNA and the mixture allowed to stand for 5min. Two immiscible layers of liquid were observed and ethidium bromide was removed in the upper butanol layer. This extraction process was repeated 3 times until no red color was observed in the bottom aqueous layer. DNA was then precipitated by adding 8mL of 95% ethanol. Centrifugation at 3000x *g* for 15min was performed and a DNA pellet was obtained. The pellet was then resuspended in 1mL deionized water.

Cell biology

2.15 Cell line culture

A HEK-293 cell line was purchased from American Type Culture Collection (ATCC). Cells were maintained in Dulbecco's Modified Eagle Medium with F12 supplement (DMEM/F12, 1:1) (Gibco, Cat# 11330) with 10% fetal bovine serum (FBS) and penicillin/streptomycin (diluted 100 times from 10000 unit/mL penicillin G sodium and 10000 μg/mL streptomycin sulphate in 0.85% saline, Gibco, Cat# 15140-122) in a 100mm culture dish. Cell cultures were kept in a humidified incubator at 37^{o}C with 5% CO_2 supply. When cultures achieved 70% confluency, cells were removed and passed on to new dishes. Medium was removed by aspiration and cells then washed in 1x phosphate-

buffered saline (PBS). After PBS was removed by aspiration, 1mL of 0.05% trypsin-EDTA solution (Gibco, Cat# 15400-054) was added to the cells and the dish put back into an incubator for 1min. Cells were then removed from the dish by adding 10mL growth medium. The cell suspension was pipetted up and down 20 times to ensure that the cells were efficiently dissociated. 2mL of the suspension was then transferred to a new culture dish with 8mL of new growth medium.

2.16 Transient transfection of HEK-293 cells

Transfection of HEK-293 cells by electroporation was carried out according to Sambrook and Russell, 2001. First, cells were removed from the 100mm dish by washing briefly in 1x PBS and 1mL 0.05% trypsin-EDTA was then added to the dish. The dish was incubated at 37^{o}C for 1min and 10mL growth medium was added to resuspend cells. After dissociation of cells by pipetting up and down, cells were spun down by centrifugation at 1000x *g* for 5min. Medium was then removed and 200µL of Opti-MEM-reduced serum medium (Gibco, Cat# 11058-021) was added to resuspend cells. To 100µL of the resuspended cells, 3µg of plasmid DNA was added and transferred to a Gene Pulser electroporation cuvette (Bio-Rad, Cat #. 1652086). The cells were electroporated using a pre-set program in the Gene Pulser XCell electroporation machine (Bio-Rad), then transferred back to a 60mm culture dish with 5mL of growth medium.

2.17 List of antibodies

Monoclonal mouse anti-KCC2 IgG, clone N1/12 (UC Davis NeuroMab facility, Cat# 75-013)

Polyclonal rabbit anti-KCC2 IgG (Millipore, Cat# 07-432)

Polyclonal rabbit anti-KCC2 phospho-Ser^{940} IgG, p-S940 (PhosphoSolutions, custom-made) (See also section 4.1)

Monoclonal mouse anti-tubulin IgG (Abcam, Cat#ab7291)

Polyclonal donkey HRP-conjugated anti-rabbit IgG (Amersham, Cat# NA934V)

Polyclonal goat HRP-conjugated anti-mouse IgG (Pierce, Cat# 1858413)

Fluorescein-conjugated donkey anti-mouse IgG (Jackson ImmunoResearch, Cat# 715-095-150)

Rhodamine-conjugated donkey anti-rabbit IgG (Jackson ImmunoResearch, Cat# 711-025-152)

2.18 Immunofluorescence staining

Staining of proteins with fluorescent antibody was performed as previously described (Kittler et al., 2000). Cells grown on 12mm glass cover slips were transferred to a 24-well culture plate with 300µL 4% paraformaldehyde/4% sucrose solution for fixation for 15min. Cells were then washed 3 times in 1x PBS and incubated with 5% milk solution in 0.2% triton (blocking solution) for 10min. Primary antibody was added to the cells in the blocking solution for 1h, the cells then washed 5 times in 1x PBS, and secondary antibody added to the cells in the blocking solution for 45min. Finally the cells were washed in 1x PBS and mounted on glass slides.

2.19 Confocal microscopy

A mounted specimen was viewed using a confocal laser-scanning microscope with a 60x oil objective. Green fluorescence protein (GFP) and fluorescein isothiocyanate (FITC) were excited by a laser of wavelength 488nm and signal received by emission filter HQ530/60. Tetramethyl rhodamine isothiocyanate (TRITC) was excited by laser of wavelength 543nm and signal received by emission filter HQ590/70. Acquisition of confocal images was carried out using Laser Sharp 2000 software from Bio-Rad. To ensure no spectral bleed through, laser scans for green and red fluorescence signal were sequentially collected. Under such conditions the green fluorescence signal during red laser illumination (and vice versa) was negligible. Pseudo color (green for GFP and FITC, red for TRITC) was assigned automatically by the software after each laser scan was acquired.

Biochemistry

2.20 Sodium dodecyl sulphate polyacrylamide gel electrophoresis (SDS-PAGE)

Acrylamide gel was set according to Sambrook and Russell, 2001 by first mixing 1.5M Tris-Cl (pH8.8), 30% acrylamide/bis solution, 29:1 (Bio-Rad, Cat# 161-0156), 10% ammonium persulphate (APS), 10% SDS, N, N, N', N'-tetramethylethylenediamine (TEMED) and deionized water and poured into the

Mini PROTEAN 3 system gel casting stand (Bio-Rad) according to manufacturer's instructions. 70% ethanol was added slowly on top of the gel layer to form a horizontal straight boundary for the gel. This served as the resolving gel. After 30min, the ethanol was washed in deionized water, dried and a second layer of acrylamide gel (stacking gel) made by mixing 1.0M Tris-Cl (pH6.8), 30% acrylamide/bis solution, 29:1, 10% APS, 10% SDS, TEMED and deionized water. The stacking gel was laid on top of the resolving gel and a plastic comb placed on top to form wells in the stacking gel for holding protein samples. After 30min, the gel was set and assembled into the Mini PROTEAN 3 system gel running tank (Bio-Rad) according to manufacturer's instructions. Gel running buffer was added to the tank and protein samples were loaded into the wells of the gel. Protein samples were separated by electrophoresis under 160V for 1h.

2.21 Electrotransfer of SDS-PAGE gels

Electrotransfer of SDS-PAGE gels was set up according to manufacturer's instructions (Bio-Rad). Acrylamide gel was taken out from the gel tank after electrophoresis. It was then transferred to a Mini Trans-Blot cell unit (Bio-Rad) in a sandwich of filter paper and sponge fiber pads on both sides. A nitrocellulose membrane was also placed directly next to the gel. The cassette was set according to manufacturer instructions and electrophoresis was carried out in a constant current at 50mA for 16h.

2.22 Western blotting

Western blotting was carried out essentially as described in McDonald et al., 1998. After electrotransfer, the nitrocellulose membrane was removed from the tank. It was washed briefly with 0.1% (w/v) ponceau S in 5% acetic acid. The ponceau S solution was washed with deionized water and the positions of the molecular markers marked using a pencil. The membrane was then washed briefly with 1x Tris-buffered saline with 0.1% Tween (TBS-T) and incubated in 5% milk in TBS-T for 1h for blocking. Primary antibody was added with proper dilution to 5% milk in TBS-T for 2h and the membrane then washed 3 times for 10min each wash with TBS-T. Secondary antibody was then added in 5% milk in TBS-T to incubate the membrane for 1h. Again, the membrane was washed 3 times for 10min with TBS-T. Finally, the membrane was dried briefly and 1mL of VisiGlo HRP Plus chemiluminescent substrate (Amresco, Cat# N219) was applied to the membrane for 1min for developing chemiluminescence. Excess fluid was dripped off from the membrane and the membrane visualized using a FujiFilm LAS-3000 chemiluminescence detection unit.

2.23 Fusion protein purification

Purification of GST-fusion protein was described previously (Moss et al., 1992). First, 20mL of bacterial culture was grown for 16h then transferred to 1L LB broth with appropriate antibiotic. The culture was allowed to grow at 37^{o}C with constant shaking at 200rpm. When the OD_{600} of the culture achieved 0.5, 47.6mg isopropyl β-D-1-thiogalactopyranoside (IPTG) (Sigma, Cat# I6758)

was added directly to the culture (0.2mM IPTG induction) to allow induction of protein expression. The culture was allowed to grow at 37^{o}C while shaken for 3h. To harvest the bacteria, the culture was transferred to a 1L bottle and centrifuged at 1000x *g* for 20min at 4^{o}C. The supernatant was removed and the bacterial pellet resuspended in 10mL of buffer (Buffer A) containing 50mM Tris-Cl (pH8.0), 25% sucrose and 10mM EDTA. The bacteria were then spun down by centrifugation at 1000x *g* for 15min and resuspended in 10mL of lysis buffer (Buffer B) containing 1% Triton X-100, 1mM EDTA, 10mM Tris-Cl (pH7.4) and protease inhibitors. The lysate was stored at -20^{o}C for 16h. The next day, bacterial lysate was thawed and sonication was applied to the lysate to assist the breakdown of the bacterial cell wall. To the lysate, 25mL of a solution (Buffer C) containing 20mM HEPES (pH7.6), 100mM KCl, 0.2mM EDTA, 20% glycerol and protease inhibitors was added. The lysate was then spun at 75000x *g* for 30min at 4^{o}C to get rid of insoluble materials. 80mg of glutathione-agarose beads (Sigma, G4510) were soaked in Buffer C for 10min at 4^{o}C and washed 3 times with Buffer C. The beads were incubated for 2h with the supernatant after centrifugation on a rotating wheel at 4^{o}C then spun down by centrifugation at 1000x *g* and washed twice with Buffer C. Finally, the beads were incubated with 2mL of 70mM glutathione (pH7.4) in PBS to elute the fusion protein. The fusion protein was dialyzed with a solution containing 20mM Tris-Cl (pH7.4) and 2mM EDTA for 16h.

His-tag fusion protein was purified from 50mL bacterial culture as described in the ProBond purification system manual (Invitrogen, Cat# K850-01). Briefly, a bacterial culture (2mL) grown for 16h was transferred to 50mL LB broth. The

culture was kept at 37°C for around 2h while being shaken until its OD_{600} achieved 0.5. 0.2mM IPTG was added to the culture and fusion protein induced at 37°C for 3h in shaker. Bacteria were then collected by centrifugation at 1000x *g* for 5min. To the bacterial pellet, 8mL of guanidium lysis buffer containing 6M guanidine HCl, 20mM $NaPO_4$ (pH7.8) and 500mM NaCl was added. The lysate was placed on a rotating wheel for 5min at room temperature and sonication was performed to assure thorough cell lysis. The cellular debris was then removed by centrifugation at 3000x *g* for 15min. To 8mL of lysate, 2mL of ProBond resin in 1:1 slurry (Invitrogen, Cat# 46-0019), which was washed by water and resuspended in denaturing binding buffer, was added. The resin was allowed to bind to fusion proteins in the lysate for 30min at room temperature on a rotating wheel. After that, the resin was collected by centrifugation at 1000x *g* and washed 2 times by 4mL denaturing binding buffer (pH6.0). The resin was then washed twice by 4mL denaturing wash buffer (pH5.3). The fusion protein was eluted from the resin by 5mL denaturing elution buffer. Finally, fusion protein was dialyzed by 1L of solution containing 10mM Tris-Cl (pH8.0), 0.1% Triton X-100 at 4°C for 16h to remove urea.

2.24 *In vitro* kinase assay

In vitro kinase assay was performed according to procedure described in Moss et al., 1992. Purified fusion protein was incubated with buffer containing 20mM 4-(2-hydroxyethyl)-1-piperazineethanesulfonic acid (HEPES) (pH7.5), 10mM $MgCl_2$, 50nM phorbol 12, 13-dibutyrate (PDBu), 0.2mM adenosine

triphosphate (ATP), 10μCi of [γ-^{32}P]ATP and 5μL of purified protein kinase C (PKC, 10ng/μL) (Millipore, Cat# 14-115) in a 50μL reaction. The reaction mixture was incubated in a water bath at 30^{o}C for 30min and the reaction terminated by adding 50μL of 2x SDS-PAGE sample buffer. Phosphorylation signal of protein (represented by ^{32}P β-radiation) was captured using a phospho-imager screen (Bio-Rad, Cat# 1707843) and visualized using a molecular imager FX machine (Bio-Rad).

The stoichiometry of phospho-proteins was calculated by the following equations:

X=specific count reading from scintillation counter by 1μL of [γ-^{32}P]ATP (CPM)

Y=amount of ATP in 1μL of [γ-^{32}P]ATP (mole)

Therefore, count/mole of ATP (CPM/mole)=X/Y

Z=specific count reading from scintillation counter by phosphorylated protein

Therefore, amount of phospho-proteins (mole)=Z/(X/Y)

2.25 Phospho-peptide mapping and phospho-amino acid analysis

Procedures of phospho-peptide mapping and phospho-amino acid analysis were modified from Moss et al., 1992. After SDS-PAGE and phospho-imager analysis, protein labeled with radioactive isotope was excised from the acrylamide gel with a scalpel. The gel was washed 3 times for 30min each wash using destaining buffer. It was then washed twice for 30min each wash using 50% (v/v) methanol. The gel was dried briefly with filter paper and

incubated with 1mL of trypsin (1mg/mL) in 50mM NH_4HCO_3 at 37^{o}C for 16h. The next day, the supernatant was collected and 0.5mL of trypsin solution was added at 37^{o}C for 2h to extract the residual phospho-protein from the gel. The trypsin solution was combined and lyophilized under centrifugation in a vacuum. The lyophilized product was dissolved in 10μL of deionized water. This trypsinized protein was applied to a thin layer chromatography (TLC) plate (Selecto Scientific, Cat# 10028) together with 1μL each of phenol red (10mg/mL) and basic fuchsin (10mg/mL). The TLC plate was pre-wet with TLC electrophoresis buffer and then subjected to electrophoresis under 500V for 2.5h. After electrophoresis the TLC plate was dried, and a liquid chromatography was performed in a vertical manner. Finally the TLC plate was dried and phospho-peptide was detected using a phospho-imager.

Phospho-amino acid analysis was carried out using 6N HCl to hydrolyzed tryptic peptides for 1h after they were recovered from the gel as described above. The hydrolyzed product was then lyophilized and dissolved in 10μL of deionized water similarly. When the sample was applied to the TLC plate, phospho-amino acid standards (phospho-serine, -threonine and -tyrosine, 10mg/mL) and phenol red (10mg/mL) were also applied and separated by electrophoresis at 500V for 1.5h. After electrophoresis the plate was dried, amino acid was stained briefly using 1% (w/v) ninhydrin solution at 60^{o}C and the TLC plate was quickly dried again. The composition of phospho-amino acid was then analyzed using a phosphor-imager.

2.26 *In vitro* phosphatase assay

In vitro phosphatase assay was performed according to Terunuma et al., 2004. Purified fusion protein was first phosphorylated using an *in vitro* kinase assay with ATP in the presence of Ni^{2+} resin (for His-tag fusion proteins) or glutathione-coated agarose beads (for GST-fusion proteins). The labeled protein was then briefly spun down using centrifugation, washed with buffer containing 50mM Tris-Cl (pH7.6) and 3µL of purified phosphatase was added to the reaction mixture and incubated at 30°C for 15min. The fusion protein was briefly spun down using centrifugation, the reaction stopped by adding 20µL of sample buffer and the fusion protein then analyzed using SDS-PAGE.

2.27 Whole-cell metabolic labeling

Whole-cell metabolic labeling experiments were carried essentially as described previously (Moss et al., 1992). Cells were washed twice with pre-warmed phosphate-free DMEM (Invitrogen, Cat# 11971) and incubated at 37°C in phosphate-free medium for 30min. 1mCi of ^{32}P in orthophosphoric acid ($H_3{}^{32}PO_4$) (PerkinElmer, Cat# NEX053 P062304W) was then added to the medium and the cells incubated at 37°C for 4h.

2.28 Biotinylation assay

Biotinylation was carried out as described previously (Fairfax et al., 2004). Cells were first washed twice with 1xPBS with 50mM $MgCl_2$ and 100mM $CaCl_2$ (PBS-CM). The cells were then incubated with 2mL of PBS-CM

containing 2mg of EZ-link Sulfo-NHS-SS-biotin (Pierce, Cat# 21331B) for 30min. After that, cells were washed 3 times with PBS-CM containing glycine and bovine serum albumin (BSA) (quench buffer). Lastly, cells were washed with 1xPBS and lysed with lysis buffer. The cell lysate was spun in a benchtop centrifuge at top speed for 10min to get rid of insoluble materials. To the supernatant, 40μL of 1:1 slurry of UltraLink immobilized Neutravidin beads (Pierce, Cat# 53150) in lysis buffer was added. The mixture was incubated at 4^{o}C on a rotating wheel for 2h. The beads were spun down using centrifugation at 1000x *g* for 2min, washed twice with lysis buffer with 0.5M NaCl and once with lysis buffer alone. Lysis buffer was removed after centrifugation and 20μL of sample buffer was added to the beads. The sample was then analyzed using SDS-PAGE.

2.29 Endocytosis assay

Hippocampal neurons were labeled with 1mg/mL EZ-link Sulfo-NHS-SS-Biotin as described above, washed with quench buffer and returned to 37^{o}C incubator for endocytosis to occur for different durations up to 20min in the presence of culture medium containing 1μM leupeptin. Cells were then quickly cooled on ice and cell surface biotin was cleaved with cleavage buffer (quench buffer containing 50mM glutathione) for 15min on ice. The internalized biotin-labeled proteins were pulled down with UltraLink immobilized Neutravidin beads and analyzed by SDS-PAGE followed by immunoblotting as described above.

2.30 Protein assay

Protein assay was performed according to manufacturer's instruction (Bio-Rad). The protein sample was diluted 20 times with deionized water. To 100μL of diluted sample, 100μL of BCA solution (a combination of 2.5mL buffer A, 2.4mL buffer B and 0.1mL buffer C from a Micro BCA protein assay kit from Pierce, Cat# 23235) was added. A protein standard curve was made by diluting 2mg/mL BSA solution in a series dilution from 100μg/mL to 10μg/mL. 100μL of BCA solution was added to 100μL of each of the BSA protein standards. The standard curve and protein sample were incubated at 60^{o}C in a 96-well plate for 1h for colorimetric development. After that, OD_{570} of each sample was measured using a microplate reader 680 (Bio-Rad). The protein concentration of each sample was calculated from the protein standard curve.

2.31 Immunoprecipitation

Immunoprecipitation of proteins was performed as described previously (Kittler et al., 2000). Cells were lyzed in 1mL lysis buffer, collected in a 1.5mL polypropylene tube and spun in a benchtop centrifuge at top speed at 4^{o}C for 10min. To the supernatant, 40μL of 1:1 slurry of protein A sepharose CL-4B beads (Amersham, Cat# 17-0780-01) in 1xPBS was added and the mixture was incubated at 4^{o}C on a rotating wheel for 2h. The beads were spun down at 1000x g for 2min and washed twice with lysis buffer containing 0.5M NaCl and once with lysis buffer alone. Lysis buffer was removed after centrifugation

and 20μL of sample buffer was added to the beads. The sample was then analyzed using SDS-PAGE.

2.32 $^{86}Rb^{+}$ influx assay

HEK-293 cells were transfected with KCC2-FL WT or a series of mutants including S728A, T787A, S940A, S1034A and double mutants S940/1034A and S728/940A. One day after transfection cells were treated with 2μM bumetanide and 100μM ouabain to inhibit Na^{+}-K^{+}-$2Cl^{-}$ co-transporter and Na^{+}-K^{+}-ATPase respectively. $^{86}Rb^{+}$ accumulation was allowed to proceed over a 3-5min time course. Cells were then washed extensively with PBS to remove extracellular $^{86}Rb^{+}$ and cells lyzed to measure radioactivity using a scintillation counter. Experiments were repeated with 100μM furosemide to inhibit KCC2 activity and the difference between samples with or without furosemide treatment was recorded as furosemide-sensitive $^{86}Rb^{+}$ influx, an indicator of KCC2 activity. As a negative control vector-transfected cells showed no $^{86}Rb^{+}$ accumulation. This experiment was performed by Jeff Williams in collaboration with the laboratory of Dr. John Payne at UC Davis.

2.33 Hydrophobicity plot

The amino acid sequence was analyzed by the software provided on the website http://www.vivo.colostate.edu/molkit/hydropathy/index.html using Kyte-Doolittle scale and window size of 20.

2.34 Statistics

Standard error of the mean (SEM) was calculated using Excel from quantified data. Student's t-test was then performed using GraphPad Software for statistical significance.

2.35 List of buffers, drugs and chemicals

The recipes of commonly used buffers, and the solvent and concentration of drugs and chemicals described in this thesis are:

GYT medium

10% (v/v) Glycerol

0.125% (w/v) Yeast extracts

0.25% (w/v) Tryptone

TAE

40mM Tris-acetate

1mM EDTA (pH8.0)

DNA sample buffer (6x)

30% (v/v) Glycerol

0.25% (w/v) Xylene cyanol

Buffers for plasmid extraction from bacteria:

1) Solution I

50mM Glucose

25mM Tris-Cl (pH8.0)

10mM EDTA (pH8.0)

2) Solution II

0.2N NaOH

1% (w/v) SDS

3) Solution III

5M Potassium acetate

11.5% (v/v) Acetic acid

Buffers for GST-fusion protein purification:

1) Buffer A

50mM Tris-Cl (pH8.0)

25% Sucrose

10mM EDTA

2) Buffer B

10mM Tris-Cl (pH7.4)

1mM EDTA

1% Triton X-100

1mM DTT

3) Buffer C

20mM HEPES-NaOH (pH7.6)

100mM KCl

0.2mM EDTA

20% Glycerol

Buffers for His-tagged fusion protein purification in denaturing condition:

Guanidinium lysis buffer

6M Guanidine HCl

20mM NaPO4, pH7.8

500mM NaCl

Denaturing binding buffer

8M Urea

20mM $NaPO_4$, pH7.8

500mM NaCl

Denaturing wash buffer

8M Urea

20mM $NaPO_4$, pH6.0

500mM NaCl

Denaturing elution buffer

8M Urea

20mM $NaPO_4$, pH4.0

500mM NaCl

Cell lysis buffer (2x)

20mM $NaPO_4$, pH7.4

10mM EDTA

10mM EGTA

200mM NaCl

20mM Sodium pyrophosphate

50mM NaF

4% Triton X-100

1% Deoxycholate

2mM Sodium orthovanadate

Coomassie blue staining solution

30% (v/v) Methanol

10% (v/v) Acetic acid

0.25% (w/v) Brilliant blue G

Destaining solution

30% (v/v) Methanol

10% (v/v) Acetic acid

SDS-PAGE running buffer

25mM Tris

250mM Glycine

0.1% (w/v) SDS

SDS-PAGE transfer buffer

48mM Tris

39mM Glycine

0.0375% SDS

Phosphate-buffered saline

137mM NaCl

2.7mM KCl

10mM Na_2HPO_4

2mM KH_2PO_4

Tris-buffered saline

8g of NaCl, 0.2g of KCl and 3g of Tris base were dissolved in 800mL deionized H_2O. The pH value of the solution was adjusted to 7.4 by slowly adding HCl and then more H_2O was added to make the solution up to 1L.

SDS-PAGE sample buffer (2x)

100mM Tris-Cl (pH6.8)

4% (w/v) SDS

0.2% Bromophenol blue

20% Glycerol

Freshly add 100mM β-mercaptoethanol into 1x buffer before use

TLC electrophoresis buffer

17.4% (v/v) Acetic acid

0.92% (v/v) Pyridine

TLC chromatography buffer

7.5% (v/v) Acetic acid

37.5% (v/v) Pyridine

25% (v/v) 1-Butanol

PBS-CM

PBS with 1mM $CaCl_2$ and 0.5mM $MgCl_2$

Quench buffer for biotinylation

PBS-CM with 50mM glycine and 0.1% (w/v) BSA

Phorbol 12,13-dibutyrate (PDBu) (Calbiochem, Cat# 524390)

0.5mM stock was dissolved in DMSO, stored at -20^{o}C and used in 500nM

GF109203X (GFX) (Tocris, Cat# 0741)

10mM stock was dissolved in DMSO, stored at -20^{o}C and used in 10μM

Calphostin C (CalC) (Calbiochem, Cat# 208725)

100μM stock was dissolved in DMSO, stored at -20^{o}C and used in 100nM

Cyclosporin A (CsA) (Calbiochem, Cat# 239835)

20mM stock was dissolved in DMSO, stored at -20^{o}C and used in 20μM

Okadaic acid (OA) (Calbiochem, Cat# 459620)

100μM stock was dissolved in DMSO, stored at -20^{o}C and used in 100nM

Sodium pervanadate (Na_3VO_4), peroxide of sodium orthovanadate (Sigma, Cat# S6508)

30mM sodium orthovanadate activated by 0.18% H_2O_2 for 15min at room temperature in the dark, freshly made and used in 100μM

PP2, a specific Src family kinase inhibitor (Calbiochem, Cat# 529573)

10mM stock was dissolved in DMSO, stored at -20^{o}C and used in 10μM

PP3, a specific EGFR kinase inhibitor (Calbiochem, Cat# 529574)

10mM stock was dissolved in DMSO, stored at -20^{o}C and used in 10μM

Chapter 3 Direct phosphorylation of KCC2 by PKC and tyrosine kinase

Introduction

It has been previously established that KCC2 activity is regulated by activators of protein kinase C (PKC), WNK family kinase 3 (WNK3), brain type creatine kinase (CKB), as well as inhibitors of serine/threonine protein phosphatases PP1 and PP2A (Kelsch et al., 2001; Song et al., 2002; Rivera et al., 2004; Kahle et al., 2005; Bergeron et al., 2006; Inoue et al., 2006), suggesting that phosphorylation of this protein may be the molecular mechanism underlying these observations. However, currently there is no evidence that KCC2 is in fact a phospho-protein (Bergeron et al., 2006). From a perspective of consensus sequence comparison (Payne et al., 1996), it has been shown that there are several putative PKC phosphorylation sites $(R/K)(X)_{1-4}(S/T)(X)_{1-3}(R/K)$(where X is any amino acid)(Kennelly and Krebs, 1991) and a protein tyrosine kinase (PTK) phosphorylation site YXXØ (where X is any amino acid and Ø is a hydrophobic residue)(Ding et al., 2003) within the intracellular domains of the KCC2 sequence. Among these sites, Ser^{728}, Thr^{787} and Ser^{1034} co-exist in other KCC members while Thr^{34} and Ser^{940} are unique to KCC2. On the other hand, the putative PTK phosphorylation site Tyr^{1087} also exists in other KCC isoforms (Strange et al., 2000) (Fig. 3.1). A list of the putative phosphorylation sites on KCC2 sequence can be found in Figure 3.1.

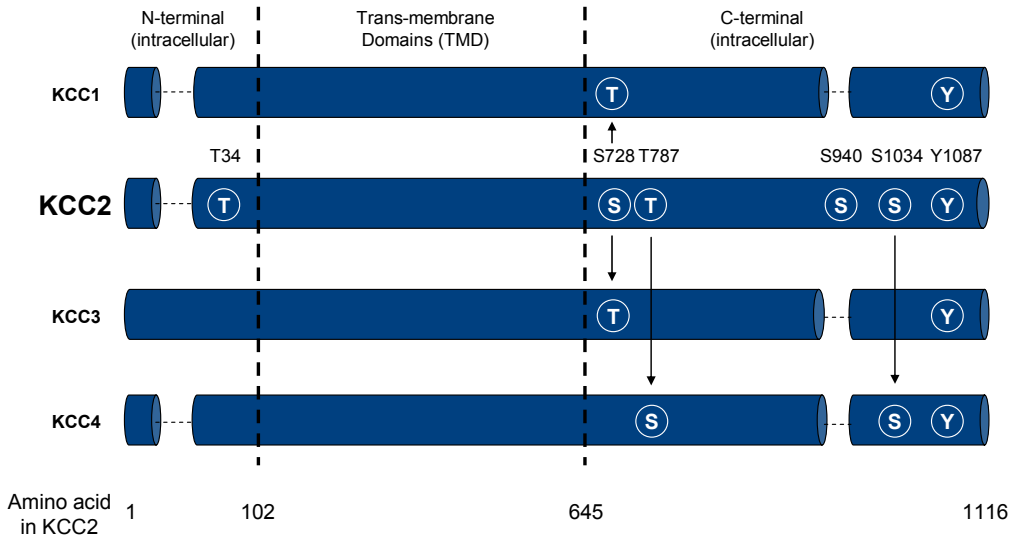

Fig. 3.1 Sequence comparison of KCC members and the locations of possible phosphorylation sites on KCC2. Putative PKC phosphorylation sites are labeled as S for serine and T for threonine. Putative PTK phosphorylation sites are labeled as Y for tyrosine. The positions of these sites in the KCC2 sequence are denoted by numbers. Phosphorylation sites co-existing in other KCC members are indicated by arrows.

Protein kinases are enzymes responsible for phosphorylation reactions that transfer phosphate groups from adenosine triphosphate (ATP) to amino acid residues in proteins such as serine, threonine or tyrosine. PKC belongs to a serine/threonine-specific kinase that plays a major role in various cellular mechanisms including cell proliferation, differentiation, protein degradation and intracellular trafficking (Connolly et al., 1999; Brandon et al., 2000; Nakashima, 2002). In mammalian neurons, expression of PKC is abundant and its activity is under tight regulation (Pascale et al., 2007). PKC can be classified as conventional (classical), unconventional (novel) or atypical (Becker and Hannun, 2005). Different classes of PKC have different requirements for activation. Conventional PKC is activated by calcium ions, diacylglycerol (DAG) and phospholipids. Unconventional PKC is activated by DAG but calcium is not required. Atypical PKC requires neither calcium nor DAG for activation. PTKs are another big class of kinases that catalyze the addition of phosphate into a tyrosine moiety. They consists of two types of enzymes: receptor tyrosine kinases (RTKs) and non-receptor protein tyrosine kinases (Hubbard and Till, 2000). RTKs typically consist of an extracellular ligand binding domain, transmembrane domain and intracellular catalytic domain which carries out a kinase reaction (Ottensmeyer et al., 2000). Upon ligand binding, dimerization of receptors occurs which leads to autophosphorylation of receptors. This conformational change then increases the accessibility of substrate and ATP to the catalytic domain such that phosphorylation is carried out. Among the non-receptor protein tyrosine kinases, v-Src is one of the first identified (Collett and Erikson, 1978). It was later classified as a member of Src family tyrosine kinases which consists of

Src, Fyn, Fgr, Lyn, Hck, Blk, Lck, Yes and Yrk. Tyrosine kinases are involved in many signal transduction pathways and are important for cellular differentiation, cell death and neurite outgrowth (Rogers et al., 1994; Wu et al., 1999).

The role of phosphorylation in regulating inhibitory transmission in the central nervous system is well documented (Moss and Smart, 1996; Belelli et al., 2006). The $GABA_A$ receptor is the main site for generating inhibitory current and has been shown to be phosphorylated by PKC and Src among many kinases (Boxall, 2000; Brandon et al., 2000; Brandon et al., 2001; Song and Messing, 2005). Since KCC2 controls the Cl^- gradient across the neuronal membrane and is critical in dictating the GABAergic response in mature neurons (Rivera et al., 1999), the roles that PKC and Src are playing in the regulation of KCC2 is of crucial importance in the research on KCC2 currently.

The use of recombinant protein systems in investigating phosphorylation of membrane proteins is popular (Krishek et al., 1994; Raymond et al., 1994; Song and Kaczmarek, 2006); for example, fusion proteins have been used extensively to investigate the phosphorylation of $GABA_A$ receptor subunits and to identify their phosphorylation sites (Moss et al., 1992; McDonald et al., 1998; Brandon et al., 2000; Houston et al., 2007). To initiate the study of KCC2 phosphorylation, fusion proteins of KCC2 intracellular domains were used coupled with an *in vitro* kinase assay. Specific sites for phosphorylation were also identified. To confirm the *in vitro* studies recombinant KCC2 proteins were expressed in HEK-293 cells.

In this chapter, the role of PKC and PTK in the phosphorylation of KCC2 was determined. This serves as the background for the study of phospho-dependent modulation of KCC2 since the identity of kinases and the kinetics of phosphorylation remain unknown. The specific aims of this chapter are:

1) To show that PKC phosphorylates KCC2 directly *in vitro.*
2) To identify the residues of KCC2 responsible for phosphorylation by PKC.
3) To show that KCC2 expressed in HEK-293 cells and endogenous KCC2 in cultured hippocampal neurons is phosphorylated by PKC.
4) To show that KCC2 is phosphorylated by Src.

Results

3.1 Expression of GST-tag and His-tag fusion proteins encoding the N-tail and C-tail of KCC2

The coding sequences of N-tail (residues 1-102) and C-tail (residues 645-1116) of KCC2 were amplified and subcloned into pGEX4T-2 (McDonald and Moss, 1994) to generate GST-tagged fusion protein in bacteria (Fig. 3.2). After induction with IPTG, bacterial lysates were resolved by SDS-PAGE and the gel stained with Coomassie blue to confirm the expression of fusion proteins. However, the attempt to purify GST-tagged fusion protein of C-tail of KCC2 was unsuccessful, mainly because the protein was expressed in the insoluble

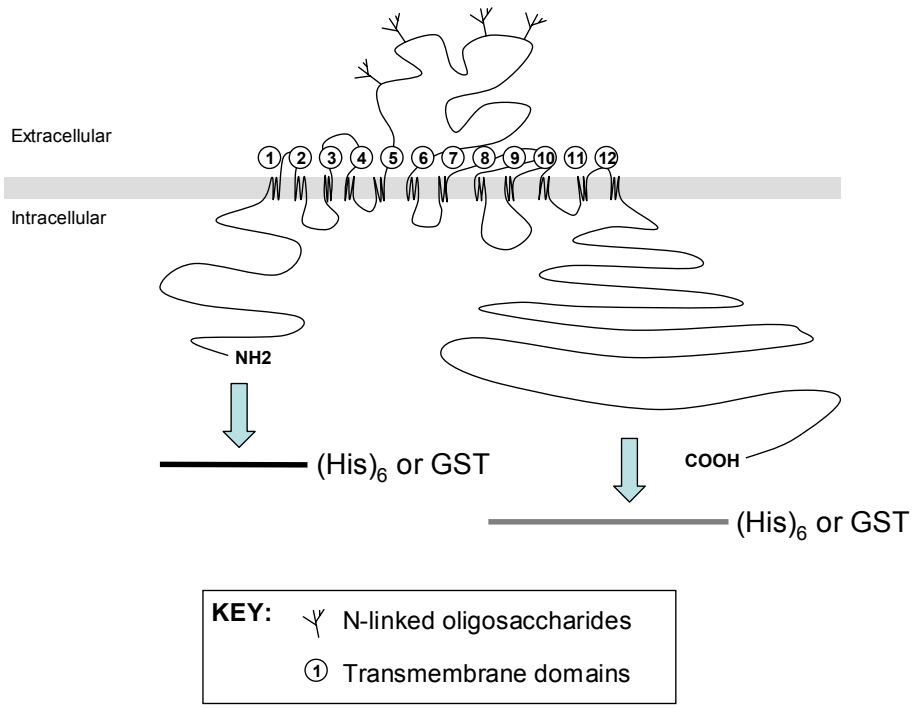

Fig. 3.2 Schematic diagram showing the molecular organization of KCC2 and cloning of fusion proteins. KCC2 is bound by intracellular N- and C-tails which span more than half of its molecular size. In between the intracellular domains there are 12 transmembrane domains, denoted by the 12 circled numbers. A relatively prominent extracellular domain is present between transmembrane domains 5 and 6, in which sites for N-linked glycosylation were found. Both intracellular N-tail (residues 1-102) and C-tail (residues 645-1116) of KCC2 were subcloned into vectors expressing fusion proteins (His-tag or GST-tag) in bacteria.

fraction (Fig. 3.3). On the other hand, GST-tagged fusion protein of N-tail of KCC2 (GST-N) was shown to be around 36kDa. Approximately 2mg of high purity of the fusion protein was obtained from 1L of bacterial culture after purification (Fig. 3.4). A hydrophobicity plot revealed that some regions within the C-tail of KCC2 are moderately hydrophobic (>1 in Kyte-Doolittle scale, Fig. 3.5), possibly contributing to the insolubility of this GST-tagged fusion protein of C-tail. To tackle this problem, the fusion proteins were purified under denaturing conditions; thus a His-tag fusion protein system was employed. The coding sequences of both N- and C-tails of KCC2 gene were subsequently subcloned into pTrcHis-2C (Invitrogen) to express a C-terminal 6xHis tagged fusion protein. Under denaturing conditions using 8M urea and 6M guanidine, His-tagged fusion proteins of N- and C-tails of KCC2 (His-N and His-C respectively) were purified. SDS-PAGE followed by Coomassie staining of the gel confirmed the expression and purity of both fusion proteins (Fig. 3.4). The molecular weight of His-N and His-C were found to be 13kDa and 47kDa respectively. Approximately 0.2mg and 0.4mg respectively of the fusion proteins were obtained from 100mL bacterial culture.

3.2 *In vitro* phosphorylation of His-C by PKC

To determine whether N- and C-tails of KCC2 can be phosphorylated, purified fusion proteins were subject to *in vitro* kinase assay using purified kinase and [γ-^{32}P]ATP as previously described (Moss et al., 1992). Both cAMP-dependent protein kinase (PKA) and Ca^{2+}/phospholipid-dependent protein kinase (PKC)

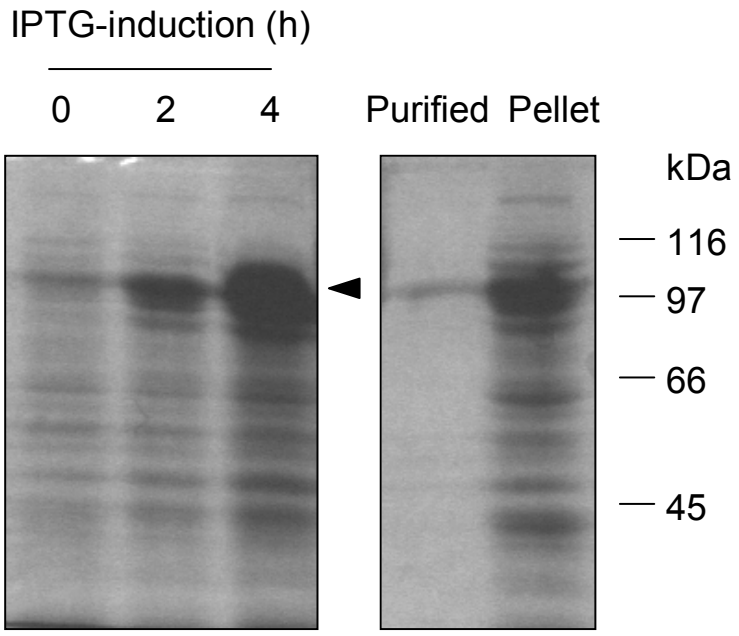

Fig. 3.3 Expression of GST-tagged C-tail fusion protein of KCC2 in E. Coli. Bacteria transformed with construct expressing GST-tagged C-tail of KCC2 were grown and fusion protein induced by 0.2mM IPTG for up to 4h. Bacterial lysates from 0, 2 and 4h after induction were resolved by SDS-PAGE and stained by Coomassie blue. Arrow indicates the expression of fusion protein at 97kDa. Purified fraction and insoluble pellet fraction during purification were resolved by SDS-PAGE and stained with Coomassie blue.

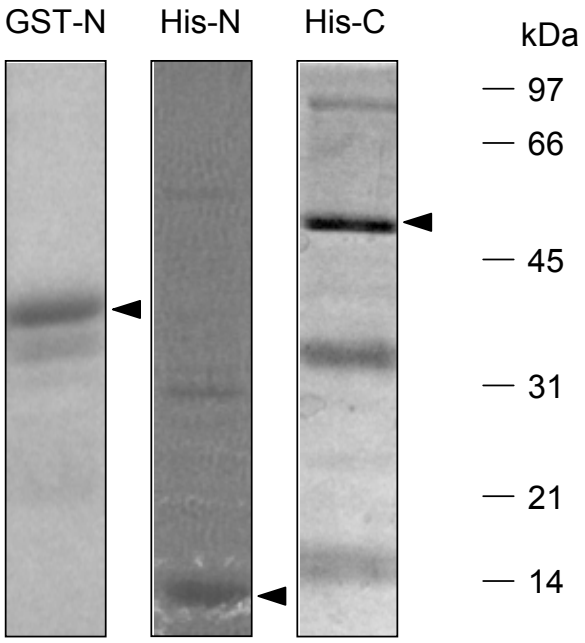

Fig. 3.4 Expression of GST-tag and His-tag fusion proteins of KCC2 in E. Coli. Purified GST-tagged N-tail (GST-N), His-tagged N-tail (His-N) and His-tagged C-tail (His-C) of KCC2 were resolved by SDS-PAGE and stained with Coomassie blue. The molecular weight of the fusion proteins are 36kDa, 13kDa and 47kDa respectively, as indicated by arrows.

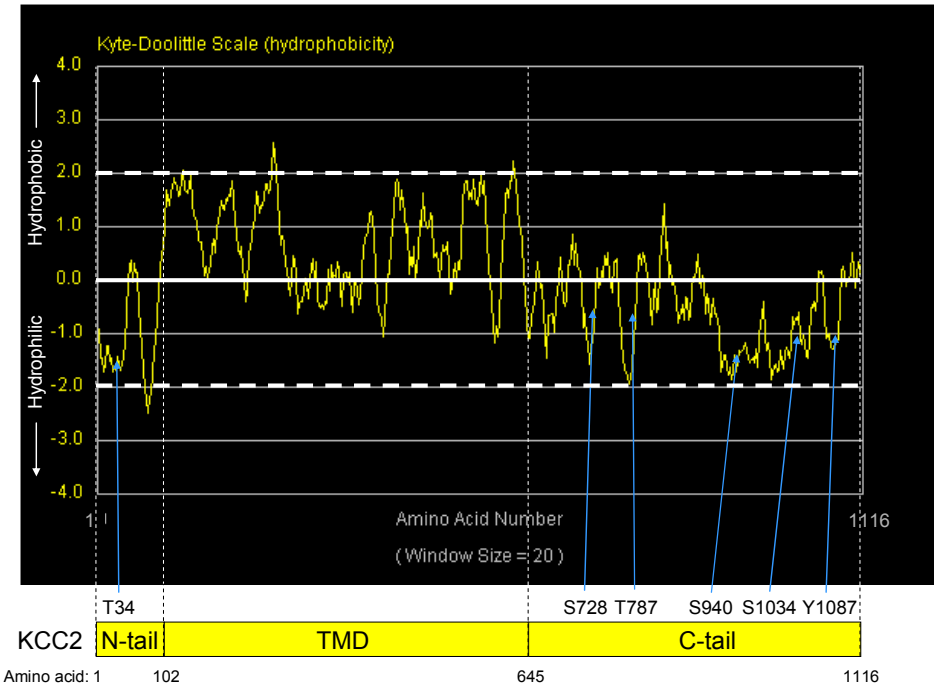

Fig. 3.5 Hydrophobicity plot of KCC2. The amino acid sequence of KCC2 was analyzed using the Kyte-Doolittle scale with a window size of 20 amino acids. Regions with a value above 0 are hydrophobic and those below 0 are hydrophilic. The N-tail, transmembrane domains (TMD) and C-tail of KCC2 are shown correspondingly as a diagram below the hydrophobicity plot. Putative PKC and PTK phosphorylation sites are indicated by arrows.

were tested. The reaction was stopped at 30min and analyzed by SDS-PAGE followed by autoradiography. It was found that GST-N cannot be phosphorylated by PKA or PKC (GST-N was minimally phosphorylated to a level similar to that of GST control); while the intracellular domain of R2-subunit of $GABA_B$ receptor and β3-subunit of $GABA_A$ receptor were highly phosphorylated under the same condition (Fig. 3.6). However, His-C was found to be phosphorylated by PKC but not PKA (Fig. 3.7). To study the kinetics of phosphorylation of His-C by PKC, reaction products from reactions of different durations were subject to scintillation count of ^{32}P. The fraction of phosphorylated fusion protein was calculated using equations from section 2.24. It was found that phosphorylation of His-C by PKC followed in a time-dependent manner. The reaction reached a plateau at about 30min at which time 0.6mole/mole of His-C was phosphorylated (Fig. 3.8).

As detailed above, by comparing with the consensus PKC phosphorylation sequence we identified several putative phosphorylation sites on both N- and C-tails of KCC2 (Fig. 3.1). However, as shown in Fig. 3.6, the N-tail of KCC2 was not phosphorylated by PKC, indicating that Thr^{34} in N-tail of KCC2 is not a PKC phosphorylation site. Nevertheless, C-tail of KCC2 was highly phosphorylated by PKC (Fig. 3.7) so phosphorylation site(s) must be present in this region. To identify the phosphorylation site(s) within the C-tail of KCC2, two truncations of His-C were constructed. First, amino acids from 932 to 1043 of C-tail of KCC2 were deleted and the result named His-C-Δ. This truncation contains possible phosphorylation sites of PKC: Ser^{728} and Thr^{787}. Secondly, the deleted 112 amino acids in His-C-Δ (i.e. 932 to 1043) were subcloned into

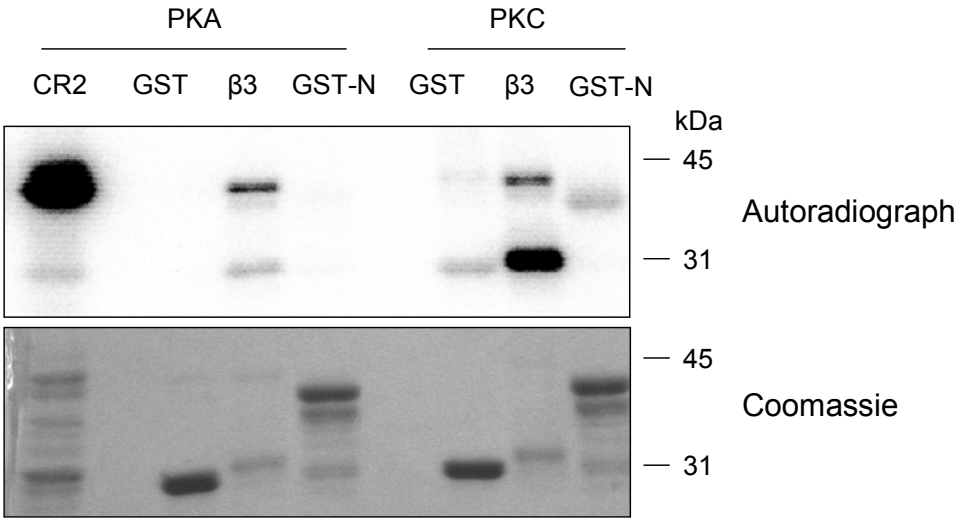

Fig. 3.6 GST-N fusion protein is not phosphorylated by PKA or PKC *in vitro*. The fusion protein was tested in an *in vitro* kinase assay using [γ-^{32}P]ATP. CR2, the intracellular domain of $GABA_B$ receptor R2-subunit, and β3, the $GABA_A$ receptor β3-subunit, were used as positive controls for both PKA and PKC phosphorylation. GST, the GST tag alone, was used as negative control for both experiments. Upper panel: autoradiograph of the kinase assay showing phosphorylation of proteins. Lower panel: Coomassie blue staining of the same gel showing the loading of the fusion proteins.

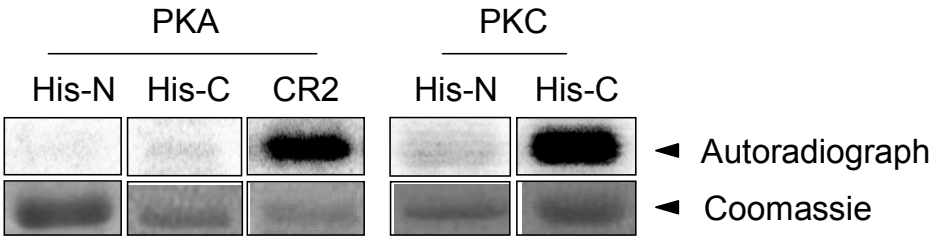

Fig. 3.7 His-C is phosphorylated by PKC but not PKA *in vitro*. His-N and His-C were tested in an *in vitro* kinase assay using [γ-^{32}P]ATP. CR2 was used as positive control for PKA phosphorylation. Reaction products were resolved by SDS-PAGE and analyzed by autoradiography showing phosphorylation of proteins. The gel was stained with Coomassie blue to show the presence of fusion proteins.

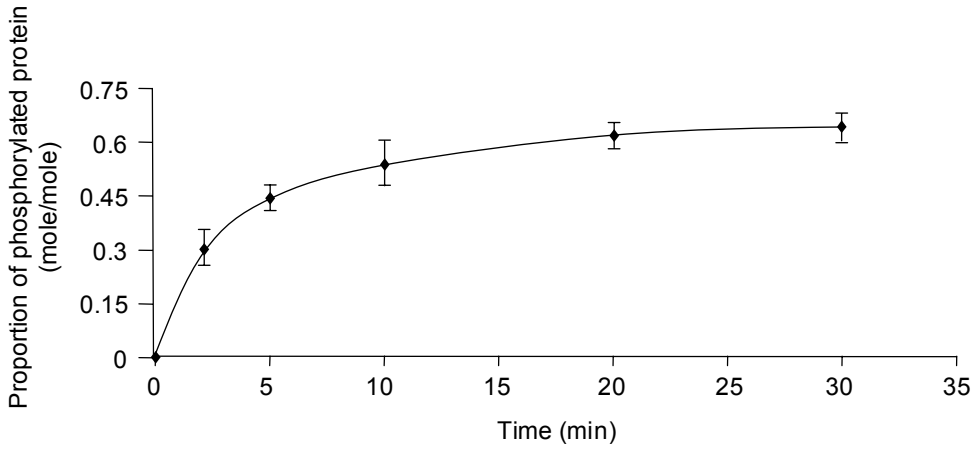

Fig. 3.8 Phosphorylation kinetics of His-C by PKC. His-C was tested in an *in vitro* kinase assay using purified PKC and [γ-^{32}P]ATP. Phosphorylation level of His-C was monitored by scintillation count of ^{32}P in the kinase reaction for up to 30min. The proportion of phosphorylated protein (in terms of mole of phosphorylated protein per mole of protein substrate, mole/mole) was calculated.

pTrcHis2C to express His-112 fusion protein. This fusion protein harbors two other putative PKC phosphorylation sites: Ser^{940} and Ser^{1034}. To determine whether these truncated fusion proteins can be phosphorylated by PKC, an *in vitro* kinase assay using [γ-^{32}P]ATP was performed. It was found that the phosphorylation level of His-C-Δ was not significantly lower compared to the highly phosphorylated His-C (Fig. 3.9), suggesting that Ser^{728} and Thr^{787} were not major PKC phosphorylation sites. On the other hand, His-112 remained highly phosphorylated (Fig. 3.9), indicating the presence of PKC phosphorylation sites in this region. To pinpoint the PKC phosphorylation sites in His-C, a series of serine-to-alanine mutations was constructed by site-directed mutagenesis. These substitution mutations essentially removed the particular site for phosphorylation (serine) but conserved the secondary and tertiary structure of expressed proteins due to the structural similarity of serine and alanine (Moss et al., 1992). All the mutant fusion proteins were purified and the expressions were confirmed by SDS-PAGE followed by Coomassie blue staining. They were then tested by an *in vitro* kinase assay using [γ-^{32}P]ATP as detailed above. The phosphorylation levels of these mutants were compared to those of the wild-type (WT) His-C (Fig. 3.10). Significantly, it was found that single mutation of Ser^{940} into alanine (S940A) reduced the level of phosphorylation to 32.5±2.5% of WT, while mutation of Ser^{728} or Ser^{1034} into alanine residues S728A and S1034A respectively remained highly phosphorylated (Fig. 3.10). Notably, double mutations (S728/940A, S940/1034A) or a triple mutation (S728/940/1034A) showed a further reduction of phosphorylation level compared to that of S940A, indicating that other possible phosphorylation sites may play a role in KCC2 phosphorylation

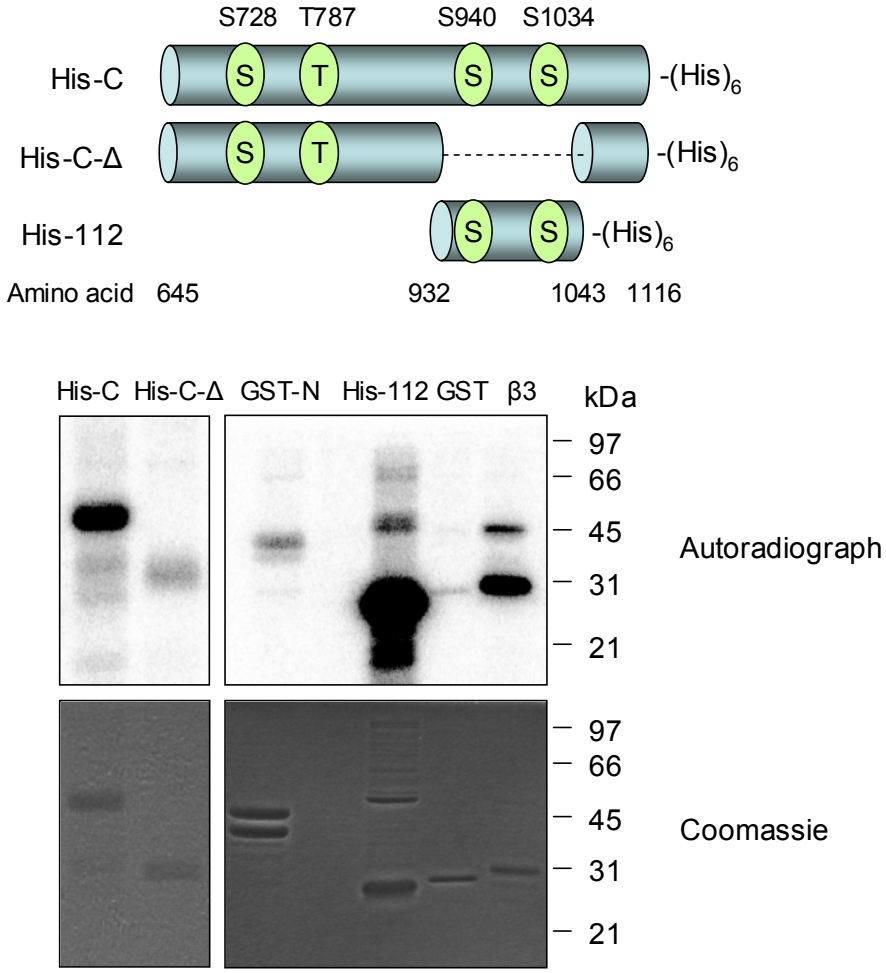

Fig. 3.9 Phosphorylation of truncated fusion proteins of His-C *in vitro*. Coding sequence of C-tail of KCC2 with a deletion of amino acids from 932-1043 was subcloned into pTrcHis2C to generate His-C-Δ fusion protein. Similarly, coding sequence of amino acids from 932-1043 of KCC2 was subcloned into pTrcHis2C to generate His-112 fusion protein. Putative PKC phosphorylation sites on the fusion proteins were indicated as S for serine and T for threonine and are numbered accordingly. Both truncation fusion proteins were tested in an *in vitro* kinase assay using PKC and [γ-^{32}P]ATP. Reaction products were resolved by SDS-PAGE and analyzed by autoradiography. GST-N was used as a negative control and β3-subunit of $GABA_A$ receptor as a positive control for PKC phosphorylation. Coomassie blue staining shows the loading of the purified fusion proteins of the same gel.

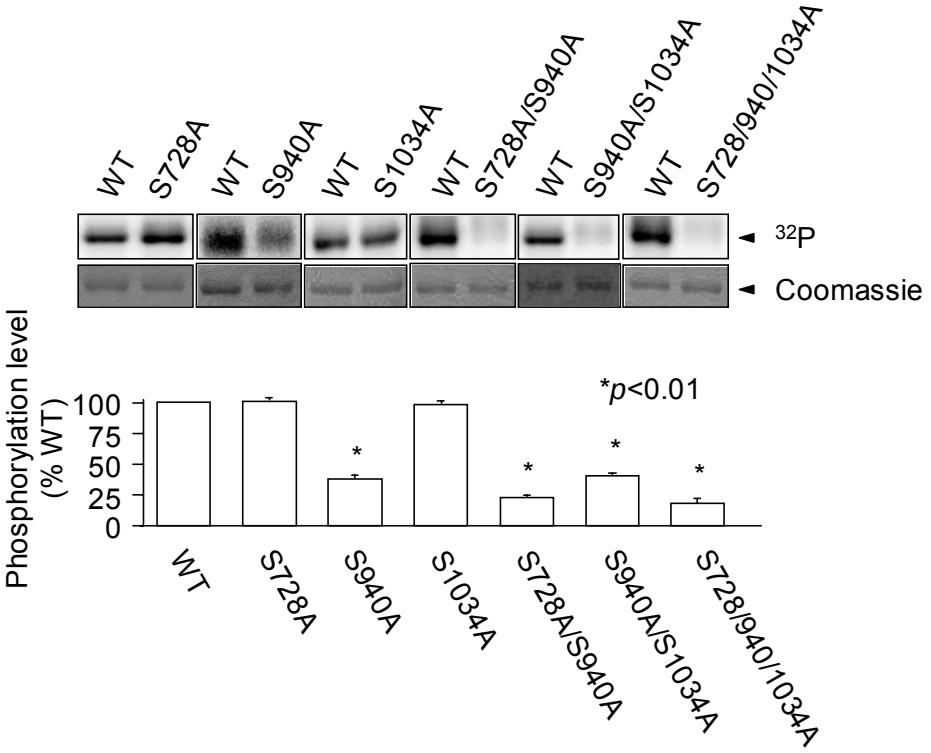

Fig. 3.10 Site-directed mutagenesis of His-C and *in vitro* kinase assay of the mutant fusion proteins. Serine-to-alanine mutations of His-C were generated by site-directed mutagenesis. Single mutations of His-C include S728A, S940A and S1034A. Double mutations include S728A/S940A and S940/S1034A. Triple mutation S728A/940/1034A was also generated. Mutant fusion proteins of His-C were tested in an *in vitro* kinase assay using PKC and [γ-^{32}P]ATP. Upper panel: autoradiograph of reaction products after SDS-PAGE shows the level of phosphorylation of each fusion protein compare to that of wild-type (WT) of His-C. Coomassie blue staining shows the equal loading of fusion proteins in each comparison. Lower panel: quantification of the autoradiograph shown on the upper panel. [*, significantly different from WT ($p < 0.01$; value = mean±SEM, Student's *t*-test, $n = 3$)]

by PKC. Together, these results strongly suggested that Ser^{940} residue is the major PKC phosphorylation site of KCC2.

To investigate the charge environment and distribution of phosphorylation sites in His-C, a phospho-peptide map was prepared (McDonald et al., 1998). The ^{32}P-labeled phosphorylated His-C fusion proteins were excised from the gel and digested with trypsin into phospho-peptides. These tryptic phospho-peptides were then separated by thin layer chromatography (TLC) including electrophoresis and chromatography in 2-dimension and visualized using a phospho-imager. It was found that there were two major positively charged phospho-peptides in WT but that one of them was removed in the S940A mutant (Fig. 3.11). Interestingly, a phospho-peptide map of His-C-Δ closely resembles that of the S940A mutant, indicating that the phospho-peptides of both fusion proteins are of similar identity (Fig. 3.11). In addition, the presence of other minor bands in the phospho-peptide maps of S940A and His-C-Δ indicated that these proteins were phosphorylated, possibly at other putative PKC phosphorylation sites. One such possible site is Ser^{728} since a minor reduction of phosphorylation level was observed in double mutant S728/940A compared to that of S940A (Fig. 3.10).

Besides phospho-peptide mapping, the composition of phospho-residues in His-C phosphorylated by PKC was investigated. The tryptic phospho-proteins were hydrolyzed by 6N HCl into single amino acids. The final products were resolved on a TLC plate using electrophoresis. Phospho-amino acids were separated due to their different mobility in electrophoresis and their positions

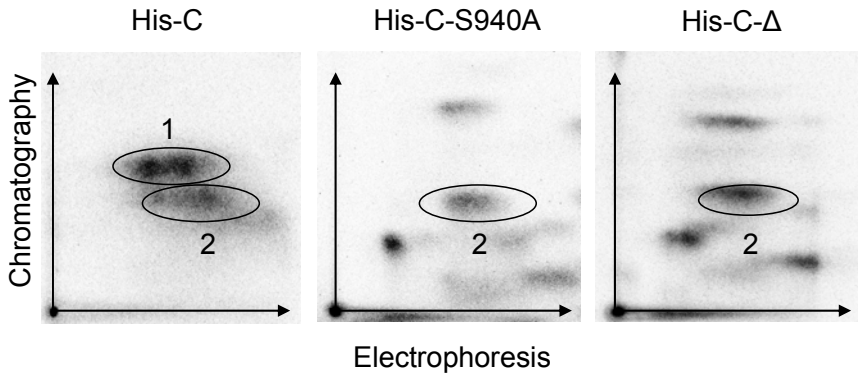

Fig. 3.11 Phospho-peptide map of His-C and its mutants. ^{32}P-labeled His-C, mutant S940A and truncation His-C-Δ fusion proteins were excised from the gel and digested with trypsin overnight to yield phospho-peptides. The digested products were separated by electrophoresis followed by chromatography in two dimensions. Autoradiography shows the locations of phospho-peptides, which were indicated and numbered on each map.

compared with those of the standards. Autoradiography of the phospho-amino acids showed that His-C was entirely phosphorylated at the serine residue, an observation similar to mutation S940A and truncation His-C-Δ (Fig. 3.12).

3.3 Expression of KCC2-FL in HEK-293 cells

In the previous sections experiments were performed using purified fusion proteins from bacteria in an *in vitro* system. In order to carry out the investigation in a more physiologically related system, KCC2 proteins were expressed in HEK-293 cells. To express KCC2 molecules in mammalian cells, the cDNA encoding the full length of KCC2 was subcloned into a pRK5 expression construct (Moss et al., 1991) to form KCC2-FL. The expression of KCC2 protein was first confirmed by western blotting using an anti-KCC2 antibody. It was found that a major band of molecular weight of 140kDa was present in KCC2-FL transfected cells but not in vector transfected control (Fig. 3.13). Furthermore, bands of molecular weight of 120kDa, 100kDa and 60kDa are degradation products and a band of 220kDa possibly results from dimerization of the KCC2 molecules (Williams et al., 1999). Interestingly, single mutations of S940A and Y1087F were expressed with identical molecular weight as WT (Fig. 3.13), suggesting that the expression of KCC2 proteins was not affected by these mutations. Immunoprecipitation of KCC2 from transfected cells showed that two bands were present, a pattern similar to that observed in transfected cells expressing KCC2 (Fig. 3.14). The appearance of KCC2 molecules as two distinct sizes may be due to the N-link glycosylation of proteins when expressed in recombinant systems as described

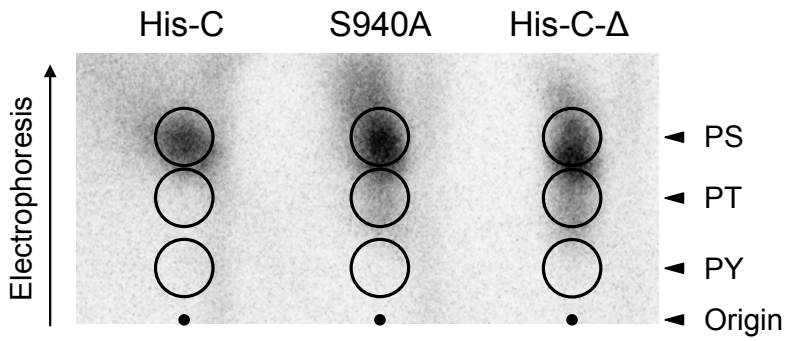

Fig. 3.12 Phospho-amino acid analysis of His-C and its mutants. ^{32}P-labeled His-C, mutant S940A and truncation His-C-Δ fusion proteins excised from the gel were hydrolyzed by 6N HCl at 100ºC for 1h to become signal amino acids. The final products were loaded onto a TLC plate together with phospho-amino acid standards and resolved by electrophoresis. Locations of phospho-serine (PS), phospho-threonine (PT), phospho-tyrosine (PY) and the origins of electrophoresis are indicated by arrows. Autoradiography shows phosphorylation of serine, threonine or tyrosine residues for each fusion protein.

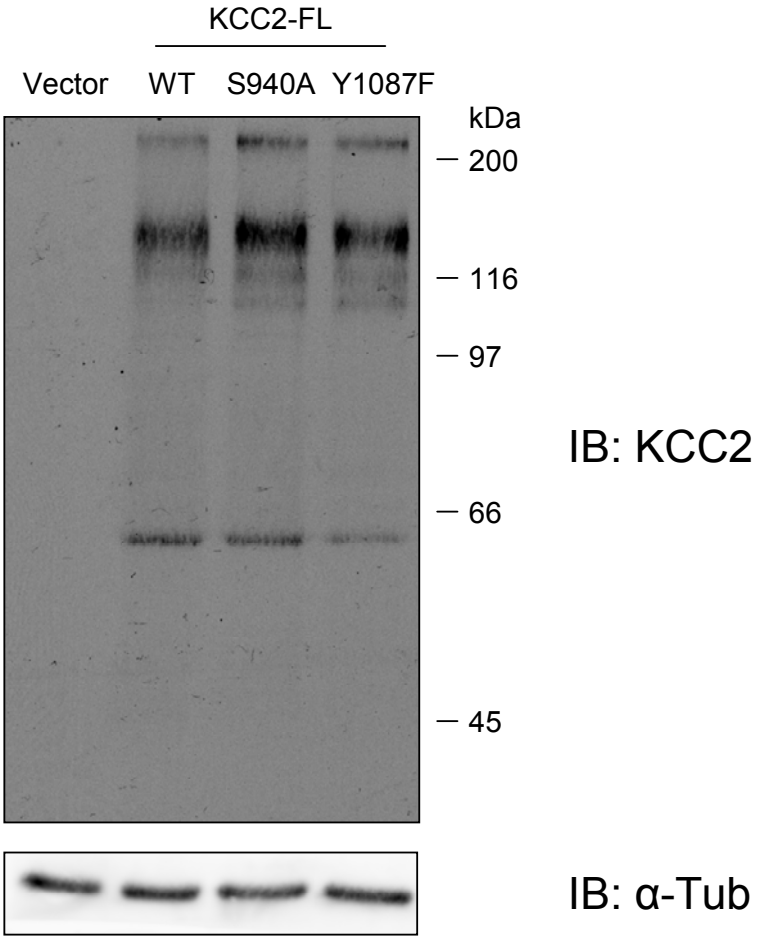

Fig. 3.13 Expression of KCC2 in HEK-293 cells. The full length coding sequence of KCC2 was subcloned into a pRK5 vector to form KCC2-FL in which the expression of KCC2 was driven by a strong mammalian cytomegalo virus (CMV) promoter. Single mutation substitution of Ser^{940} by alanine (S940A) and Tyr^{1087} by phenylalanine (Y1087F) were made subsequently by site-directed mutagenesis. Purified plasmids of wild-type (WT) KCC2-FL, mutants and pRK5 vector were transfected into HEK-293 cells. One day after transfection cells were harvested and the cell lysates analyzed by SDS-PAGE followed by western blotting. Expression of KCC2 was detected by immunoblotting (IB) with anti-KCC2 antibody. An antibody against α-tubulin (α-Tub) was used to show equal loading of proteins in SDS-PAGE.

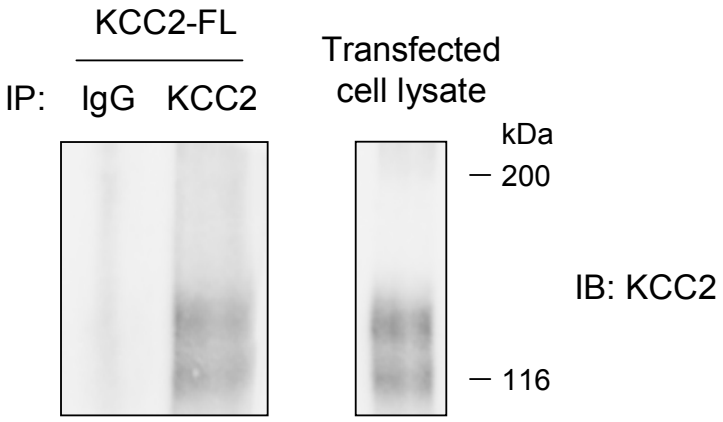

Fig. 3.14 Immunoprecipitation of KCC2-FL from HEK-293 cells. Cells transfected with KCC2-FL plasmid were lyzed and KCC2 immunoprecipitated (IP) by polyclonal rabbit anti-KCC2 antibody coupled to protein A-sepharose. The product was resolved by SDS-PAGE followed by immunoblotting (IB) using monoclonal mouse anti-KCC2 antibody. Non-specific rabbit IgG was used as control in immunoprecipitation. Transfected cell lysate before immunoprecipitation was also analyzed by western blotting.

previously (Williams et al., 1999). It was shown that treatment of N-glycosidase of cell lysate expressing KCC2 before SDS-PAGE and western blotting significantly reduced the molecular weight of KCC2 to around 120kDa, the size predicted from its cDNA (Williams et al., 1999).

To analyze KCC2 in transfected cells, a metabolic whole-cell labeling experiment using ^{35}S-methionine was also performed. Cells were incubated with ^{35}S-methionine for 4h before immunoprecipitation of KCC2. Two bands of approximately 120kDa and 140kDa were observed in cells transfected with KCC2-FL but not in control vector (Fig. 3.15). Importantly, expression levels of mutant S728A and S940A were similar to that of WT, indicating that expression and degradation of KCC2 proteins were not affected by these mutations.

3.4 Phosphorylation of KCC2-FL in HEK-293 cells

From the previous *in vitro* kinase assay, it has been shown that Ser^{940} is the major PKC phosphorylation site on KCC2. To confirm that this residue is phosphorylated by PKC in cells, a metabolic whole-cell labeling method using [^{32}P]orthophosphoric acid was employed. Cells transfected with KCC2-FL expression constructs were incubated with [^{32}P]orthophosphoric acid to allow incorporation of ^{32}P into the proteins. KCC2 molecules were then immunoprecipitated as described previously (Fig. 3.14) and resolved by SDS-PAGE. Phosphorylation level of KCC2 was then monitored by autoradiography. It was found that WT KCC2 was basally phosphorylated and

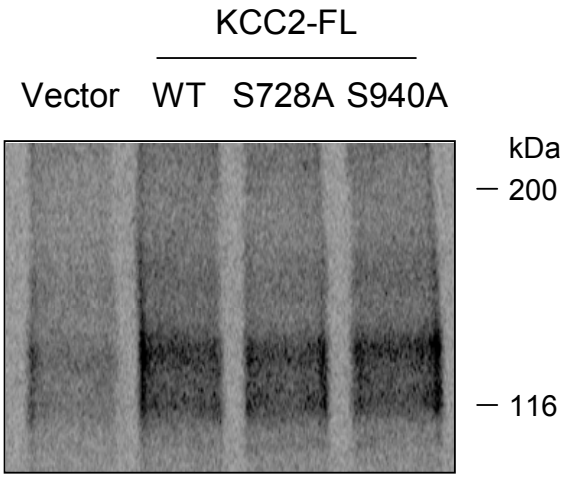

Fig. 3.15 Metabolic ^{35}S-methionine labeling of KCC2-FL in HEK-293 cells. Cells transfected with KCC2-FL WT, mutants (S728A and S940A) and pRK5 vector alone were labeled with ^{35}S-methionine for 4h before immunoprecipitation using polyclonal rabbit anti-KCC2 antibody. The products were resolved by SDS-PAGE and the incorporation of radioisotope ^{35}S monitored by phospho-imager.

that the phosphorylation level was significantly increased (p<0.01) by the 15min treatment of 100nM PDBu, a specific PKC activator, to 195.7±5.6% of basal condition (Fig. 3.16). Interestingly, mutant S940A was also basally phosphorylated; however the effect seen in WT by PDBu was totally blocked by this mutation (Fig. 3.16). These results strongly suggested that Ser^{940} is the major site of PKC phosphorylation in KCC2.

3.5 Expression of endogenous KCC2 in cultured hippocampal neurons

As detailed above phosphorylation of the intracellular domains of KCC2 expressed in HEK-293 cells has been examined. The advantages of using such recombinant systems to investigate phosphorylation are that the protein in question (i.e. KCC2) is expressed in high abundance and mutations can be introduced to pinpoint the site(s) of phosphorylation. However, these experiments serve only as a guide to possible events in neurons. The availability of kinase(s) to KCC2 in neurons may be different from that in recombinant systems. Therefore it is crucial to analyze the phosphorylation of KCC2 in neurons. Studies have revealed that expression of KCC2 is high in cortex and hippocampus (Woo et al., 2002; Bayatti et al., 2007; Molinaro et al., 2007; Pathak et al., 2007). Since hippocampus is the primary region for learning and memory and has been investigated extensively in GABAergic function (Cooper et al., 1999; Brunig et al., 2001; Coulter and Carlson, 2007), cultured hippocampal neurons were used in the following studies.

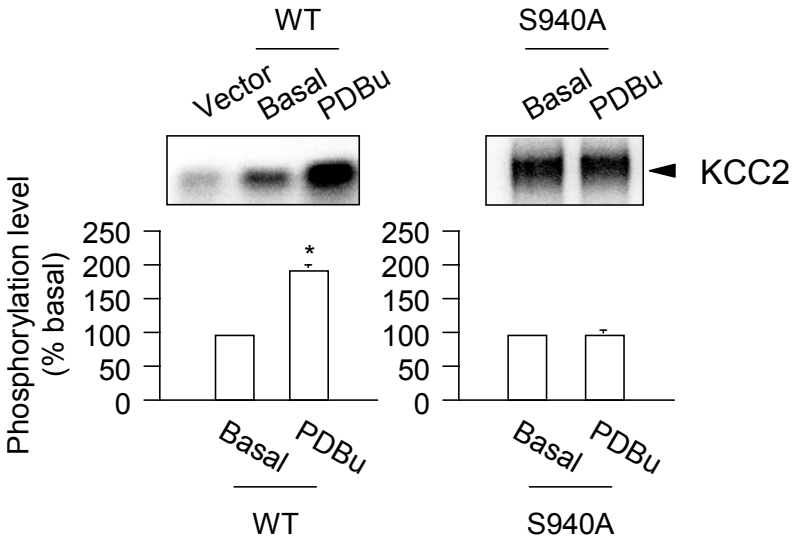

Fig. 3.16 Metabolic ^{32}P labeling of KCC2-FL in HEK-293 cells. Cells were transfected with WT KCC2-FL and its mutant S940A. One day after transfection cells were labeled with [^{32}P]orthophosphoric acid for 4h. KCC2 proteins from cells under basal condition or those treated with 500nM PDBu for 15min were immunoprecipitated and resolved by SDS-PAGE. Phosphorylation of KCC2 was monitored by phospho-imager. Upper panel: autoradiograph showing phosphorylation of immunoprecipitated KCC2. Lower panel: quantification of autoradiograph. [*, significantly different from basal condition ($p < 0.01$; value = mean±SEM, Student's *t*-test, $n = 3$)]

Hippocampal neurons from E18 pups of rat were dissected and plated on culture dishes. The cell lysates of different age (weeks) of culture were analyzed by SDS-PAGE and the amount of KCC2 expression visualized by western blotting. It was found that endogenous KCC2 proteins have a molecular weight of 120kDa as predicted from its coding sequence, and that its expression level increased from week 2 to week 5 (Fig. 3.17), which approximates with the results of other studies (Ludwig et al., 2003). Therefore cultures of 4 to 5 weeks were used in further studies. First we examined if KCC2 could be immunoprecipitated from these cells. To do so cultures were lyzed and detergent soluble fractions were immunoprecipitated with non-specific rabbit IgG and anti-KCC2 antibody. It was found that a band at around 120kDa was observed when using anti-KCC2 antibody but not in non-specific rabbit IgG control (Fig. 3.18).

3.6 Phosphorylation of endogenous KCC2 in cultured hippocampal neurons

To investigate phosphorylation of endogenous KCC2, whole-cell labeling experiments using [^{32}P]orthophosphoric acid were performed. 4h after ^{32}P incubation, neurons were lyzed and endogenous KCC2 proteins were immunoprecipitated. The proteins were resolved by SDS-PAGE and monitored by phospho-imager. It was found that KCC2 was basally phosphorylated (Fig. 3.19). Treatment with 500nM PDBu for 15min before cell lysis significantly increased (p<0.01) the phosphorylation level of KCC2 to 395.5±22.3% of basal condition (Fig. 3.19). Interestingly, treatment with 10μM GF109203X, a

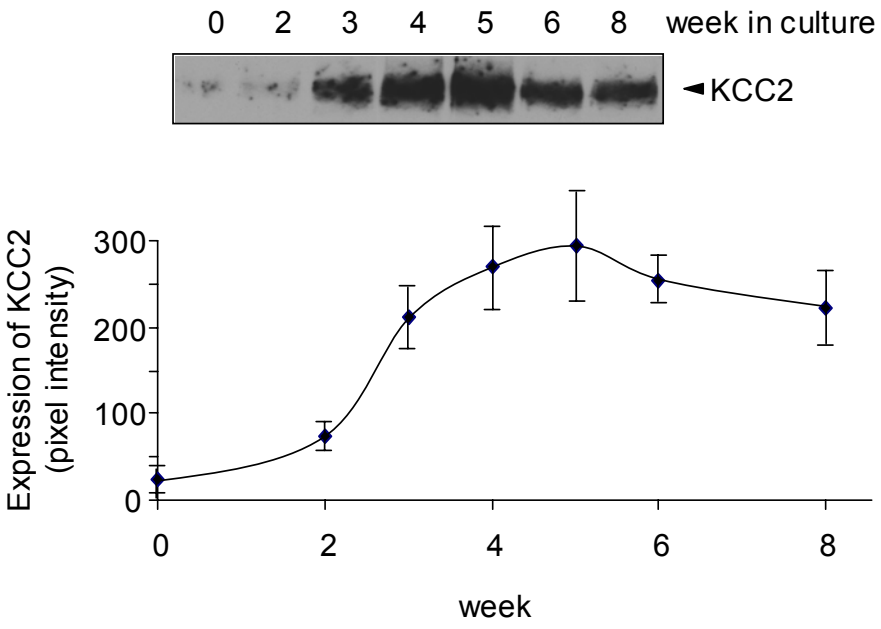

Fig. 3.17 Expression of KCC2 in cultured hippocampal neurons from 0 to 8 weeks. Hippocampal neurons from rat E18 pups were maintained in culture medium for up to 8 weeks. Cell lysates of different age (weeks) neurons were collected and resolved by SDS-PAGE followed by western blotting using anti-KCC2 antibody. The lower panel shows the quantification of KCC2 expression in 8 weeks of cultures.

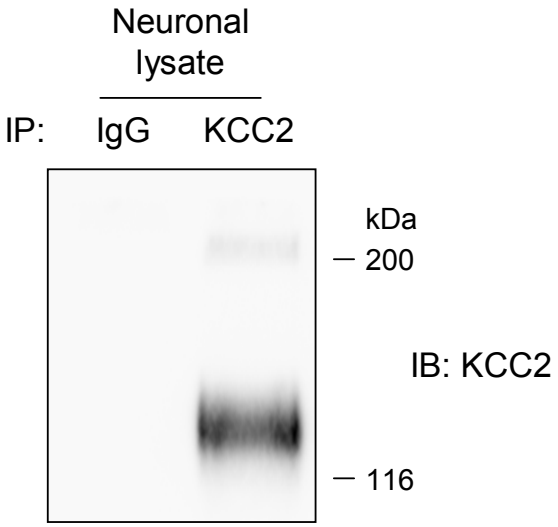

Fig. 3.18 Immunoprecipitation of endogenous KCC2 from cultured hippocampal neurons. Endogenous KCC2 proteins from cultured hippocampal neurons were immunoprecipitated using polyclonal rabbit anti-KCC2 antibody and resolved by SDS-PAGE followed by western blotting. Non-specific rabbit IgG was used as control in immunoprecipitation.

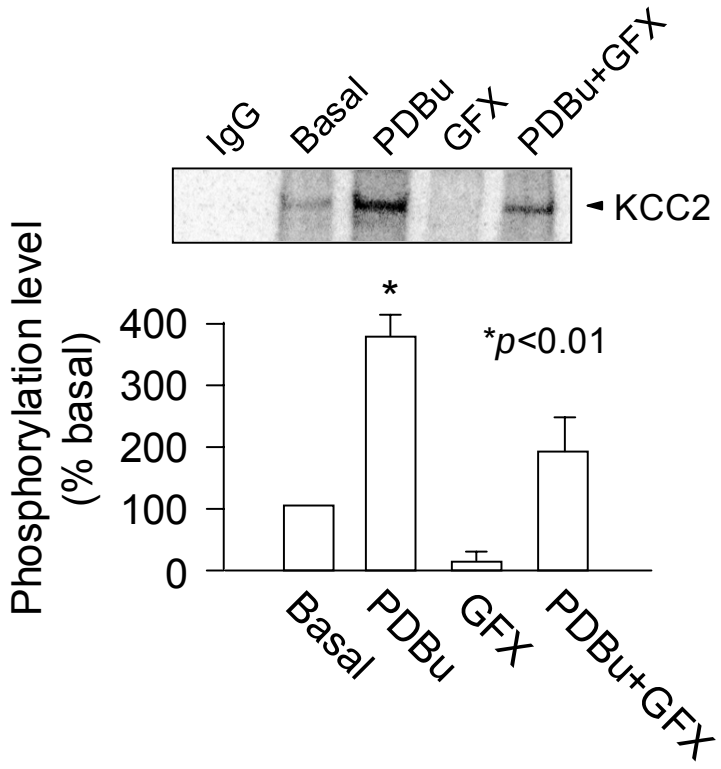

Fig. 3.19 Metabolic ^{32}P labeling of KCC2 in cultured hippocampal neurons. Four-week-old cultured hippocampal neurons were labeled with [^{32}P]orthophosphoric acid for 4h and endogenous KCC2 immunoprecipitated and resolved by SDS-PAGE. Phosphorylation of KCC2 was monitored using a phospho-imager. Upper panel: autoradiograph of immunoprecipitated KCC2 from neurons. Non-specific rabbit IgG was used as control for immunoprecipitation. 500nM PDBu was used for PKC activation and 10μM GF109203X (GFX) was used as a specific PKC inhibitor. Lower panel: quantification of the phospho-imager results. [*, significantly different from basal condition ($p < 0.01$; value = mean±SEM, Student's *t*-test, $n = 3$)]

specific PKC inhibitor, significantly reduced (p<0.01) basal phosphorylation of KCC2 to 15.5±3.5% of basal and blocked the effect of PDBu treatment. Thus endogenous KCC2 in hippocampal neurons is phosphorylated by PKC activation.

To further study phosphorylation of endogenous KCC2 in neurons, phospho-peptide map and phospho-amino acid analysis were performed. Phospho-peptide mapping of endogenous KCC2 revealed that there were two major phospho-peptides after PDBu treatment (Fig. 3.20), a pattern resembling that of His-C (Fig. 3.11). Intriguingly, phospho-amino acid analysis showed that endogenous KCC2 is phosphorylated on serine residues under basal conditions (Fig. 3.21), which is similar to that of His-C (Fig. 3.12). Furthermore, PDBu treatment stimulated phosphorylation on tyrosine residues, an effect blocked by 100nM calphostin C (CalC), a specific PKC inhibitor (Fig. 3.21).

3.7 Phosphorylation of KCC2-FL at tyrosine residue in HEK-293 cells

In addition to serine/threonine protein kinase PKC, phosphorylation of KCC2 by tyrosine kinase was also studied. In particular Tyr^{1087} has been shown to modulate KCC2 expression but whether this residue is actually phosphorylated remain to be addressed (Wake et al., 2007). Immunoprecipitation of KCC2 proteins from HEK-293 cells transfected with KCC2-FL constructs (WT and Y1087F) followed by immunoblotting using phospho-tyrosine antibody showed that KCC2 was not phosphorylated at tyrosine residue but only if 100μM of sodium pervanadate (Na_3VO_4) was added to the culture 1h before

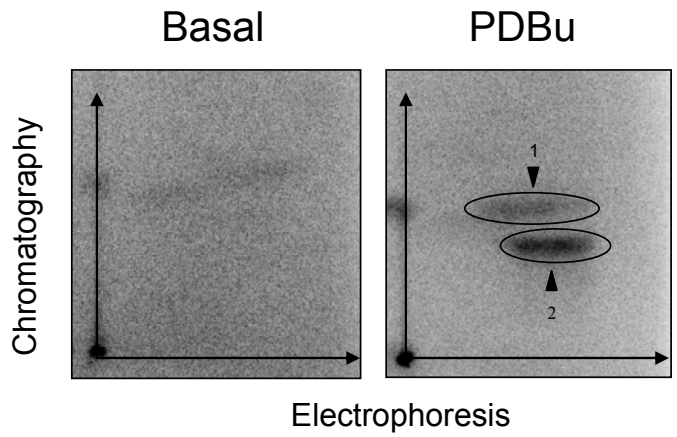

Fig. 3.20 Phospho-peptide map of KCC2 in cultured hippocampal neurons. ^{32}P-labeled endogenous KCC2 proteins before (basal) and after PDBu treatment (PDBu) were immunoprecipitated and resolved by SDS-PAGE. The phosphorylated protein was excised from the gel and digested overnight by trypsin to yield phospho-peptides. The product was then loaded onto a TLC plate and subject to electrophoresis and chromatography in 2 dimensions. The phospho-peptides are indicated by arrows.

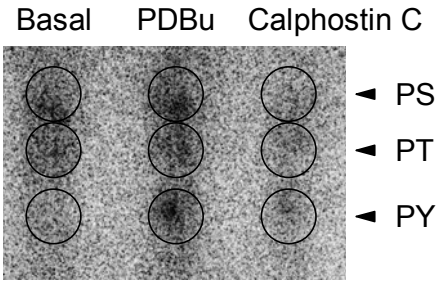

Fig. 3.21 Phospho-amino acid analysis of endogenous KCC2 in cultured hippocampal neurons. ^{32}P-labeled endogenous KCC2 proteins were hydrolyzed by 6N HCl to become single amino acids. The final products were loaded onto a TLC plate with phospho-amino acid standards and separated by electrophoresis. KCC2 proteins from neurons at basal condition, 500nM PDBu treated neurons and 100nM calphostin C treated neurons were tested. Location of phospho-serine (PS), phospho-threonine (PT) and phospho-tyrosine (PY) are indicated by arrows.

cell lysis (542±19% of control, Fig. 3.22). This indicated that endogenous phosphatase activity in cultured cells is high. Interestingly, mutation at Tyr^{1087}, the putative tyrosine phosphorylation site of KCC2, did not significantly reduce tyrosine phosphorylation of KCC2 under Na_3VO_4 treatment (Fig. 3.22), suggesting the presence of other tyrosine phosphorylation site(s) in the sequence of KCC2.

To investigate whether KCC2 expressed in cells can be phosphorylated by Src tyrosine kinase, v-Src, the constitutively active form of Src, was co-expressed with KCC2-FL in HEK-293 cells. V-Src is closely related to proto-oncogene c-Src but its inhibitory phosphorylation site was removed so v-Src becomes constitutively active (Roskoski, 2004). V-Src has also been shown to phosphorylate $GABA_A$ receptor at tyrosine residue (Moss et al., 1993); thus it is a good candidate to study tyrosine phosphorylation of KCC2. Since it has been shown that endogenous tyrosine phosphatase activity in cultured neurons is high (Fig.3.22), cells were treated with Na_3VO_4 for 1h before lysis and KCC2 proteins were immunoprecipitated followed by immunoblotting using phospho-tyrosine antibody. It was found that co-expression of v-Src significantly increased ($p<0.01$) the phospho-tyrosine level of KCC2 to 385.5±22.2% of control (Fig. 3.23). Intriguingly, mutant Y1087F did not reduce tyrosine phosphorylation level of KCC2 when v-Src was co-expressed (Fig. 3.23), suggesting that v-Src kinase phosphorylated other site(s) on KCC2 but not Tyr^{1087}.

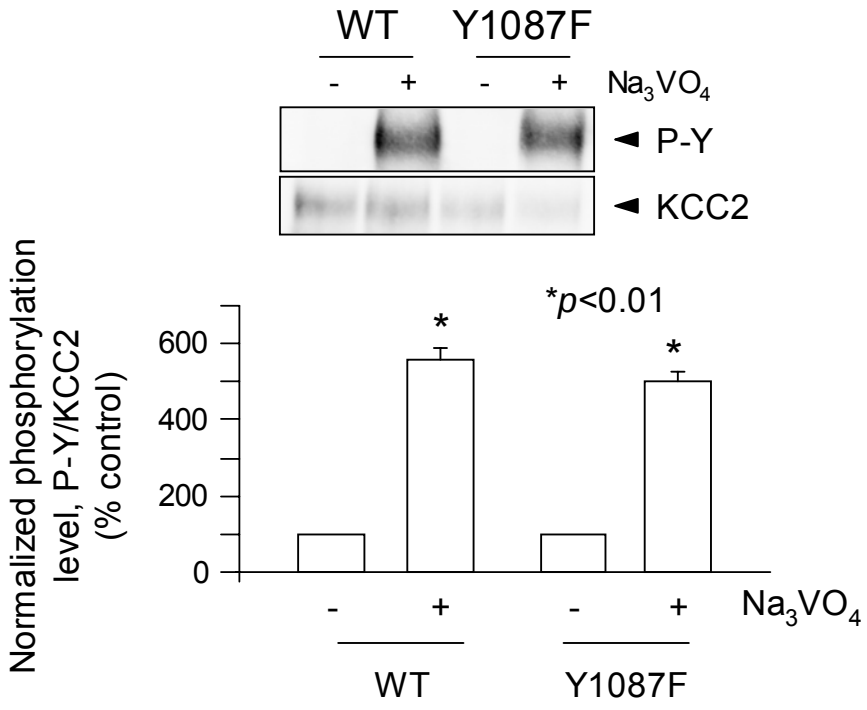

Fig. 3.22 KCC2-FL was phosphorylated at tyrosine residue in HEK-293 cells. HEK-293 cells were transfected with KCC2-FL (WT and Y1087F) and treated with (+) or without (-) 100μM Na_3VO_4 for 1h. KCC2 was immunoprecipitated and the proteins resolved by SDS-PAGE followed by western blotting using anti-phospho-tyrosine antibody (P-Y). Cell lysates before immunoprecipitation were also analyzed by western blotting using anti-KCC2 antibody. The phosphorylation level of KCC2 was normalized with the total amount of KCC2 expression. [*, significantly different from control (p < 0.01; value = mean±SEM, Student's t test, n = 4)]

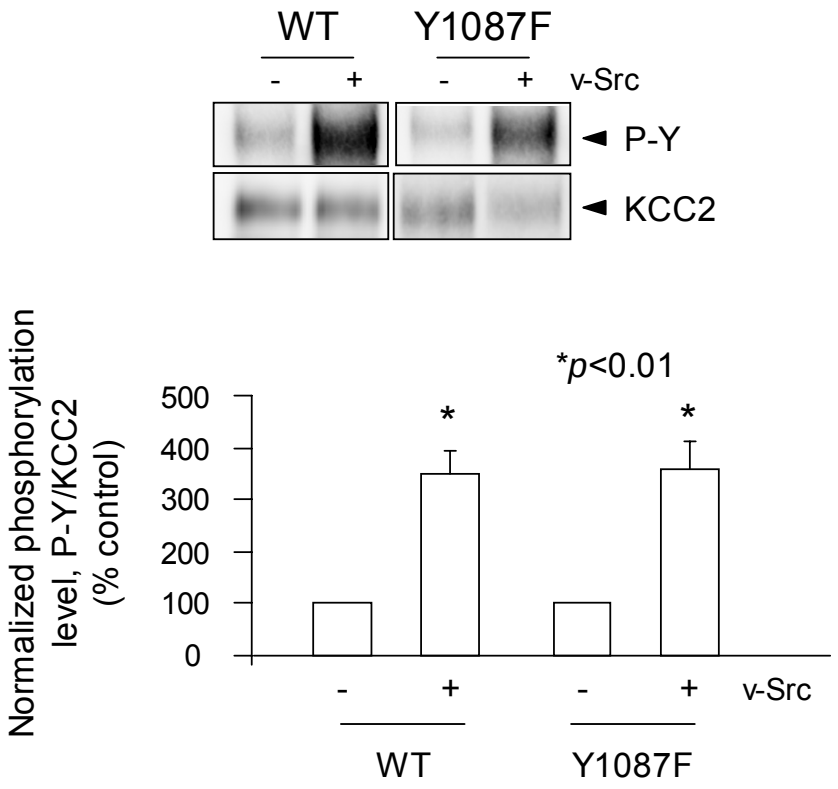

Fig. 3.23 KCC2-FL was phosphorylated by v-Src, a constitutively active form of Src tyrosine kinase, in HEK-293 cells. HEK-293 cells were transfected with KCC2-FL (WT or Y1087F) and v-Src (+) or empty vector (-). One day after transfection cells were treated with 100μM Na_3VO_4 for 1h. KCC2 proteins were then immunoprecipitated, resolved by SDS-PAGE and analyzed by western blot using anti-phospho-tyrosine antibody (P-Y). Cell lysates before immunoprecipitation were also analyzed by western blotting using anti-KCC2 antibody. The phosphorylation level of KCC2 was normalized with the total amount of KCC2 expression. [*, significantly different from vector control ($p < 0.01$; value = mean±SEM, Student's *t*-test, $n = 3$)]

3.8 Phosphorylation of endogenous KCC2 at tyrosine residue in cultured hippocampal neurons

In the previous section it was shown that KCC2 proteins expressed in HEK-293 cells were phosphorylated at tyrosine residue. To investigate whether endogenous KCC2 was also phosphorylated on tyrosine residues, similar experiments were performed on cultured hippocampal neurons. It was found that endogenous KCC2 was phosphorylated at tyrosine residue when Na_3VO_4 was added to the culture (811±18.4% of control, Fig. 3.24), indicating that endogenous tyrosine phosphatase activity in cultured neurons was also high. To show that tyrosine phosphorylation of KCC2 proteins in neurons is mediated by Src family kinase, PP2, a selective inhibitor of Src family protein tyrosine kinase, was treated with Na_3VO_4 on cultured hippocampal neurons for 30min before cell lysis. Results showed that PP2 significantly reduced (p<0.01) the phospho-tyrosine level of KCC2 to 22.5±7.1% of control condition but that PP3, a negative control compound for PP2, which inhibits the activity of epidermal growth factor receptor (EGFR) kinase, did not significantly reduce tyrosine phosphorylation of KCC2 (Fig. 3.25). These results indicated that KCC2 proteins in neurons were phosphorylated by Src family kinase.

Discussion

In this chapter the phosphorylation of KCC2 was investigated using a range of different approaches.

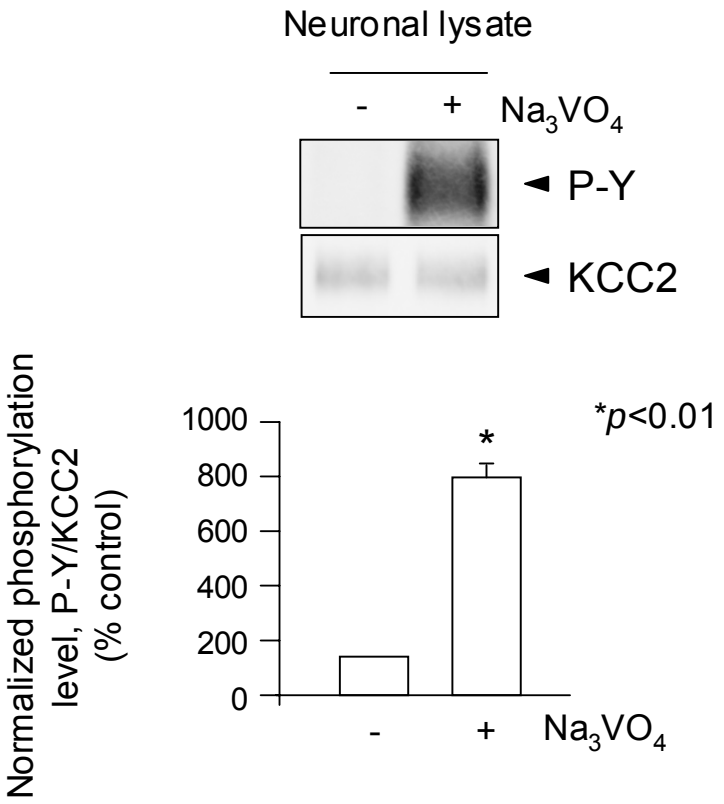

Fig. 3.24 Endogenous KCC2 in cultured hippocampal neurons was phosphorylated at tyrosine residue. Cultured hippocampal neurons were treated with (+) or without (-) 100μM Na_3VO_4 for 1h and endogenous KCC2 proteins immunoprecipitated. Phosphorylation of tyrosine residue was monitored by western blotting using anti-phospho-tyrosine antibody (P-Y). Cell lysates before immunoprecipitation were also analyzed by western blotting using anti-KCC2 antibody. The phosphorylation level of KCC2 was normalized with the total amount of KCC2 expression. [*, significantly different from control ($p < 0.01$; value = mean±SEM, Student's *t*-test, $n = 3$)]

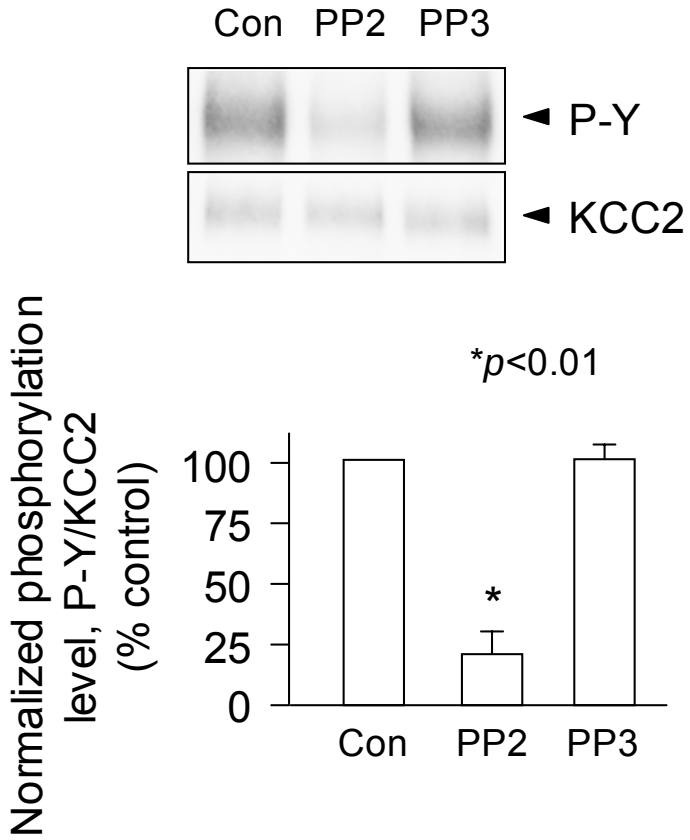

Fig. 3.25 Phosphorylation of endogenous KCC2 in cultured hippocampal neurons was inhibited by PP2, a Src family kinase inhibitor. Na_3VO_4 was added to the neurons 1h before lysis to block endogenous tyrosine phosphatase activity. 10μM PP2, Src family kinase inhibitor, and 10μM PP3, a control compound for PP2, were added 30min before lysis. KCC2 proteins were immunoprecipitated from cell lysates and resolved by SDS-PAGE followed by western blotting using anti-phospho-tyrosine antibody (P-Y). [*, significantly different from control ($p < 0.01$; value = mean±SEM, Student's *t*-test, $n = 3$)]

The investigation of phosphorylation of KCC2 was initiated by *in vitro* studies using fusion proteins of N-tail (residues 1-102) and C-tail (residues 645-1116) intracellular domains of KCC2 expressed and purified from E. coli. It was found that C-tail but not N-tail of KCC2 can be phosphorylated by PKC to high stoichiometry. This indicated that the putative phosphorylation site on N-tail of KCC2 (Payne et al., 1996) was not a phosphorylation site for PKC. This can be explained by the fact that protein folding around the putative site makes it inaccessible by PKC. Indeed, putative phosphorylation sites are deduced from consensus sequence; thus biochemical analyses are needed to prove their true identities. Peptide mapping and phospho-amino acid analysis revealed that the C-tail fusion protein was phosphorylated at serine residue within two major phospho-peptides. Interestingly, mutation of Ser^{940} into alanine significantly reduced phosphorylation of this fusion protein to around 25% of control and ablated one of the major phospho-peptides seen on phosphorylation of WT protein. However, the further reduction of phosphorylation in double or triple mutants of His-C indicates that Ser^{728} or Ser^{1034} may play a less significant role in phosphorylation of KCC2 that that of Ser^{940}. This notion is further supported by the phospho-peptide map of S940A mutant in which one of the peptides observed in His-C was not ablated (Fig. 3.11). To support the *in vitro* study, full-length KCC2 was expressed in HEK-293 cells and its phosphorylation was measured by immunoprecipitation after metabolic labeling with [^{32}P]orthophosphoric acid. This method allows the analysis of the overall change in phosphorylation of a protein in cultured cells (Moss et al., 1992). In conjunction with phospho-peptide mapping and phospho-amino acid analysis, the number of phosphorylation sites and the residues on which phosphorylation

occurs (i.e. serine, threonine or tyrosine) can be investigated (Moss et al., 1992). It was found that expressed KCC2 was basally phosphorylated and phosphorylation was increased robustly by activation of PKC, an effect that was blocked by mutation of Ser^{940}. Together, it was concluded that KCC2 is a substrate of PKC and that the major phosphorylation site within the major intracellular domain of KCC2 is Ser^{940}.

In addition to recombinant systems, phosphorylation of KCC2 in neurons was investigated using immunoprecipitation after metabolic labeling with [^{32}P]orthophosphoric acid. Hippocampal neurons grown in culture for four weeks were chosen for the study due to their high expression of KCC2. It was found that neuronal KCC2 was basally phosphorylated and that activation of PKC significantly increased phosphorylation of KCC2 at serine, threonine and tyrosine residues. Interestingly, this observation is different from that in recombinant KCC2-expressed HEK-293 cells in which only serine residue was phosphorylated. This can be explained by the fact that the availability of kinases in HEK-293 cells and hippocampal neurons are different. At the same time, this finding strongly suggested that a signaling pathway involving tyrosine kinase was co-activated in regulating KCC2 when PKC was activated. This potentially involves a cross-talk between PTK and PKC signaling in cultured neurons (Fig. 3.26) (See also section 6.1). To compare phosphorylation of recombinant and neuronal KCC2, phospho-peptide mapping was used. Interestingly, neuronal KCC2 was phosphorylated at three distinct phospho-peptides after PKC activation, two of them highly resembling those observed in recombinant KCC2. Combining results from recombinant

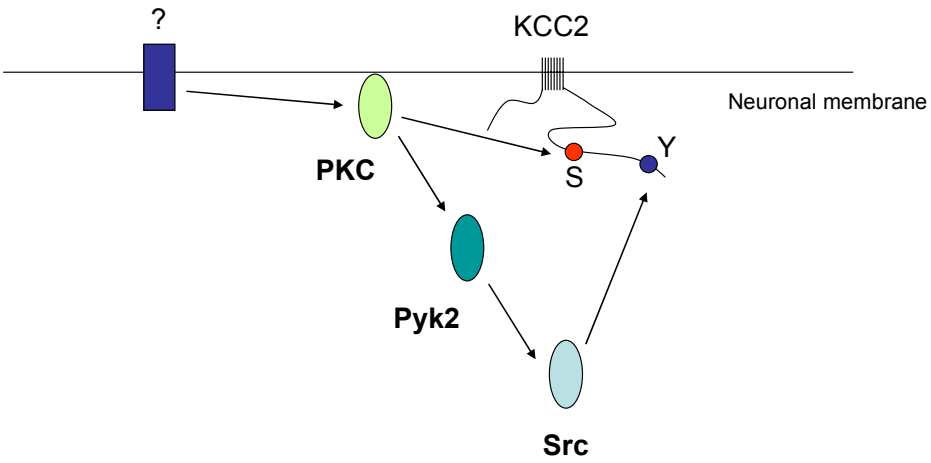

Fig. 3.26 Putative cross-talk between PKC and PTK. Schematic diagram showing the activation of Src (a member of PTK) followed by activation of PKC. PKC is capable of phosphorylation of Ser^{940} (S) in KCC2 on activation (physiological activation mechanism unknown). Pyk2, a member of the focal adhesion kinase family, is in turn activated by PKC, producing a Src homology 2 (SH2) binding domain to activate Src kinase. Activated Src kinase then phosphorylates tyrosine residue(s) (Y) of KCC2.

system and cultured neurons, it was concluded that neuronal KCC2 is a substrate of PKC and that its phosphorylation was increased upon PKC activation.

A recent report has also shown that KCC2 is phosphorylated on tyrosine residues upon oxidative stress and/or high metabolic activity (Wake et al., 2007). Consensus sequence analysis also showed that there is a putative tyrosine kinase phosphorylation site Tyr^{1087} on KCC2 (Payne et al., 1996). To investigate if this residue is phosphorylated, immunoprecipitation of KCC2 expressed in HEK-293 cells followed by immunoblotting using a phospho-tyrosine antibody was employed. Intriguingly, phosphorylation of KCC2 at tyrosine residues was robust upon blocking of tyrosine phosphatase, consistent with the previous study (Wake et al., 2007). However, mutation of Tyr^{1087} did not significantly reduce tyrosine phosphorylation, suggesting that other tyrosine residues are involved in this phosphorylation. In fact, a study has suggested that Tyr^{1087} is involved in regulation of KCC2 function, possibly through protein-protein interaction, but it lacks evidence that Tyr^{1087} itself is phosphorylated (Strange et al., 2000). The result presented here is thus the first confirmation that Tyr^{1087} is not a tyrosine kinase substrate in KCC2. Furthermore, the involvement of v-Src in phosphorylation of KCC2 was demonstrated by co-expression of this tyrosine kinase with KCC2 in HEK-293 cells. To compare with recombinant results, neuronal KCC2 was analyzed similarly. It was found that neuronal KCC2 was also phosphorylated at tyrosine residues upon inhibition of tyrosine phosphatase, an effect reversed by inhibiting Src family kinase but not receptor tyrosine kinase EGFR. Together,

it was demonstrated that tyrosine phosphorylation of KCC2 is mediated by Src family kinase, and that dephosphorylation of tyrosine residues in KCC2 in cultured cells is carried out by the high activity of tyrosine phosphatase.

Chapter 4 Development of a phospho-specific antibody against Ser^{940} of KCC2 and its use to analyze KCC2 dephosphorylation

Introduction

In the last chapter data were presented to show that KCC2 is phosphorylated by PKC on Ser^{940} within its major intracellular C-terminal domain using metabolic labeling with [^{32}P]orthophosphoric acid coupled with immunoprecipitation. However, the use of radioisotopes in studying protein phosphorylation serves to measure only the overall phosphorylation level of a protein, not the phosphorylation state of a particular site (Moss et al., 1992). For example, it was demonstrated that both serine and tyrosine residues were phosphorylated in KCC2 upon PKC activation in neurons (Fig. 3.21) although Ser^{940} was the major PKC phosphorylation site in KCC2. Therefore, to study phosphorylation at Ser^{940} specifically, an antibody against the phosphorylation state of Ser^{940}, namely p-S940, was developed using a previously described technique (Czernik et al., 1991; Jovanovic et al., 1996). The advantage of using p-S940 over a commercially available phospho-serine antibody is that it is specific to Ser^{940} of KCC2, enabling phosphorylation of Ser^{940} to be studied individually. Furthermore, it is possible to carry out immunofluorescence staining of KCC2 molecules phosphorylated at Ser^{940} in mounted cells with this phospho-specific antibody (Xu et al., 1998). In fact, such use of a phospho-specific antibody has been widely used to investigate phosphorylation of other proteins including GABA receptors (Jovanovic et al., 2004; Kuramoto et al., 2007).

As p-S940 was initially developed in our laboratory it needs to be characterized for its specificity against the phosphorylation state of its target residue, Ser^{940} (Czernik et al., 1991; Kuramoto et al., 2007). Characterization of p-S940 was carried out by western blotting using His-C and cultured cells expressing KCC2 and its specificity against the phosphorylation state of Ser^{940} confirmed using immunofluorescence staining. After establishing specificity of p-S940, this antibody was used to investigate the regulation of phosphorylation of Ser^{940} by PKC activity. The identities of phosphatases responsible for dephosphorylation of this critical residue were also investigated.

Regulation of phosphorylation at Ser^{940} is of particular interest in the study of KCC2. It has been shown that Ser^{940} is the major PKC phosphorylation site within its intracellular domain (Figs. 3.10, 3.16). In fact, phosphorylation events mediated through PKC play an important role in controlling K^+-Cl^- co-transport activities in different cell types (Adragna et al., 2004; Bergeron et al., 2006); however, a direct link between PKC phosphorylation on the KCC2 molecule and its functional modification on co-transport activity has yet to be established (Strange et al., 2000). On the other hand, phosphorylation is also tightly regulated by phosphatases, which catalyze the removal of the phosphate group from a phosphorylated residue. Previous studies have indicated that phosphatases play regulatory roles in cation chloride co-transporters (CCC) (Flatman, 2002; Liedtke et al., 2005). Given the functional relevance and structural similarities between members of the CCC family (Gamba, 2005), phosphatases may be important in the regulation of phosphorylation of KCC2.

This chapter describes the development of a phospho-specific antibody of KCC2 and its application in the study of phosphorylation and dephosphorylation of residue Ser^{940} of KCC2. Specifically the aims of this chapter are:

1) To show the phosphorylation-specificity of p-S940 by western blotting on recombinant and neuronal KCC2.
2) To show the phosphorylation-specificity of p-S940 by immunofluorescence staining.
3) To study regulation of phosphorylation of Ser^{940} using p-S940.
4) To show that particular phosphatases are responsible for dephosphorylation of Ser^{940} of KCC2.

Results

4.1 Production of the phospho-specific antibody of KCC2, p-S940

To generate p-S940 the phospho-peptide around residue Ser^{940} of KCC2 intracellular domain (P-pep-S940) was first designed to be suitable for immunization. The peptide sequence for immunization is:

DESRG<u>S</u>IRRKN

in which the underlined <u>S</u> is Ser^{940} that was chemically phosphorylated during peptide synthesis. The design of this immunizing antigen was based on several criteria. First, the peptide length was short at around 10 amino acids such that the phospho-serine residue was forced into the epitope recognized by the

antibody. Second, the sequence was subjected to a Blast search to reduce the chance of cross-reactivity with homologous protein. It is important to note that the region around Ser^{940} is unique to KCC2 among KCC members. Finally, an N-terminal cysteinyl residue was added for conjugation of carrier protein and coupling to affinity column. After chemical synthesis of the phospho-peptide, it was injected into two rabbits and three subsequent boosts were administered within a 3-month period. The immunization schedule is listed below:

Week	Injection procedure
0	Intradermal, 0.6mg of peptides in Complete Freund's Adjuvant
2	Subcutaneous, 0.3mg of peptides in Incomplete Freund's Adjuvant
4	Subcutaneous, 0.3mg of peptides in Incomplete Freund's Adjuvant
5	Serum collection
6	Serum collection
7	Serum collection
8	Subcutaneous, 0.3mg of peptides in Incomplete Freund's Adjuvant
9	Serum collection
10	Serum collection
11	Serum collection
12	Subcutaneous, 0.3mg of peptides in Incomplete Freund's Adjuvant

Approximately 15mL serum from the animal was then collected after the first injection. This serum was purified with affinity column coupled with phospho-peptides. Chemical synthesis of peptides, injection of phospho-peptides into rabbits and purification of antibodies were all carried out by PhosphoSolutions.

4.2 Phosphorylation-specificity of purified p-S940 determined by western blotting

To characterize p-S940 His-C and its S940A mutant were subjected to an *in vitro* kinase assay by PKC in the presence or absence of ATP. The reaction products were resolved by SDS-PAGE and analyzed by western blotting using p-S940. It was found that p-S940 recognized only WT His-C in the presence of ATP (Fig. 4.1), consistent with results shown in Fig. 3.10 in which His-C was highly phosphorylated by PKC but blocked significantly by S940A mutant.

To further confirm the specificity of p-S940 HEK-293 cells expressing KCC2-FL and the S940A mutant were used as in Fig. 3.13. Prior to cell lysis, cells were treated with 500nM PDBu for 15min to activate PKC. The cell lysates were then analyzed by SDS-PAGE and western blotting. It was found that there was basal phosphorylation of KCC2-FL in HEK-293 cells in the absence of PDBu (Fig. 4.2); however, treatment with PDBu significantly ($p<0.01$) increased the signal of p-S940 in WT to 218±68% of basal condition. Importantly, no signal was detected in S940A mutant (Fig. 4.2), indicating that the antibody is specific to the phosphorylation of Ser^{940} of KCC2 expressed in the recombinant system.

To determine if p-S940 could be used to examine the phosphorylation of neuronal KCC2 lysates of hippocampal neurons were immunoblotted with this antibody. Using this approach a major band of 120kDa and some very weak

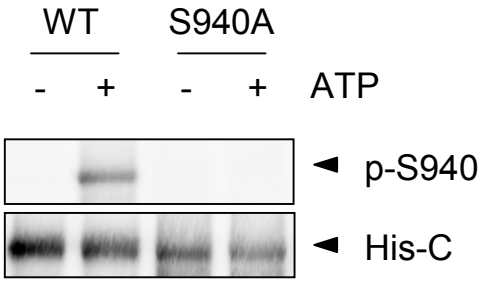

Fig. 4.1 p-S940 is specific to the phosphorylation of His-C *in vitro*. His-C (WT and S940A) was subject to *in vitro* kinase assay in the presence (+) and absence (-) of ATP. The reaction products were then resolved by SDS-PAGE followed by western blotting using p-S940. The amount of His-C used in the reactions was determined using anti-KCC2 antibody on a separate blot with the same amount of proteins loaded.

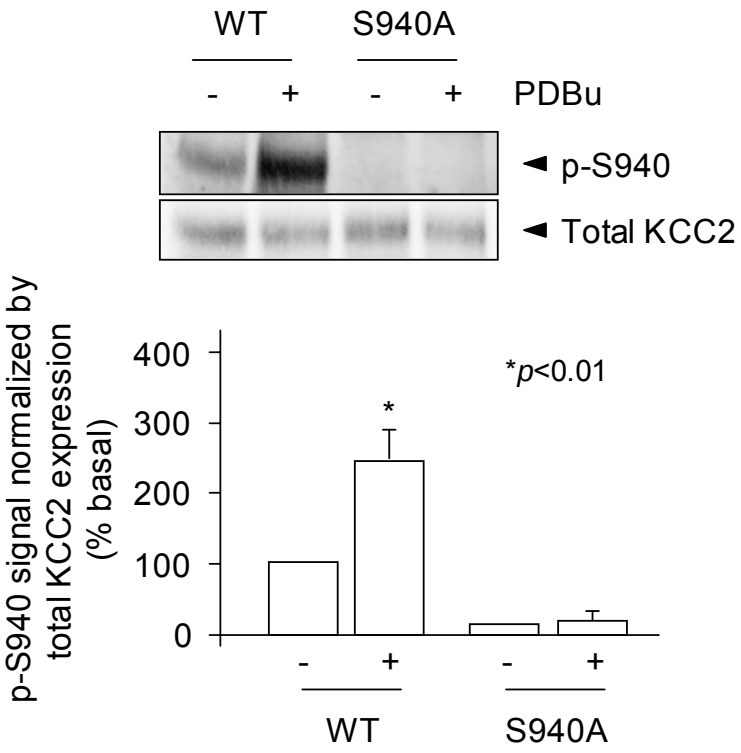

Fig. 4.2 p-S940 is specific to the phosphorylation of KCC2 expressed in HEK-293 cells. Cells transfected with KCC2-FL (WT and S940A) were treated with (+) or without (-) 500nM PDBu for 15min before cell lysis. Cell lysates were analyzed by SDS-PAGE and western blotting using p-S940. Anti-KCC2 antibody was used to detect the total amount of KCC2 on a separate blot to show equal loading of proteins. Quantification of p-S940 signal was normalized with that of total expression of KCC2. [*, significantly different from basal condition ($p < 0.01$; value = mean±SEM, Student's *t*-test, $n = 5$)]

bands between 150kDa and 180kDa were seen with p-S940. Detection of these bands was abolished with a molar excess (1mg/mL) of P-pep-S940. However, the signal of p-S940 was not affected by incubation of non-phospho-peptide, pep-S940 (Fig. 4.3). Another weak band above 200kDa was seen in different treatments of the blots, indicating that this is not specific to phosphorylation of Ser^{940}. Interestingly, when the blot was incubated with λ-phosphatase before incubation of p-S940, the phospho-specific signals were all removed (Fig. 4.4). λ-phosphatase is known to be a Mn^{2+}-dependent phosphatase that removes the phosphate group from serine, threonine and tyrosine residues (Cohen and Cohen, 1989). Therefore, the removal of p-S940 signal by λ-phosphatase treatment suggested that p-S940 specifically recognized the phosphate group of KCC2 on the blot.

In addition, KCC2 proteins were immunoprecipitated by anti-KCC2 antibody from cultured neurons and the products immunoblotted with p-S940. Results showed that treatment of PDBu significantly ($p<0.01$) increased phosphorylation of KCC2 by 195.4±55% compared to basal condition (Fig. 4.5). Interestingly, this result resembled that observed in whole-cell labeling experiments using [^{32}P]orthophosphoric acid (Fig. 3.19). Together, these results showed that p-S940 is specific to the phosphorylation of Ser^{940} of KCC2 by PKC in cultured hippocampal neurons.

4.3 Phosphorylation-specificity of purified p-S940 as determined by immunofluorescence staining

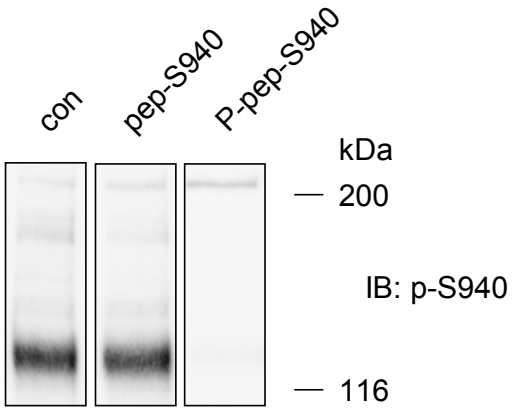

Fig. 4.3 Competition assay using phospho- and non-phospho-peptides of Ser^{940} of KCC2 in western blots of neuronal lysates. Cell lysate of cultured hippocampal neurons was resolved by SDS-PAGE followed by immunoblotting. During incubation of primary antibody p-S940, non-phospho-peptide (pep-S940) or phospho-peptide (P-pep-S940) was added in molar excess amount. In control experiment (con) neither of the peptides was added. The binding of p-S940 to the membrane was recognized by HRP-conjugated polyclonal anti-rabbit IgG.

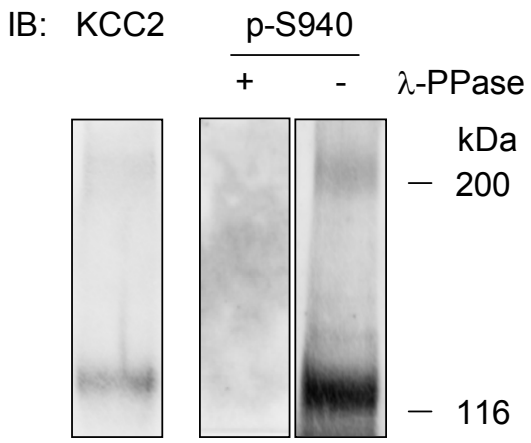

Fig. 4.4 The effect of λ-phosphatase treatment on western blots before p-S940 incubation. Cell lysate from cultured hippocampal neurons was resolved by SDS-PAGE and proteins transferred onto nitrocellulose membrane. Blots were treated with (+) or without (-) λ-phosphatase (λ-PPase). The treated membranes were then immunoblotted with p-S940. On a separate blot, the expression of total KCC2 was determined by immunoblotting with anti-KCC2 antibody.

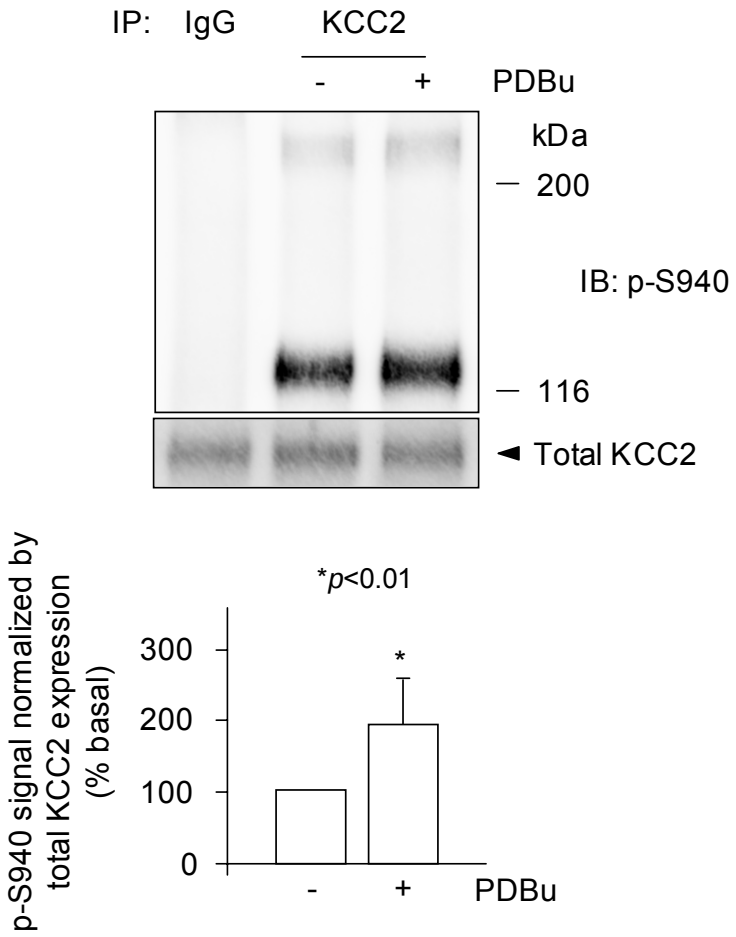

Fig. 4.5 p-S940 is specific to the phosphorylation of immunoprecipitated KCC2 from hippocampal neurons. Cultured hippocampal neurons were treated with (+) or without (-) 500nM PDBu for 15min before cell lysis and immunoprecipitation (IP) of KCC2. Non-specific rabbit IgG was a negative control for IP. Proteins after IP were resolved by SDS-PAGE followed by immunoblotting (IB) using p-S940. The total amount of KCC2 in each lane was analyzed by anti-KCC2 antibody on a separate blot. Quantification of p-S940 signal was normalized with that of total expression of KCC2. [*, significantly different from basal condition ($p < 0.01$; value = mean±SEM, Student's *t*-test, $n = 3$)]

In addition to western blotting the specificity of p-S940 was tested in immunofluorescence staining using HEK-293 cells expressing KCC2-FL and the S940A mutant. After PKC activation, cells were fixed and immunostained with anti-KCC2 antibody and p-S940 coupled to fluorescein isothiocyanate (FITC)- and tetramethyl rhodamine isothiocyanate (TRITC)-conjugated secondary antibodies respectively. It was found that p-S940 staining co-localized exclusively with KCC2 staining, indicating its specificity to KCC2. Furthermore, p-S940 can detect basal phosphorylation of WT KCC2 expressed in HEK-293 cells (Fig. 4.6). Significantly, the signal detected by p-S940 appeared to be increased by exposure to PDBu (Fig. 4.6). On the other hand, anti-KCC2 recognized the expression of S940A mutant of KCC2 in HEK-293 cells; however, no signal was detected by p-S940 in these cells before and after treatment of PDBu (Fig. 4.6), indicating the specificity of p-S940 to PKC phosphorylation of KCC2 in an immunostaining application. To complement these experiments with recombinant KCC2, cultured hippocampal neurons were also used for immunostaining experiments. After PKC activation hippocampal neurons were stained with anti-KCC2 antibody and p-S940 coupled to FITC- and TRITC- conjugated secondary antibodies respectively. Twenty cells each from a PKC-activated dish and a control dish were randomly chosen and for each cell a stack of confocal images along the vertical axis were taken. Each stack of confocal images was compressed together using the MetaMorph program to form a 3-D reconstruction of a neuronal cell. The pixel intensity of KCC2 staining and p-S940 staining of the dendritic regions of each cell was recorded. Similar to the results in HEK-293 cells, p-S940 staining

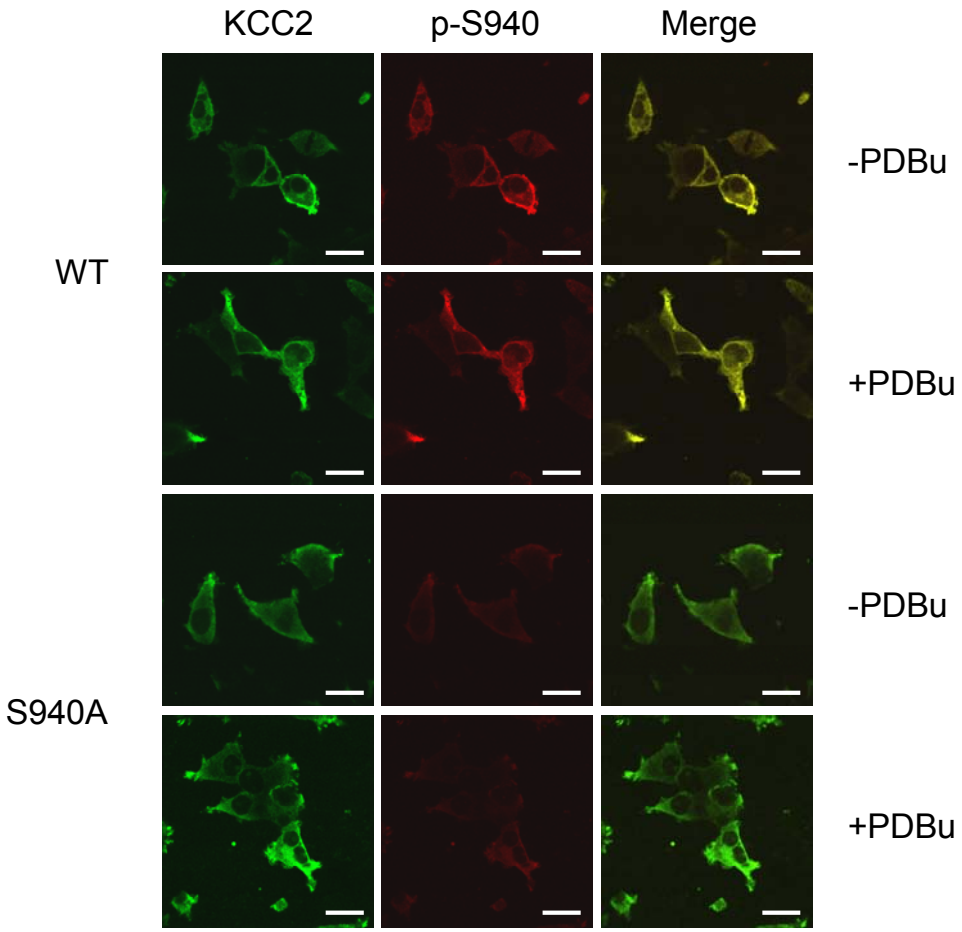

Fig. 4.6 Immunofluorescence staining showing that p-S940 is specific to phosphorylation of KCC2 expressed in HEK-293 cells. Cells expressing KCC2 (WT and S940A) were subjected to immunostaining in the presence (+) or absence (-) of 500nM PDBu. Anti-KCC2 antibody and p-S940 were used and were coupled to FITC- and TRITC-conjugated secondary antibodies respectively. Scale bar = 50μm.

overlaps exclusively with KCC2. Interestingly, endogenous KCC2 proteins were also shown to be basally phosphorylated (Fig. 4.7). Furthermore, treatment of PDBu significantly (p<0.005) increased p-S940 signal in dendrites to 205.6±45.5% of basal value after normalized with that of total KCC2 (Fig. 4.7). These experiments reinforced that p-S940 is specific to phosphorylation of KCC2 at Ser^{940} and again showed the utility of this antibody in immunostaining applications.

4.4 Regulation of Ser^{940} phosphorylation by PKC activity in cultured neurons

Given the ability of p-S940 to specifically detect KCC2 phosphorylated on Ser^{940} the role that PKC activity plays in regulating the phosphorylation of this individual residue was addressed. To achieve this goal 4-5 week-old cultures were treated with PDBu for 10, 20 and 30min before cell lysis. This experiment serves to determine whether phosphorylation at Ser^{940} is stable upon PKC activation since the phosphorylation of many proteins appears to be biphasic (Brandon et al., 2000). It was found that phosphorylation of Ser^{940} was increased significantly (p<0.01) to 223±5.4% of basal value in 10min (Fig. 4.8). Intriguingly, this increase in phosphorylation was maintained steadily throughout a 30-min period while total expression of KCC2 remained unchanged.

To further examine the role of PKC in mediating phosphorylation of Ser^{940} the effects of calphostin C (CalC), a specific PKC inhibitor on basal

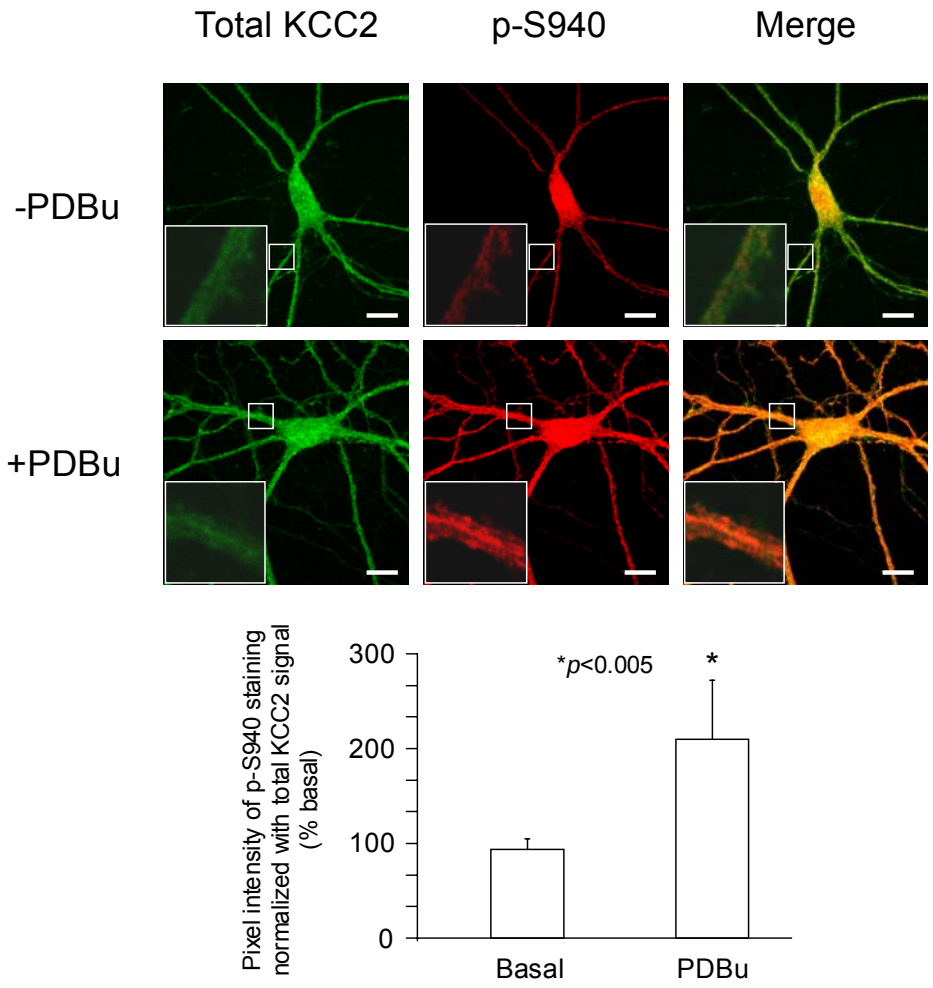

Fig. 4.7 Immunofluorescence staining showing that p-S940 is specific to phosphorylation of KCC2 in cultured hippocampal neurons. Cultured hippocampal neurons were subjected to immunostaining under basal conditions (-PDBu) or after treatment of 500nM PDBu for 15min (+PDBu). Anti-KCC2 antibody and p-S940 were used and coupled to FITC- and TRITC-conjugated secondary antibodies respectively. The level of p-S940 signal was quantified and normalized with that of total KCC2 expression in the lower panel. Scale bar = 50μm. [*, significantly different from basal condition ($p < 0.005$; value = mean±SEM, Student's *t*-test, $n = 15$)]

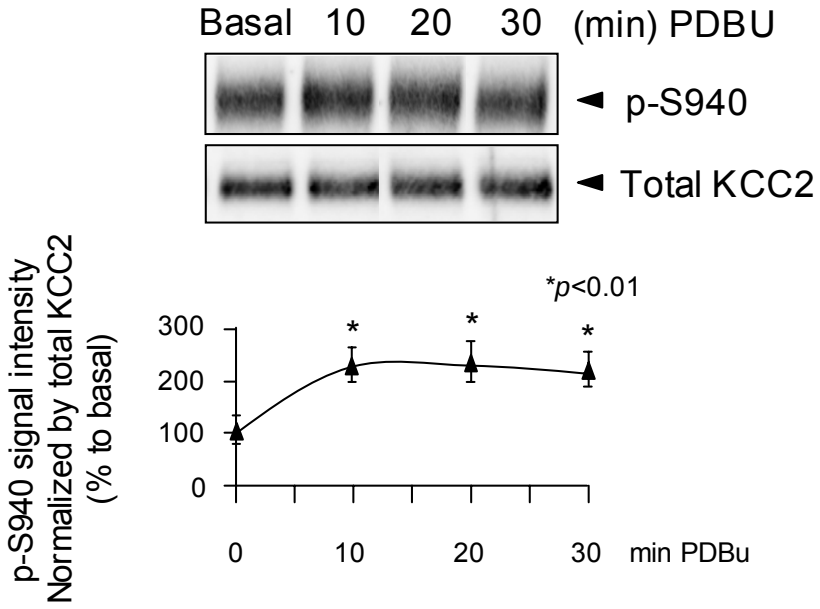

Fig. 4.8 Activation of PKC by PDBu was detected by p-S940 antibody. Cultured hippocampal neurons were treated with 500nM PDBu from 10min to 30min. Cell lysates were then collected and resolved by SDS-PAGE followed by western blotting. Upper panel: p-S940 antibody was used in western blotting to detect phosphorylation of KCC2. Anti-KCC2 antibody was used on another blot to show equal amount of total KCC2 protein. Lower panel: the amount of phosphorylation of KCC2 during 30min of PDBu treatment was quantified. [*, significantly different from basal condition ($p < 0.01$; value = mean±SEM, Student's *t*-test, $n = 3$)]

phosphorylation of this residue, were analyzed. Using 100nM CalC, the phosphorylation level of Ser^{940} was reduced significantly ($p<0.01$) to 78.09±8.18% of control (Fig. 4.9). These results thus suggest that phosphorylation of Ser^{940} is regulated by PKC activity. However, the incomplete blockade of basal phosphorylation by CalC suggests that phosphorylation of Ser^{940} is likely mediated by other kinases.

4.5 The dephosphorylation of Ser^{940} is mediated via PP1/PP2A/PP2C

The dephosphorylation of serine/threonine residues is mediated via the specific protein phosphatase (PP) including PP1, PP2A, PP2B and PP2C (Cohen, 1989). To find out which phosphatase was responsible for dephosphorylation of Ser^{940}, okadaic acid (OA) was employed. As measured using *in vitro* analysis OA inhibits PP1 with an IC_{50} of 20nM, PP2A with an IC_{50} of 0.2nM, while PP2B is much less sensitive to this agent (IC_{50} = 5μM) (Cohen, 1989). In contrast PP2C is not sensitive to OA. Treatment of 4-5 week-old cultured neurons with OA at 100nM significantly increased phosphorylation of Ser^{940} to 192±14.4% of control (Fig. 4.10). This indicated that dephosphorylation of Ser^{940} was carried out by PP1 and PP2A. To investigate whether PP2B or calcineurin was involved in regulation of Ser^{940} phosphorylation cyclosporin A, a specific inhibitor of calcineurin, was used. Interestingly, it was found that cyclosporin A did not significantly change the phosphorylation level of Ser^{940} (Fig. 4.11), suggesting that calcineurin is not involved in dephosphorylation of Ser^{940}. Together these results suggest a predominant role for PP1/PP2A, but not PP2B, in dephosphorylation of Ser^{940} in KCC2.

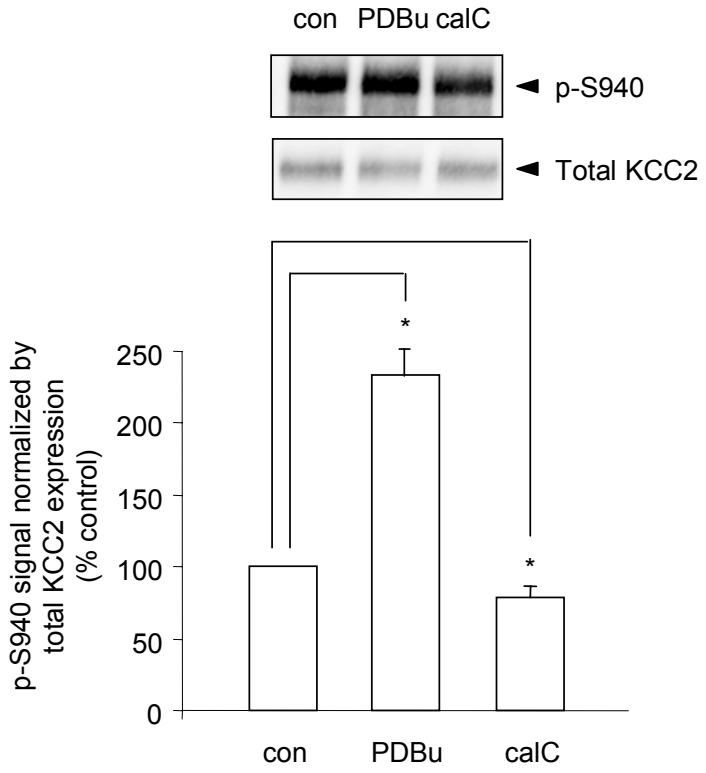

Fig. 4.9 The effect of PKC inactivation on Ser^{940} phosphorylation. Cultured hippocampal neurons were treated with 100nM PDBu (PDBu) or 100nM calphostin C (CalC) for 10min before cell lysis. Proteins were resolved by SDS-PAGE followed by immunoblotting using p-S940. Signals from p-S940 between control (con), PDBu and CalC were quantified and compared. [*, significantly different from control condition ($p < 0.01$; value = mean±SEM, Student's *t*-test, $n = 3$)]

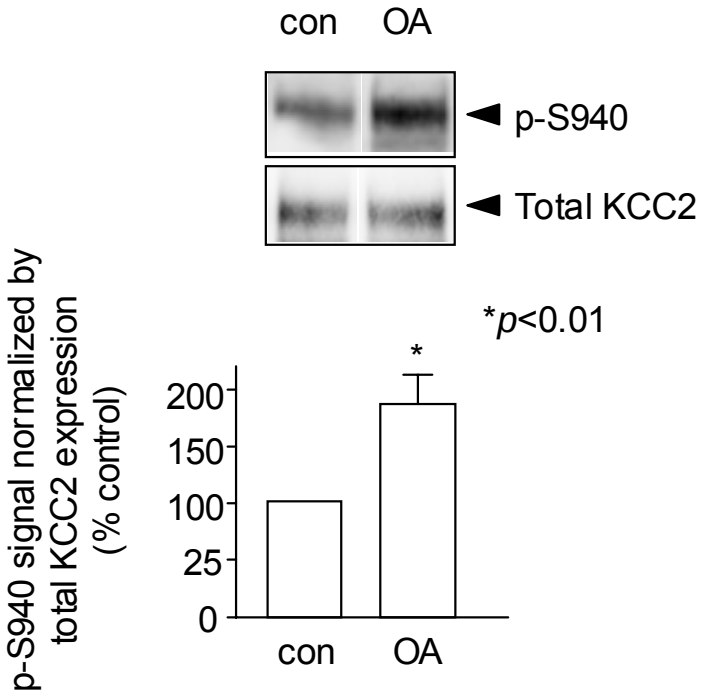

Fig. 4.10 The effect of phosphatase inhibitor on Ser^{940} phosphorylation. Cultured hippocampal neurons were treated with 100nM okadaic acid (OA) for 15min before cell lysis. Cell lysates were resolved by SDS-PAGE followed by western blotting using p-S940 antibody. Signals from p-S940 between control (con) and OA were quantified and compared. [*, significantly different from control ($p < 0.01$; Student's t test, $n = 3$)]

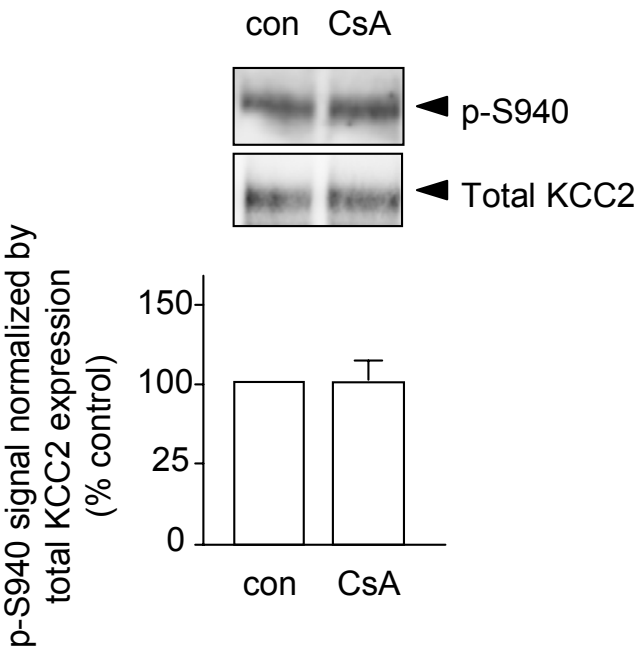

Fig. 4.11 The effect of calcineurin inhibitor on Ser^{940} phosphorylation. Four-week-old cultured hippocampal neurons were treated with 20μM cyclosporin A (CsA), a specific calcineurin inhibitor, for 15min. Proteins collected after cell lysis were resolved by SDS-PAGE and analyzed by western blotting using p-S940. Signals from p-S940 between control (con) and CsA were quantified and compared.

Because it is difficult to control for drug penetration in these experiments the dephosphorylation of Ser^{940} was also analyzed *in vitro* using purified kinase preparations. For these experiments His-C was first phosphorylated by purified PKC *in vitro* in the presence of ATP for 15min. The products were then washed extensively with PBS to stop kinase activity. The phosphorylated proteins were incubated with different purified phosphatases and respective buffers (refer to section 2 methods) for 15min at 30ºC. For control experiment, proteins were incubated with buffers without phosphatase. It was found that PP1 and PP2A were involved in dephosphorylation of Ser^{940} (Fig. 4.12). The phosphorylation level was reduced to 28.3±15.5% and 38±6.4% of that of control respectively. Importantly, PP2B did not change the level of phosphorylation of His-C significantly (Fig. 4.12). These results were consistent with the studies in neurons using OA and cyclosporin A (Figs. 4.10 and 4.11). Moreover, it was found that PP2C was able to dephosphorylate His-C *in vitro* to 42.1±9.4% of control value (Fig. 4.12).

Discussion

In this chapter, the development of a polyclonal antibody specific to the phosphorylation state of Ser^{940} of KCC2, namely p-S940, was documented. Since this phospho-specific antibody was newly raised in our laboratory, it is crucial to test for its specificity using different techniques, including western blotting and immunocytochemistry as described previously (Jovanovic et al., 2004; Kuramoto et al., 2007).

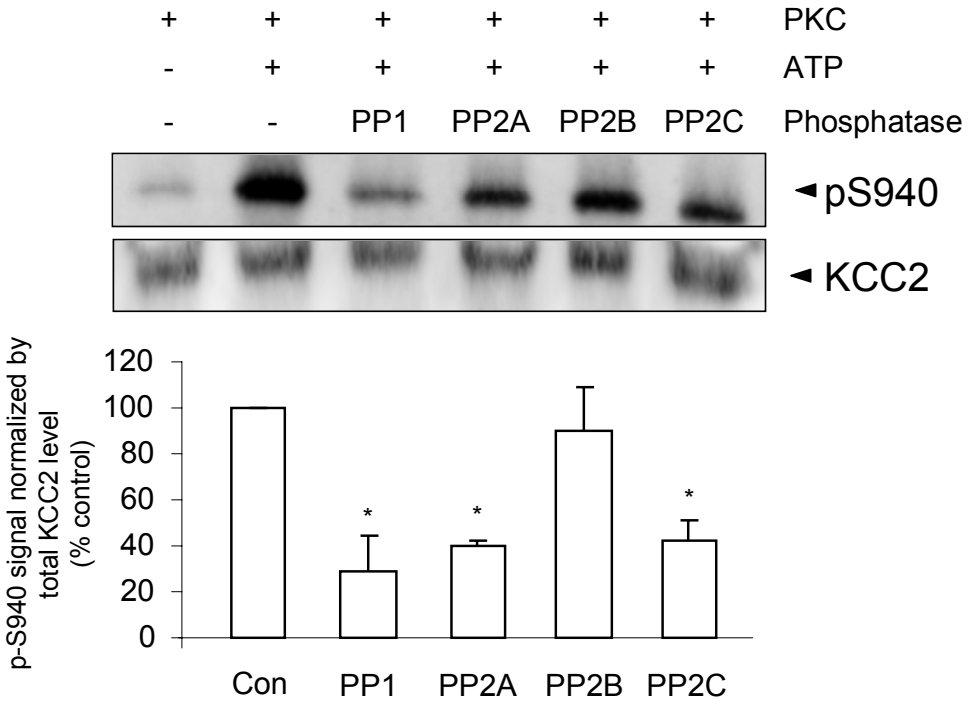

Fig. 4.12 Dephosphorylation of His-C *in vitro*. Purified His-C was first phosphorylated in an *in vitro* kinase assay using ATP and purified PKC. Phosphorylated proteins were bound to Ni^{2+} resin and washed extensively before incubation with phosphatases including PP1, PP2A, PP2B and PP2C for 15min. Proteins were then washed again and resolved by SDS-PAGE. Phosphorylation of the proteins was monitored using p-S940 antibody. Phosphorylation level of His-C after dephosphorylation was compared to that of control (without phosphatase incubation). Antibody against KCC2 was used to demonstrate the presence of equal amount of His-C in each reaction. [*, significantly different from control ($p < 0.01$; Student's t test, $n = 3$)]

The antibody was first tested using fusion protein His-C, which was phosphorylated by PKC *in vitro*. It was shown that p-S940 could recognize His-C on western blots when phosphorylated. By contrast, non-phosphorylated His-C was not recognized by p-S940.

In addition to studies using fusion proteins, specificity of p-S940 was demonstrated in cultured cells using western blotting. Here, KCC2 expressed in HEK-293 cells and endogenous KCC2 in cultured hippocampal neurons was shown to have basal phosphorylation at Ser^{940}. Moreover, activation of PKC significantly increased the signal of p-S940, while total KCC2 level was not affected. These results are similar to those seen in whole-cell labeling experiments using [^{32}P]orthophosphoric acid in the previous chapter. However, the increase in p-S940 signal upon PKC activation was less than the overall increase using the same treatment observed in whole-cell labeling experiments. This can be explained by the fact that phosphorylation sites other than Ser^{940} were phosphorylated upon PKC activation. In chapter 3 it was shown that Ser^{728} and Ser^{1034} may play roles in phosphorylation of KCC2. Tyrosine phosphorylation of KCC2 was also observed using tyrosine phosphatase inhibitor sodium pervanadate. There is a possible cross-talk between PKC and PTK signaling pathways (Burry, 1998; Morishita et al., 2007) (See also section 6.1). Apart from PKC activation, specificity of p-S940 was further demonstrated by λ-phosphatase treatment of western blot and competition assay using a phospho-peptide of Ser^{940}. The complete removal of p-S940 signal in those experiments strongly suggests that this antibody is specific to the phosphorylation state of Ser^{940}.

In addition to western blotting, immunocytochemistry was employed to demonstrate the specificity of p-S940. When KCC2 was expressed in HEK-293 cells, p-S940 recognized phosphorylation only of WT KCC2, not S940A mutant. Furthermore, PKC activation increased p-S940 signal of WT KCC2, indicating its specificity. Similarly, immunostaining of cultured hippocampal neurons using p-S940 revealed that phosphorylation of KCC2 was significantly increased by activation of PKC, a result consistent with western blot studies.

After establishing the specificity of p-S940, this antibody was employed to further investigate the phosphorylation of Ser^{940}. First, phosphorylation of Ser^{940} was investigated in a time course of PKC activation. It was found that the phosphorylation of Ser^{940} in mature neurons was increased during 10min of PKC activation and its level stayed the same for 30min, which is comparable to that observed in *in vitro* phosphorylation of His-C. Phosphorylation depends on an orchestrated action of kinases and phosphatases inside cells; therefore the identity of the phosphatase that dephosphorylates Ser^{940} was also explored. Using selective inhibitors of phosphatases, it was shown that both PP1 and PP2A dephosphorylated Ser^{940}, while PP2B did not. To complement this study, an *in vitro* dephosphorylation assay using His-C and [γ-^{32}P]ATP was employed. In addition to PP1 and PP2A, PP2C was also found to be involved in the dephosphorylation of Ser^{940}.

Chapter 5 Phospho-dependent modulation of KCC2 cell surface expression and activity

Introduction

It was established in the previous chapters that KCC2 is directly phosphorylated by PKC and the Src family tyrosine kinase. To study how these phosphorylation events regulate the function of KCC2, its cell surface expression and co-transport activities were investigated. KCC2 carries out its function by co-transporting K^+ and Cl^- across the neuronal membrane; therefore its cell surface expression is crucial in determining its efficacy in co-transport function. To measure the cell surface expression of KCC2, a biotinylation assay was employed as described previously (Fairfax et al., 2004). First, the amount of cell surface KCC2 under PKC activation was determined by immunoblotting. Using a biotinylation method, labeled proteins were allowed to undergo endocytosis and the rate of endocytosis of KCC2 was also determined. To demonstrate the essential role of Ser^{940} in KCC2 cell surface expression and endocytosis, mutant S940A was expressed in HEK-293 cells and its response to PKC activation was compared to that of WT KCC2. Immunostaining of KCC2 was employed to confirm the results from cell surface biotinylation. Here, the subcellular distribution of KCC2 was recorded by measuring the signal intensity of a line scan across a cell expressing KCC2 molecules. The effect of PKC activation on the distribution of KCC2 was then compared.

KCC2 co-transport activity was also directly assessed by an $^{86}Rb^{+}$ influx assay in HEK-293 cells. Due to the similar atomic size between $^{86}Rb^{+}$ and K^{+}, the former was used as a substitute for K^{+} to monitor the influx rate of ions in an isotonic condition. The role of PKC activation on KCC2 activity was first demonstrated in HEK-293 cells expressing KCC2 molecules. To investigate the role of Ser^{940} in mediating KCC2 function under PKC activation, S940A mutant was used and compared to WT KCC2. Overall, this chapter focuses on the functional consequence of phosphorylation of KCC2 molecules. Specifically, the aims of this chapter are:

1) To show that cell surface expression of KCC2 is modified upon phosphorylation by PKC.
2) To show that endocytosis of KCC2 is modified upon phosphorylation by PKC and that phosphorylation of Ser^{940} is essential in this process.
3) To show that subcellular distribution of KCC2 is modified upon phosphorylation by PKC.
4) To show that KCC2 co-transport activity is altered by phosphorylation mediated by PKC.

Results

5.1 Investigation of cell surface expression of KCC2 using biotinylation

The biotinylation labeling method was used to quantify the amount of KCC2 expressed on the cell surface of HEK-293 cells. Cell surface proteins were

labeled with Sulfo-NHS-SS-Biotin (Thermo Fisher Scientific, Inc.), which binds covalently to any available primary amines. After extensive washing, HEK-293 cells expressing KCC2 were lysed and proteins labeled with Sulfo-NHS-SS-Biotin were captured by NeutrAvidin resin. Labeled proteins were eluted by reducing reaction using 0.2M β-mercaptoethanol and resolved by SDS-PAGE. The amount of cell surface KCC2 was then quantified by immunoblotting with anti-KCC2 antibody and expressed as a percentage of the total fraction of the cell. It was found that 22.9±4.5% of WT KCC2 was present on the cell surface at steady state, and this could be increased significantly (p<0.01) to 40.6±5.4% in 15min upon activation of PKC (Fig. 5.1). Interestingly, 38.7±4.6% of S940A mutant of KCC2 was found in biotin-labeled fraction at steady state, a level significantly higher than that of WT. However, PDBu treatment did not significantly increase the cell surface expression of this mutant (Fig. 5.1), suggesting that phosphorylation of Ser^{940} is essential to the change of KCC2 cell surface level upon PKC activation. To confirm this result, a biotinylation assay was performed on cultured hippocampal neurons. It was found that activation of PKC with PDBu produced a significant increase (p<0.001) in neuronal cell surface KCC2 to 395.6±9.9% of control, an effect that was blocked by a specific PKC inhibitor, calphostin C (Fig.5.2).

5.2 Endocytosis of KCC2 in HEK-293 cells is modified by PKC activation

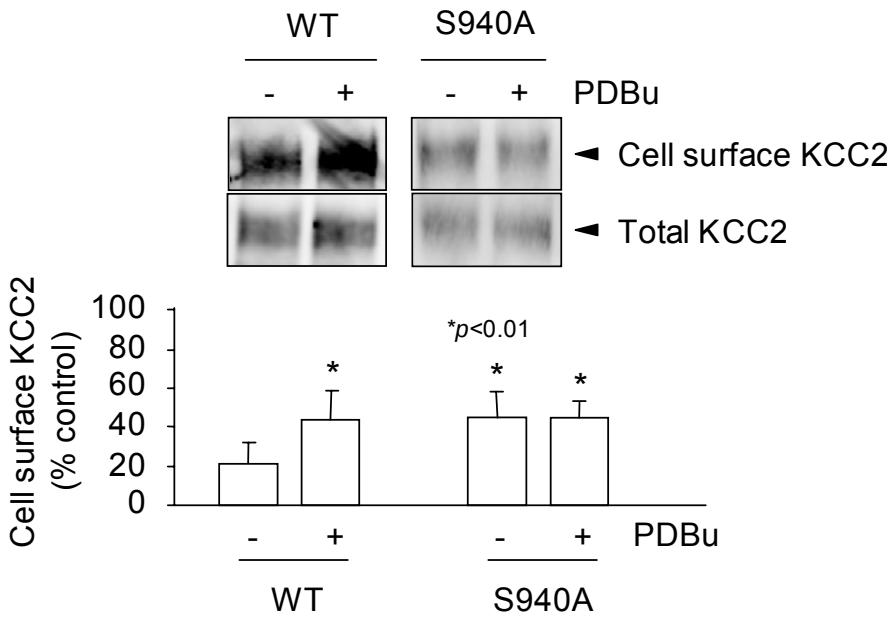

Fig. 5.1 Biotinylation assay of KCC2 expressed in HEK-293 cells. Cells transfected with KCC2-FL (WT and S940A mutant) were treated with (+) or without (-) 500nM PDBu for 15min. Cell surface proteins labeled by Sulfo-NHS-SS-Biotin were pulled down by NeutrAvidin resin. Proteins were then resolved by SDS-PAGE followed by western blot. On a separate blot, 1% of total lysate was loaded and the amount of KCC2 was determined by anti-KCC2 antibody. [*, significantly different from basal condition ($p < 0.01$; value = mean±SEM, Student's *t*-test, $n = 4$)]

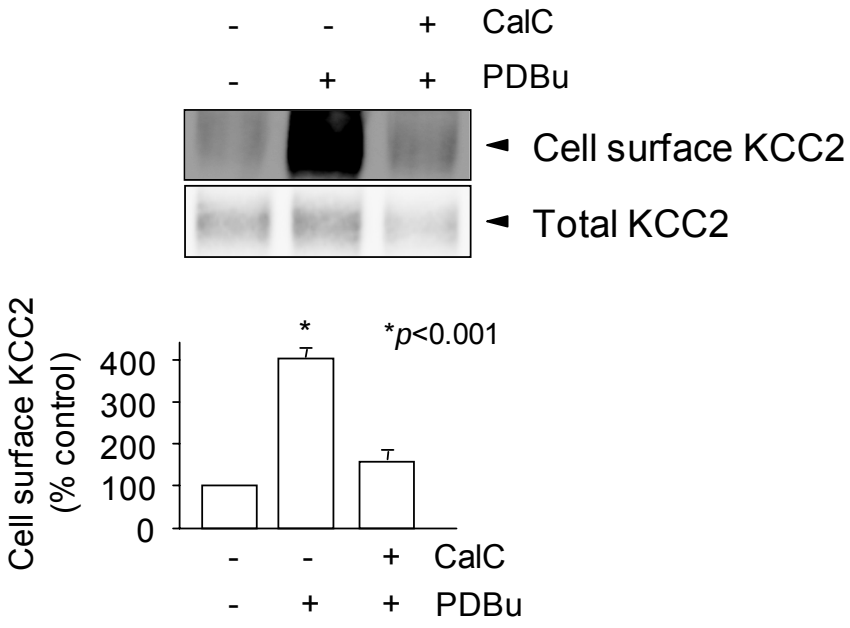

Fig. 5.2 The effect of PKC activation on cell surface KCC2 in cultured hippocampal neurons. Cultured hippocampal neurons were treated with 500nM PDBu for 15min or co-treated with 100nM Calphostin C (CalC) before cell surface proteins were labeled with Sulfo-NHS-SS-Biotin. Biotin-labeled cell surface proteins were purified on NeutrAvidin resin and resolved by SDS-PAGE. Western blotting using anti-KCC2 antibody was used to quantify the amount of KCC2 in cell surface fraction and in total lysate. [*, significantly different from basal condition ($p < 0.001$; value = mean±SEM, Student's *t*-test, $n = 5$)]

The cell surface stability of a protein is affected by several factors, including the rate of endocytosis, the rate of surface insertion, and the rate of protein recycling (Fig. 5.3). To examine if PKC modulates KCC2 endocytosis, HEK-293 cells transfected with KCC2-FL WT and S940A mutant were labeled with Sulfo-NHS-SS-Biotin and endocytosis was allowed to proceed at 37ºC for up to 20min. To prevent lysozomal degradation of any internalized proteins, 1μM leupeptin was added. After endocytosis and cleavage of remaining cell surface biotin with reduced glutathione, cells were lyzed and internalized biotinylated proteins captured by NeutrAvidin resin. The isolated proteins were then resolved by SDS-PAGE and analyzed by western blotting using KCC2 antibody.

It was found that the entire cell surface population of KCC2 was endocytosed within 10min under basal condition (Fig. 5.4). The process was linear over the initial 5min period of the assay (Fig. 5.4). Under control conditions 80.7±8.2% of the total cell surface population of KCC2 was internalized within 5min, whereas in the presence of PDBu internalization was reduced significantly (p<0.001) to 30.5±4.5% (Fig. 5.5). Interestingly, the endocytosis of the S940A mutant of KCC2 appeared to be significantly slower than that of WT over a time course of 20min in the presence or absence of PKC activation (Fig. 5.4). At 5min under control conditions, the amount of endocytosed KCC2 S940A was 15.6±3.2% of total cell surface population, a level significantly lower than that of WT (Fig. 5.5). However, in contrast to WT, PDBu treatment did not significantly alter the endocytosis of S940A mutant (Fig. 5.5).

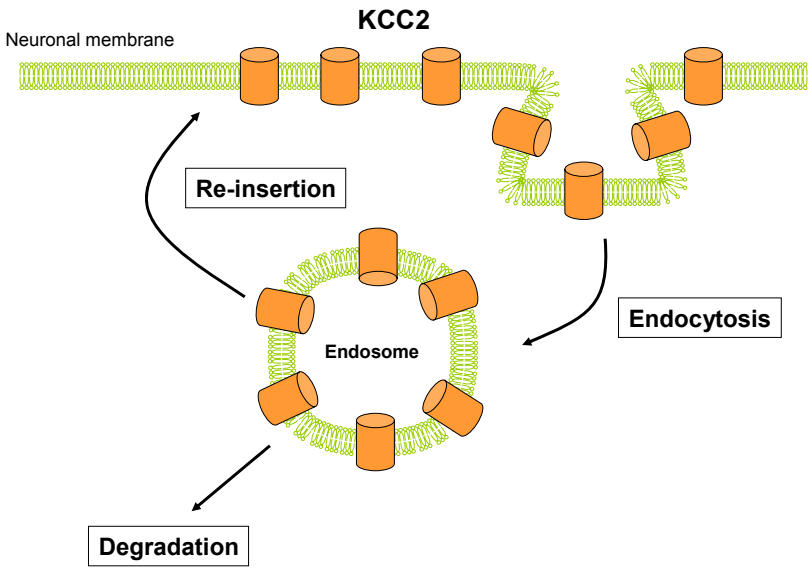

Fig. 5.3 Factors contributing to cell surface stability of KCC2. Cell surface protein expression is a summation of endocytosis, re-insertion, and degradation. The expression of KCC2 on neuronal membrane is used as a model in this diagram.

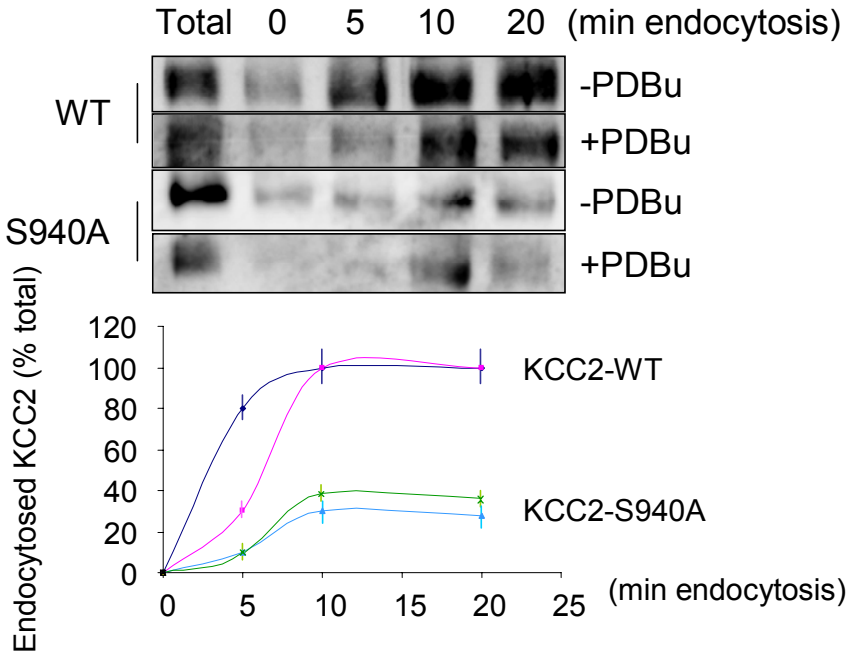

Fig. 5.4 Endocytosis of KCC2 in HEK-293 cells. Cells transfected with WT or S940A mutant of KCC2-FL were labeled with Sulfo-NHS-SS-Biotin and then incubated for varying time periods in the absence (-) or presence (+) of 500nM PDBu at 37°C to allow endocytosis. After cleavage by reduced glutathione the remaining biotinylated proteins were pulled down by NeutrAvidin resin and immunoblotted with KCC2 antibody. The percentage of endocytosed proteins was determined compared to total cell surface fraction (without cleavage).

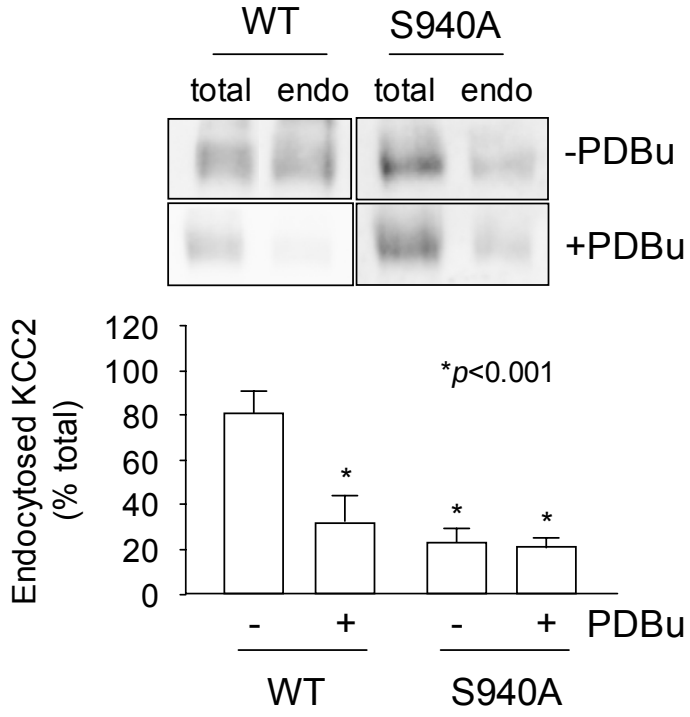

Fig. 5.5 Endocytosis of KCC2 in HEK-293 cells at 5min. The amount of cell surface KCC2 (WT and S940A) before endocytosis (total) and after 5min of endocytosis (endo) was compared. In addition, the effect of 500nM PDBu treatment on KCC2 endocytosis was shown. [*, significantly different from basal condition ($p < 0.001$; value = mean±SEM, Student's *t*-test, $n = 3$)]

5.3 Subcellular distribution of KCC2 shown by immunocytochemistry coupled to confocal imaging

To confirm the results using biotinylation, immunocytochemistry was used to measure the subcellular distribution of KCC2. HEK-293 cells transfected with KCC2-FL WT or S940A were fixed, permeabilized and stained with KCC2 antibody. Confocal images were taken from individual cells and the pixel intensity along a line scan of the mid-plane of each cell was recorded. In this way, the ratio of protein at cell periphery region to cytosol fraction can be calculated and this ratio can be an estimation of the distribution of a protein (KCC2 molecules) at a subcellular level. The effect of PKC activation on the subcellular distribution of KCC2 was also determined. It was found that PDBu significantly increased (p<0.01) the ratio of WT KCC2 molecules associated with the cell periphery by 182±7.2% of control (Fig. 5.6). However, in cells expressing S940A mutant, PDBu did not significantly change the subcellular distribution of KCC2 molecules (Fig. 5.6), results are consistent with those observed using a biotinylation method as outlined in section 5.1.

This immunocytochemistry experiment was repeated in cultured hippocampal neurons. Here, the level of KCC2 membrane expression was measured by the ratio of fluorescence signals associated with the cell surface and the cytoplasm of individual proximal dendrites along a line scan of a mid-plane as shown (Fig. 5.7). It was revealed that treatment of neurons with PDBu significantly increased (p<0.01) the level of KCC2 immunoreactivity at the periphery of dendrites to 175.5±19% of that of control neurons, but this effect was reduced

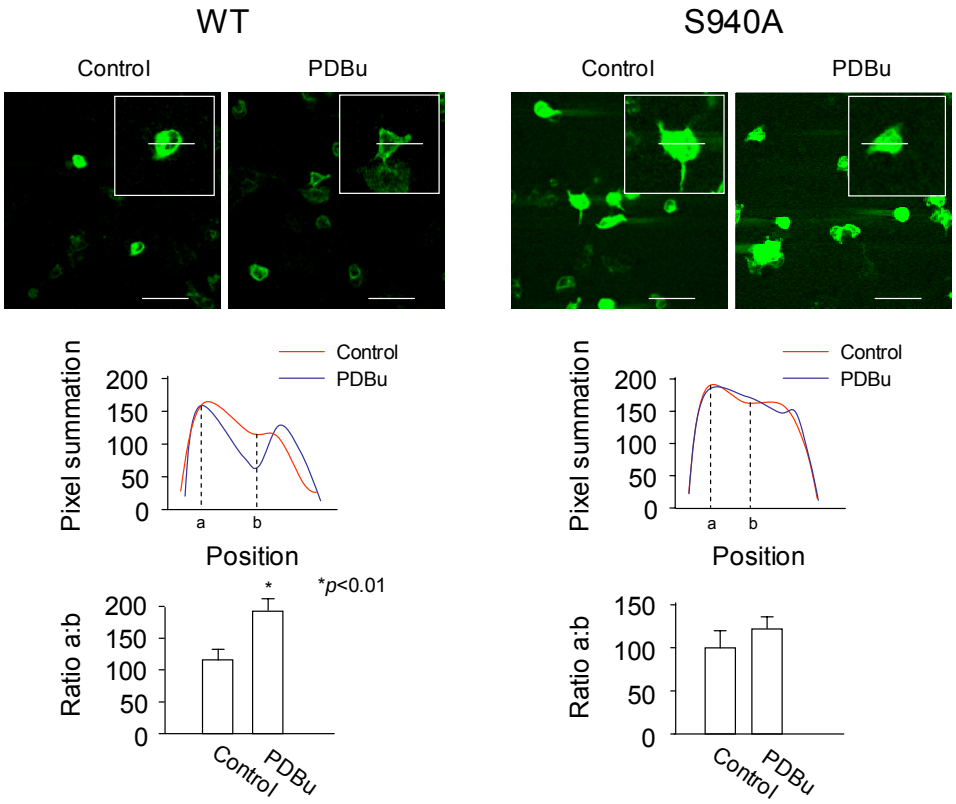

Fig. 5.6 Subcellular distribution of KCC2 in HEK-293 cells. HEK-293 cells transfected with KCC2-FL was fixed, permeabilized and immunostained with anti-KCC2. Confocal images of the cells were acquired and a line scan was performed along the mid-plane of the cells. The pixel summation of the line was quantified and the profile of cells under control conditions and treated with 500nM PDBu before fixation was compared. The ratio of signal intensity between membrane (position a) and cytoplasm (position b) of individual cells was also calculated and compared. Scale bar = 50μm. [*, significantly different from control condition ($p < 0.01$; value = mean±SEM, Student's *t*-test, $n = 15$)]

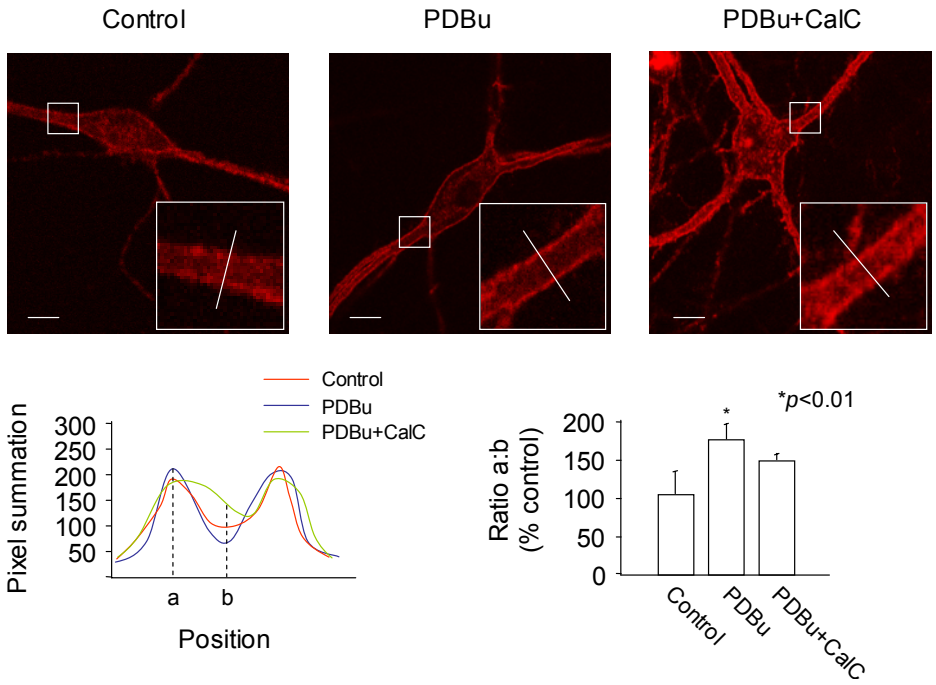

Fig. 5.7 Subcellular distribution of endogenous KCC2 in hippocampal neurons. Four-week-old hippocampal neurons were treated with 500nM PDBu and/or 100nM CalC for 10min. Neurons were fixed, permeabilized and stained with KCC2 antibody coupled to a TRITC-conjugated secondary antibody. Confocal images were then taken from the bottom to top of proximal dendrites and line scans across the dendrites performed on the mid-plane of the images as shown in insets. The summation of pixel intensity was calculated for cells with different drug treatments. The ratio of signal intensity between plasma membrane (position a) to cytosol (position b) was also calculated. Scale bar = 25μm. [*, significantly different from control ($p < 0.01$; value = mean±SEM, Student's *t*-test, $n = 20$)]

by inhibition of PKC (Fig. 5.7). In accordance with the biotinylation results, it appeared that PKC activation increased expression of KCC2 on neuronal cell surface.

5.4 K^+-Cl^- cotransport activity in HEK-293 cells

Using biochemistry and immunofluorescence it was shown in the previous sections that activation of PKC increased cell surface expression of KCC2 in HEK-293 cells and cultured hippocampal neurons. To directly investigate the functional activity of KCC2 upon PKC activation, a furosemide-sensitive $^{86}Rb^+$ influx assay was employed. This experiment was conducted by Jeff Williams in collaboration with the laboratory of Dr. John Payne at UC Davis. HEK-293 cells were initially transfected with KCC2-FL WT or a series of mutants including S728A, T787A, S940A, S1034A and double mutants S940/1034A and S728/940A. On the day of experiment cells were treated with bumetanide and ouabain to inhibit Na^+-K^+-$2Cl^-$ co-transporter and Na^+-K^+-ATPase respectively. KCC2 activity was then measured by $^{86}Rb^+$ accumulation over a 3-5min time course. Experiments were repeated with furosemide to inhibit KCC2 activity and the difference was recorded as furosemide-sensitive $^{86}Rb^+$ influx, an indicator of KCC2 activity. As a negative control vector-transfected cells showed no $^{86}Rb^+$ accumulation. By contrast, KCC2-FL WT-transfected cells showed a basal activity represented by $^{86}Rb^+$ accumulation. This activity was increased by 15min pre-incubation with N-ethylmaleimide (NEM), an accepted activator of KCC2 (Payne, 1997) (Fig. 5.8). Interestingly, treatment of

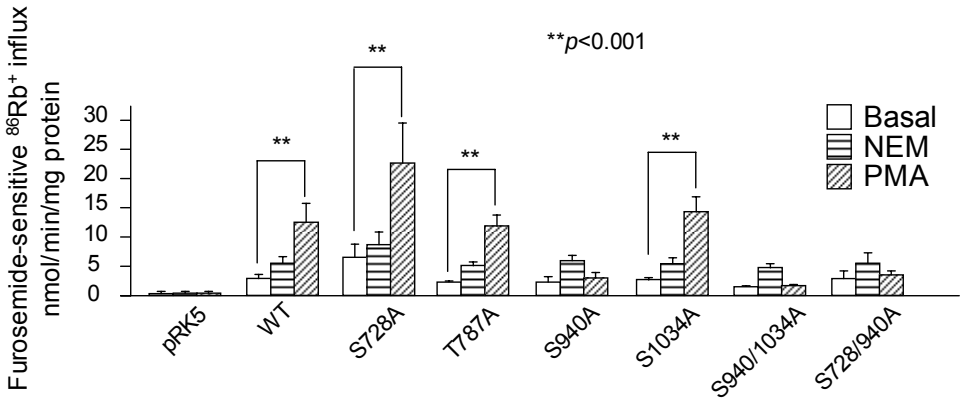

Fig. 5.8 PKC-dependent phosphorylation of KCC2 Ser^{940} modulates KCC2 activity. K^+-Cl^- co-transport activity was monitored 48h after transfection by measuring the furosemide-sensitive $^{86}Rb^+$ influx in cells expressing a series of KCC2 constructs or vector. Influx of $^{86}Rb^+$ was linear for 10min in all KCC2 constructs, and 3-5min influxes were routinely performed. HEK-293 cells were pretreated with 2μM bumetanide prior to the influx assay to inhibit endogenous Na^+-K^+-$2Cl^-$ co-transporter activity and 100μM ouabain to inhibit endogenous Na^+-K^+-ATPase. The level of $^{86}Rb^+$ influx is indicated under basal conditions or in the presence of 100nM PMA or 50μM NEM over a time course of 3-5min. [**, significantly different from basal condition (p < 0.001; value = mean±SEM, Student's t-test, n = 3)]

phorbol 12-myristate-13-acetate (PMA) significantly increased (p<0.001) KCC2 activity to 420±80.2% of basal condition (Fig. 5.8). Moreover, all other mutants of KCC2-FL showed comparable basal activity that was elevated by treatment with NEM; however, the effect of PMA was totally blocked by S940A alone (Fig. 5.8). This result demonstrated that KCC2 activity is modulated by direct phosphorylation of KCC2 Ser^{940}. The fact that mutant S940A is activated by NEM, indicates that NEM activates KCC2 in a manner that is perhaps not mediated by PKC.

Discussion

In this chapter, the effect of phosphorylation of KCC2 molecules on their cell surface stability and function was investigated. It was found that phosphorylation exerts a profound influence on KCC2 function in terms of its cell surface expression and co-transport function. KCC2 is a membrane protein that co-transports K^+ and Cl^- across neuronal membrane; therefore its cell surface expression is a major factor contributing to its overall function. A biotinylation method was first employed to investigate the cell surface expression of KCC2. Interestingly, results showed that activation of PKC significantly increased KCC2 expression at cell surface, which is in accord with a functional assay using $^{86}Rb^+$ to study co-transport activity. The endocytic rate of cell surface KCC2 was measured and compared during phosphorylation. The investigation of endocytosis of cell surface KCC2 serves to provide a cellular mechanism to regulate its cell surface expression. It was found that phosphorylation of KCC2 by PKC significantly slowed its rate of

endocytosis, thereby increasing its cell surface expression. In addition to biotinylation, immunocytochemistry was employed as a tool to study the subcellular distribution of KCC2 under the effect of activation of PKC. Intriguingly, activation of PKC promoted an accumulation of KCC2 proteins at the periphery of cells expressing KCC2 and also in the dendritic regions of cultured hippocampal neurons. These findings are also in accord with the biotinylation experiments and confirm the findings that activation of PKC promotes cell surface expression of KCC2 and hence its co-transport functions.

The possible mechanism of such accumulation of KCC2 after PKC activation may be due to its reduced binding to the clathrin adaptor protein AP2 in the endocytic pathway (Kittler et al., 2005). Since the association between AP2 and the protein is an essential step in this clathrin-mediated endocytosis, phosphorylation of KCC2 may structurally modify its binding site, and thus endocytosis is slowed. This in turn promotes an accumulation of KCC2 on cell surface. However, to date there is no direct evidence that Ser^{940} is a binding motif of AP2 and future investigation will be needed.

The role of Ser^{940} in the functional regulation of KCC2 was also investigated in this chapter. Mutant S940A was compared to WT in the biotinylation and immunocytochemistry experiments. It was found that S940A completely blocked the effect of PKC activation on KCC2 cell surface accumulation. S940A appeared to be more stable on the cell surface in steady state than was WT KCC2. From the endocytosis assay it was shown that S940A was less

effectively endocytosed, suggesting that phosphorylation of Ser^{940} is important for endocytosis of KCC2. This endocytosis assay also explained the fact that S940A is more stable on cell surface than is WT due to a reduced efficacy in endocytosis of KCC2 molecules in this phosphorylation-deficient mutant.

An augmented level of cell surface KCC2 molecules in the S940A mutant may imply a higher overall co-transport activity. However, in the $^{86}Rb^{+}$ flux assay it was found that the co-transport activity of S940A was not significantly different from that of WT, suggesting that S940A is intrinsically less effective in ion co-transport function. Furthermore, activation of PKC did not affect the co-transport function of S940A, indicating that functional regulation by PKC on this mutant is lost.

Chapter 6 Final discussion

To date the roles that post-translational modifications of KCC2 play in regulating its functional expression have remained elusive; however, while there has been no documentation of direct phosphorylation of KCC2, this process has been implicated in regulating its activity (Bergeron et al., 2006; Wake et al., 2007). Based on recent studies of KCC2 and other members of cation chloride co-transporters, the objectives of this study were: 1) to demonstrate that KCC2 is phosphorylated on specific residue(s) and identify the kinase(s) activities responsible for this phosphorylation, 2) to develop a phospho-specific antibody as a molecular tool to examine KCC2 phosphorylation, 3) to examine whether phosphorylation of KCC2 modulates its cell surface stability and membrane trafficking, and 4) to examine whether phosphorylation of KCC2 modulates its co-transport activities. This study therefore aims to provide a molecular understanding of the post-translational modifications that regulate KCC2 functional expression.

6.1 Evidence that PKC phosphorylates Ser^{940} in KCC2

To study phosphorylation of KCC2, a consensus sequence motif search was initially performed to identify putative phosphorylation sites in KCC2. It was revealed that both intracellular N-tail and C-tail of KCC2 contain PKC phosphorylation sites and a tyrosine phosphorylation site (Fig. 1.1). To evaluate the results from this sequence motif search, *in vitro* kinase assays were employed. Fusion proteins of intracellular domains of KCC2 (N-tail and C-tail)

were constructed with a C-terminal His-tag and purified from bacteria. It was found that PKC could phosphorylate the fusion protein of the C-tail, but not the N-tail, of KCC2. Interestingly, a single mutation of Ser^{940} in the C-tail intracellular domain of KCC2 significantly reduced the phosphorylation level of this fusion protein by PKC, suggesting an important role for Ser^{940} in KCC2 phosphorylation.

To confirm my *in vitro* studies, the phosphorylation of KCC2 was examined in cultured HEK-293 cells and hippocampal neurons. Whole-cell labeling experiments using [^{32}P]orthophosphoric acid were performed. The results confirmed that: 1) there is basal phosphorylation of KCC2, 2) activation of PKC increases phosphorylation of KCC2, and 3) mutation of Ser^{940} blocked the effect of PKC activation on KCC2 phosphorylation. These results provide the first evidence that KCC2 is directly phosphorylated. Significantly, Ser^{940} lies in a region unique to KCC2 as compared to other KCC members, suggesting a distinct role in neuronal-specific regulation.

The phosphorylation of KCC2 was also analyzed in hippocampal neurons. This analysis revealed that activation of PKC increases phosphorylation in serine residues and induces tyrosine phosphorylation (Fig. 3.21). Interestingly, the pharmacological agent used in this experiment was specific to activation of PKC. The observed tyrosine phosphorylation of KCC2 in neurons after PKC activation therefore suggested that tyrosine kinase may be activated by a PKC-dependent pathway which in turn phosphorylates KCC2. Interestingly, Pyk2, a member of the focal adhesion kinase family, is implicated as a molecular link

between PKC and Src (Lev et al., 1995). After activation by PKC, Pyk2 autophosphorylates on its residue Tyr^{402} (Girault et al., 1999), creates a Src homology 2 (SH2) ligand through which Pyk2 binds to the SH2 domain of Src (Dikic et al., 1996) and activates Src kinase by relieving autoinhibition (Thomas and Brugge, 1997). In chapter 3, experiments showed that tyrosine phosphorylation of KCC2 is strictly regulated by an unknown tyrosine phosphatase and Src kinase.

The study of phosphorylation at Ser^{940} was extended by the development of a phospho-specific antibody of KCC2. This antibody, p-S940, proved to be specific to the phosphorylated Ser^{940} in a number of tests including western blotting and immunofluorescence staining. This tool was first employed to study the dephosphorylation of Ser^{940}. It is known that dephosphorylation of the serine residue can be carried out by serine/threonine-specific protein phosphatases PP1, PP2A, PP2B and PP2C (Cohen, 1989). Western blotting using p-S940 in the presence of phosphatase inhibitor okadaic acid showed that PP1 and PP2A are responsible for dephosphorylation of KCC2 at Ser^{940}. These results were confirmed by *in vitro* phosphatase assay.

6.2 Phosphorylation of Ser^{940} modulates KCC2 trafficking and activity

Phosphorylation is the addition of a negatively charged phosphate group to serine, threonine or tyrosine residues of a protein (Edelman et al., 1987; Carpenter, 1992). This process usually results in a change of protein conformation and micro-domain environment of a protein. Studies have shown

that phosphorylation regulates numerous cellular processes including the intracellular trafficking of proteins (Billingsley and Kincaid, 1997), the degradation and the recycling of proteins (Evans and Cousin, 2005). In chapter 5, the effects of phosphorylation of KCC2 on its cell surface stability and functional activity were documented.

It was demonstrated that PKC activation increases cell surface expression of KCC2. This change in cell surface stability was blocked by a PKC-specific inhibitor and mutation of Ser^{940}. These results were confirmed using immunocytochemistry methods. Importantly, co-transport activity of KCC2 was also shown to be increased by PKC activation. This increase was blocked by a PKC-specific inhibitor and mutation of Ser^{940}.

The mechanism by which cell surface expression of KCC2 is modulated by PKC activity was also investigated. Steady-state cell surface expression of membrane proteins is dependent upon the relative rates of endocytosis, degradation and insertion (Turner et al., 1999; Evans and Cousin, 2005; Kittler et al., 2005). It was found that endocytosis of KCC2 was significantly reduced upon PKC activation, explaining the increase in cell surface stability observed in previous sections. Mutation of Ser^{940} confirmed that: 1) phosphorylation of Ser^{940} slows endocytosis of KCC2, and 2) Ser^{940} is responsible for regulation of KCC2 cell surface stability by PKC activity. Together, these results suggest a distinct role for Ser^{940} in KCC2 trafficking (Fig. 6.1).

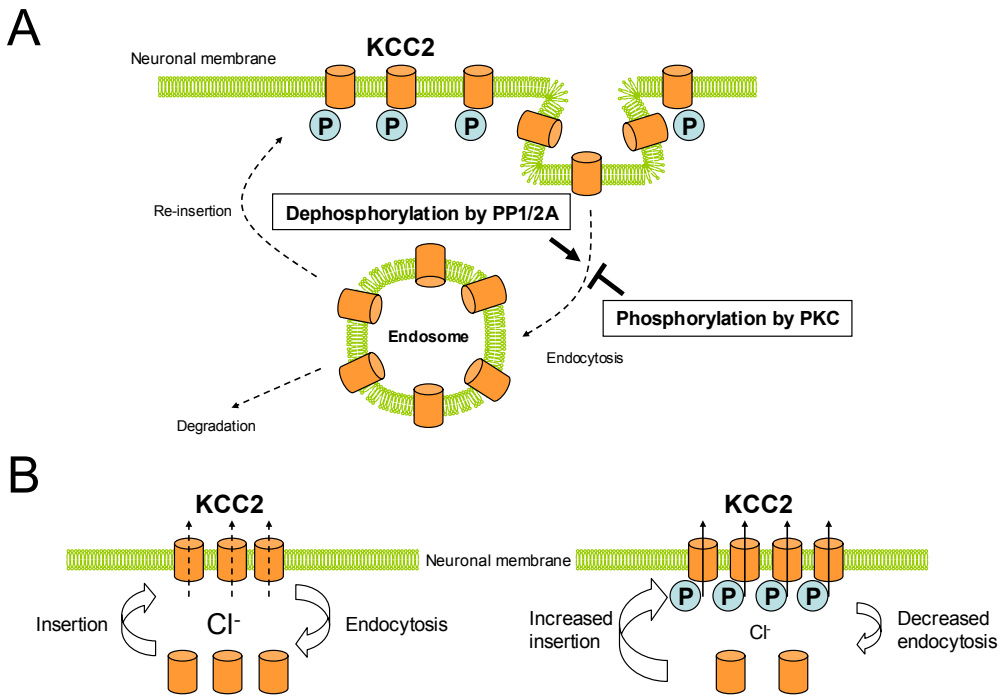

Fig. 6.1 Phospho-dependent modulation of KCC2 cell surface stability and function. A. Cell surface stability of KCC2 is affected by its endocytosis from cell membrane, degradation in intracellular compartment and re-insertion into cell membrane. Phosphorylation of KCC2 by PKC blocks the endocytosis of KCC2 while dephosphorylation of KCC2 mediated through PP1 and PP2A promotes endocytosis. **B.** At steady-state KCC2 plays a central role as the major Cl^- extruder in neurons. Phosphorylation of KCC2 increases its cell surface expression by decreasing its endocytosis and possibly increasing its insertion rate. This leads to an overall increase in co-transport function.

6.3 Modulation of KCC2 activity and its implication in neurological disorders

It has been shown that KCC2 activity generates a transmembrane Cl^- gradient in mature neurons such that activation of $GABA_A$ receptor results in an inward Cl^- current leading to hyperpolarization (Rivera et al., 1999). During neuronal development, the expression of KCC2 is up-regulated while the Cl^- importer NKCC1 is down-regulated (Wang et al., 2002). To date KCC2 has been found to function primarily as a molecular switch to determine the GABAergic response during neuronal development and the strength of synaptic inhibition in mature neurons (Rivera et al., 1999).

Since the expression and activity of KCC2 are highly associated with inhibitory synaptic transmission, precise regulation of KCC2 is crucial for fine-tuning of neuronal network activity. Malfunction or reduced expression of KCC2 has been reported in disease models related to epilepsy, a state in which neuronal network inhibition is compromised (Reid et al., 2001; Jin et al., 2005; Pathak et al., 2007; Shimizu-Okabe et al., 2007). There is also increasing evidence that disruption of the KCC2 gene leads to hyperexcitability or a decrease in the threshold of seizure generation (Woo et al., 2002; Tornberg et al., 2005); thus by regulating the activity of KCC2, the efficacy of inhibitory neurotransmitter can be modified. Results presented in this thesis show that PKC and tyrosine kinases regulate KCC2 phosphorylation. Activation of PKC increases co-transport function of KCC2 by increasing its cell surface stability, suggesting that PKC is an important target for altering neuronal inhibition. Furthermore, in

epilepsy models PKC and tyrosine kinase are regulated in an opposite manner (Funke et al., 1998; Pathak et al., 2007). This suggests that phosphorylation by PKC and tyrosine kinase may have profound effects on KCC2 function in epilepsy.

A recent study has shown that KCC2 is vital in neuronal development as it interacts structurally with cytoskeletal elements depending on the intracellular C-terminal domain of KCC2 (Li et al., 2007). However, this intracellular domain spans over 500 amino acids in length and the specific region responsible for this interaction remains unknown.

6.4 Future directions

In this thesis direct phosphorylation of KCC2 was first described and the functional consequences of this covalent modification were examined. However, KCC2 can also be regulated by other cellular modulators such as glycosylation, alkylation, protein interaction and ubiquitination. It will be interesting to evaluate whether KCC2 activity and its intracellular trafficking is affected by these cellular processes. For example, site-directed mutagenesis of putative glycosylation sites may be performed to investigate the effect of glycosylation on KCC2 cell surface expression and activity. Furthermore, the role of tyrosine phosphorylation in regulation of KCC2 needs to be explored. Activators or inhibitors of PTK can be employed to investigate the effect of tyrosine phosphorylation on KCC2 activity. It also remains unclear how KCC2 is endocytosed back to the intracellular domain, although the mechanism likely

involves the clathrin-coated pits of the AP2 complex. Experiments such as *in vitro* binding assay can be performed to investigate the association between KCC2 and AP2 complex.

Functionally, phosphorylation enhances KCC2 activity by increasing its cell surface expression. However, whether this process also modulates the intrinsic activity of KCC2 (i.e. the co-transport activity of each KCC2 molecule *per se*) requires further investigation.

A linkage between functional modulation of KCC2 activity and human pathology can be drawn. It is evident that KCC2 contributes to the onset of epilepsy due to an alteration in transmembrane Cl^- potential. Therefore an animal model with a mutated Ser^{940} site engineered into its KCC2 gene will give insights into how this residue is involved in KCC2 function *in vivo* and in such neuronal disorders as epilepsy. By deciphering the molecular mechanism that regulates KCC2 in disease states, therapeutic strategies can be designed based on enhancing KCC2 function.

6.5 Summary

KCC2 is subject to direct phosphorylation by PKC and tyrosine kinase Src in neurons. In particular, Ser^{940} in the intracellular domain of KCC2 is a major substrate of PKC. Studies using a phospho-specific antibody of KCC2 revealed that PKC and protein phosphatases PP1 and PP2A regulate phosphorylation of Ser^{940}. Activation of PKC increases cell surface expression of KCC2 and

promotes a subcellular distribution of KCC2 towards the axonal membrane. The accumulation of cell surface KCC2 upon PKC activation is due to a reduction in endocytosis, a process blocked by mutation of Ser^{940}. PKC activation also increases co-transport activity of KCC2. Mutation of Ser^{940} renders KCC2 insensitive to regulation by PKC. Together, this thesis describes an important regulatory role for PKC phosphorylation on cell surface expression, endocytosis and co-transport activity of KCC2 through the site Ser^{940} found in the intracellular domain of this co-transporter.

References

Adragna NC, Di Fulvio M, Lauf PK (2004) Regulation of K-Cl cotransport: from function to genes. The Journal of membrane biology 201:109-137.

Aguado F, Carmona MA, Pozas E, Aguilo A, Martinez-Guijarro FJ, Alcantara S, Borrell V, Yuste R, Ibanez CF, Soriano E (2003) BDNF regulates spontaneous correlated activity at early developmental stages by increasing synaptogenesis and expression of the K+/Cl- co-transporter KCC2. Development 130:1267-1280.

Bayatti N, Moss JA, Sun L, Ambrose P, Ward JF, Lindsay S, Clowry GJ (2007) A Molecular Neuroanatomical Study of the Developing Human Neocortex from 8 to 17 Postconceptional Weeks Revealing the Early Differentiation of the Subplate and Subventricular Zone. Cereb Cortex.

Becker KP, Hannun YA (2005) Protein kinase C and phospholipase D: intimate interactions in intracellular signaling. Cell Mol Life Sci 62:1448-1461.

Beckman ML, Bernstein EM, Quick MW (1998) Protein kinase C regulates the interaction between a GABA transporter and syntaxin 1A. J Neurosci 18:6103-6112.

Belelli D, Herd MB, Mitchell EA, Peden DR, Vardy AW, Gentet L, Lambert JJ (2006) Neuroactive steroids and inhibitory neurotransmission: mechanisms of action and physiological relevance. Neuroscience 138:821-829.

Belenky MA, Yarom Y, Pickard GE (2008) Heterogeneous expression of gamma-aminobutyric acid and gamma-aminobutyric acid-associated receptors and transporters in the rat suprachiasmatic nucleus. The Journal of comparative neurology 506:708-732.

Belousov AB, Hunt ND, Raju RP, Denisova JV (2002) Calcium-dependent regulation of cholinergic cell phenotype in the hypothalamus in vitro. Journal of neurophysiology 88:1352-1362.

Ben-Ari Y (2002) Excitatory actions of gaba during development: the nature of the nurture. Nature reviews 3:728-739.

Bergeron MJ, Gagnon E, Caron L, Isenring P (2006) Identification of key functional domains in the C terminus of the K+-Cl- cotransporters. The Journal of biological chemistry 281:15959-15969.

Billingsley ML, Kincaid RL (1997) Regulated phosphorylation and dephosphorylation of tau protein: effects on microtubule interaction, intracellular trafficking and neurodegeneration. The Biochemical journal 323 (Pt 3):577-591.

Binder DK, Croll SD, Gall CM, Scharfman HE (2001) BDNF and epilepsy: too much of a good thing? Trends Neurosci 24:47-53.

Bonifacino JS, Traub LM (2003) Signals for sorting of transmembrane proteins to endosomes and lysosomes. Annual review of biochemistry 72:395-447.

Boxall AR (2000) GABAergic mIPSCs in rat cerebellar Purkinje cells are modulated by TrkB and mGluR1-mediated stimulation of Src. The Journal of physiology 524 Pt 3:677-684.

Brandon NJ, Jovanovic JN, Smart TG, Moss SJ (2002) Receptor for activated C kinase-1 facilitates protein kinase C-dependent phosphorylation and functional modulation of GABA(A) receptors with the activation of G-protein-coupled receptors. J Neurosci 22:6353-6361.

Brandon NJ, Delmas P, Hill J, Smart TG, Moss SJ (2001) Constitutive tyrosine phosphorylation of the GABA(A) receptor gamma 2 subunit in rat brain. Neuropharmacology 41:745-752.

Brandon NJ, Uren JM, Kittler JT, Wang H, Olsen R, Parker PJ, Moss SJ (1999) Subunit-specific association of protein kinase C and the receptor for activated C kinase with GABA type A receptors. J Neurosci 19:9228-9234.

Brandon NJ, Delmas P, Kittler JT, McDonald BJ, Sieghart W, Brown DA, Smart TG, Moss SJ (2000) GABAA receptor phosphorylation and functional modulation in cortical neurons by a protein kinase C-dependent pathway. The Journal of biological chemistry 275:38856-38862.

Brunig I, Penschuck S, Berninger B, Benson J, Fritschy JM (2001) BDNF reduces miniature inhibitory postsynaptic currents by rapid

downregulation of GABA(A) receptor surface expression. The European journal of neuroscience 13:1320-1328.

Burbaeva G, Savushkina OK, Boksha IS (2003) Creatine kinase BB in brain in schizophrenia. World J Biol Psychiatry 4:177-183.

Burry RW (1998) PKC activators (phorbol ester or bryostatin) stimulate outgrowth of NGF-dependent neurites in a subline of PC12 cells. Journal of neuroscience research 53:214-222.

Carpenter G (1992) Receptor tyrosine kinase substrates: src homology domains and signal transduction. FASEB J 6:3283-3289.

Chudotvorova I, Ivanov A, Rama S, Hubner CA, Pellegrino C, Ben-Ari Y, Medina I (2005) Early expression of KCC2 in rat hippocampal cultures augments expression of functional GABA synapses. The Journal of physiology 566:671-679.

Cohen P (1989) The structure and regulation of protein phosphatases. Annual review of biochemistry 58:453-508.

Cohen PT, Cohen P (1989) Discovery of a protein phosphatase activity encoded in the genome of bacteriophage lambda. Probable identity with open reading frame 221. The Biochemical journal 260:931-934.

Collett MS, Erikson RL (1978) Protein kinase activity associated with the avian sarcoma virus src gene product. Proceedings of the National Academy of Sciences of the United States of America 75:2021-2024.

Collins BM, McCoy AJ, Kent HM, Evans PR, Owen DJ (2002) Molecular architecture and functional model of the endocytic AP2 complex. Cell 109:523-535.

Connolly CN, Kittler JT, Thomas P, Uren JM, Brandon NJ, Smart TG, Moss SJ (1999) Cell surface stability of gamma-aminobutyric acid type A receptors. Dependence on protein kinase C activity and subunit composition. The Journal of biological chemistry 274:36565-36572.

Cooper EJ, Johnston GA, Edwards FA (1999) Effects of a naturally occurring neurosteroid on GABAA IPSCs during development in rat hippocampal or cerebellar slices. The Journal of physiology 521 Pt 2:437-449.

Coull JA, Boudreau D, Bachand K, Prescott SA, Nault F, Sik A, De Koninck P, De Koninck Y (2003) Trans-synaptic shift in anion gradient in spinal

lamina I neurons as a mechanism of neuropathic pain. Nature 424:938-942.

Coulter DA (2001) Epilepsy-associated plasticity in gamma-aminobutyric acid receptor expression, function, and inhibitory synaptic properties. International review of neurobiology 45:237-252.

Coulter DA, Carlson GC (2007) Functional regulation of the dentate gyrus by GABA-mediated inhibition. Progress in brain research 163:235-243.

Cupello A, Gasparetto B, Mainardi P, Vignolo L, Robello M (1993) Effect of protein kinase C activators on the uptake of GABA by rat brain synaptosomes. Int J Neurosci 69:131-136.

Czernik AJ, Girault JA, Nairn AC, Chen J, Snyder G, Kebabian J, Greengard P (1991) Production of phosphorylation state-specific antibodies. Methods in enzymology 201:264-283.

De Franceschi L, Ronzoni L, Cappellini MD, Cimmino F, Siciliano A, Alper SL, Servedio V, Pozzobon C, Iolascon A (2007) K-CL co-transport plays an important role in normal and beta thalassemic erythropoiesis. Haematologica 92:1319-1326.

Delpy A, Allain AE, Meyrand P, Branchereau P (2008) NKCC1 cotransporter inactivation underlies embryonic development of chloride-mediated inhibition in mouse spinal motoneuron. The Journal of physiology 586:1059-1075.

Dikic I, Tokiwa G, Lev S, Courtneidge SA, Schlessinger J (1996) A role for Pyk2 and Src in linking G-protein-coupled receptors with MAP kinase activation. Nature 383:547-550.

Ding J, Soule G, Overmeyer JH, Maltese WA (2003) Tyrosine phosphorylation of the Rab24 GTPase in cultured mammalian cells. Biochemical and biophysical research communications 312:670-675.

Edelman AM, Blumenthal DK, Krebs EG (1987) Protein serine/threonine kinases. Annual review of biochemistry 56:567-613.

Ehrlich I, Lohrke S, Friauf E (1999) Shift from depolarizing to hyperpolarizing glycine action in rat auditory neurones is due to age-dependent Cl- regulation. The Journal of physiology 520 Pt 1:121-137.

Evans GJ, Cousin MA (2005) Tyrosine phosphorylation of synaptophysin in synaptic vesicle recycling. Biochem Soc Trans 33:1350-1353.

Fairfax BP, Pitcher JA, Scott MG, Calver AR, Pangalos MN, Moss SJ, Couve A (2004) Phosphorylation and chronic agonist treatment atypically modulate GABAB receptor cell surface stability. The Journal of biological chemistry 279:12565-12573.

Flatman PW (2002) Regulation of Na-K-2Cl cotransport by phosphorylation and protein-protein interactions. Biochimica et biophysica acta 1566:140-151.

Funke MG, Amado D, Cavalheiro EA, Naffah-Mazzacoratti MG (1998) Tyrosine phosphorylation is increased in the rat hippocampus during the status epilepticus induced by pilocarpine. Brain Res Bull 47:87-93.

Gagnon E, Bergeron MJ, Brunet GM, Daigle ND, Simard CF, Isenring P (2004) Molecular mechanisms of Cl- transport by the renal Na(+)-K(+)-Cl- cotransporter. Identification of an intracellular locus that may form part of a high affinity Cl(-)-binding site. The Journal of biological chemistry 279:5648-5654.

Gamba G (2005) Molecular physiology and pathophysiology of electroneutral cation-chloride cotransporters. Physiological reviews 85:423-493.

Gamba G, Miyanoshita A, Lombardi M, Lytton J, Lee WS, Hediger MA, Hebert SC (1994) Molecular cloning, primary structure, and characterization of two members of the mammalian electroneutral sodium-(potassium)-chloride cotransporter family expressed in kidney. The Journal of biological chemistry 269:17713-17722.

Ganguly K, Schinder AF, Wong ST, Poo M (2001) GABA itself promotes the developmental switch of neuronal GABAergic responses from excitation to inhibition. Cell 105:521-532.

Gillen CM, Brill S, Payne JA, Forbush B, 3rd (1996) Molecular cloning and functional expression of the K-Cl cotransporter from rabbit, rat, and human. A new member of the cation-chloride cotransporter family. The Journal of biological chemistry 271:16237-16244.

Girault JA, Costa A, Derkinderen P, Studler JM, Toutant M (1999) FAK and PYK2/CAKbeta in the nervous system: a link between neuronal activity, plasticity and survival? Trends Neurosci 22:257-263.

Gulacsi A, Lee CR, Sik A, Viitanen T, Kaila K, Tepper JM, Freund TF (2003) Cell type-specific differences in chloride-regulatory mechanisms and

GABA(A) receptor-mediated inhibition in rat substantia nigra. J Neurosci 23:8237-8246.

Gulyas AI, Sik A, Payne JA, Kaila K, Freund TF (2001) The KCl cotransporter, KCC2, is highly expressed in the vicinity of excitatory synapses in the rat hippocampus. The European journal of neuroscience 13:2205-2217.

Haas M, Forbush B, 3rd (1998) The Na-K-Cl cotransporters. J Bioenerg Biomembr 30:161-172.

Houston CM, Lee HH, Hosie AM, Moss SJ, Smart TG (2007) Identification of the sites for CaMK-II-dependent phosphorylation of GABA(A) receptors. The Journal of biological chemistry 282:17855-17865.

Hubbard SR, Till JH (2000) Protein tyrosine kinase structure and function. Annual review of biochemistry 69:373-398.

Huberfeld G, Wittner L, Clemenceau S, Baulac M, Kaila K, Miles R, Rivera C (2007) Perturbed chloride homeostasis and GABAergic signaling in human temporal lobe epilepsy. J Neurosci 27:9866-9873.

Inoue K, Ueno S, Fukuda A (2004) Interaction of neuron-specific K+-Cl- cotransporter, KCC2, with brain-type creatine kinase. FEBS letters 564:131-135.

Inoue K, Yamada J, Ueno S, Fukuda A (2006) Brain-type creatine kinase activates neuron-specific K+-Cl- co-transporter KCC2. Journal of neurochemistry 96:598-608.

Jin X, Huguenard JR, Prince DA (2005) Impaired Cl- extrusion in layer V pyramidal neurons of chronically injured epileptogenic neocortex. Journal of neurophysiology 93:2117-2126.

Jovanovic JN, Thomas P, Kittler JT, Smart TG, Moss SJ (2004) Brain-derived neurotrophic factor modulates fast synaptic inhibition by regulating GABA(A) receptor phosphorylation, activity, and cell-surface stability. J Neurosci 24:522-530.

Jovanovic JN, Benfenati F, Siow YL, Sihra TS, Sanghera JS, Pelech SL, Greengard P, Czernik AJ (1996) Neurotrophins stimulate phosphorylation of synapsin I by MAP kinase and regulate synapsin I-actin interactions. Proceedings of the National Academy of Sciences of the United States of America 93:3679-3683.

Kahle KT, Rinehart J, de Los Heros P, Louvi A, Meade P, Vazquez N, Hebert SC, Gamba G, Gimenez I, Lifton RP (2005) WNK3 modulates transport of Cl- in and out of cells: implications for control of cell volume and neuronal excitability. Proceedings of the National Academy of Sciences of the United States of America 102:16783-16788.

Kanematsu T, Yasunaga A, Mizoguchi Y, Kuratani A, Kittler JT, Jovanovic JN, Takenaka K, Nakayama KI, Fukami K, Takenawa T, Moss SJ, Nabekura J, Hirata M (2006) Modulation of GABA(A) receptor phosphorylation and membrane trafficking by phospholipase C-related inactive protein/protein phosphatase 1 and 2A signaling complex underlying brain-derived neurotrophic factor-dependent regulation of GABAergic inhibition. The Journal of biological chemistry 281:22180-22189.

Karadsheh MF, Delpire E (2001) Neuronal restrictive silencing element is found in the KCC2 gene: molecular basis for KCC2-specific expression in neurons. Journal of neurophysiology 85:995-997.

Kelsch W, Hormuzdi S, Straube E, Lewen A, Monyer H, Misgeld U (2001) Insulin-like growth factor 1 and a cytosolic tyrosine kinase activate chloride outward transport during maturation of hippocampal neurons. J Neurosci 21:8339-8347.

Kennelly PJ, Krebs EG (1991) Consensus sequences as substrate specificity determinants for protein kinases and protein phosphatases. The Journal of biological chemistry 266:15555-15558.

Kittler JT, Delmas P, Jovanovic JN, Brown DA, Smart TG, Moss SJ (2000) Constitutive endocytosis of GABAA receptors by an association with the adaptin AP2 complex modulates inhibitory synaptic currents in hippocampal neurons. J Neurosci 20:7972-7977.

Kittler JT, Chen G, Honing S, Bogdanov Y, McAinsh K, Arancibia-Carcamo IL, Jovanovic JN, Pangalos MN, Haucke V, Yan Z, Moss SJ (2005) Phospho-dependent binding of the clathrin AP2 adaptor complex to GABAA receptors regulates the efficacy of inhibitory synaptic transmission. Proceedings of the National Academy of Sciences of the United States of America 102:14871-14876.

Kittler JT, Chen G, Kukhtina V, Vahedi-Faridi A, Gu Z, Tretter V, Smith KR, McAinsh K, Arancibia-Carcamo IL, Saenger W, Haucke V, Yan Z, Moss SJ (2008) Regulation of synaptic inhibition by phospho-dependent binding of the AP2 complex to a YECL motif in the GABAA receptor gamma2 subunit. Proceedings of the National Academy of Sciences of the United States of America 105:3616-3621.

Krishek BJ, Xie X, Blackstone C, Huganir RL, Moss SJ, Smart TG (1994) Regulation of GABAA receptor function by protein kinase C phosphorylation. Neuron 12:1081-1095.

Kuramoto N, Wilkins ME, Fairfax BP, Revilla-Sanchez R, Terunuma M, Tamaki K, Iemata M, Warren N, Couve A, Calver A, Horvath Z, Freeman K, Carling D, Huang L, Gonzales C, Cooper E, Smart TG, Pangalos MN, Moss SJ (2007) Phospho-dependent functional modulation of GABA(B) receptors by the metabolic sensor AMP-dependent protein kinase. Neuron 53:233-247.

Lauf PK (1985) K+:Cl- cotransport: sulfhydryls, divalent cations, and the mechanism of volume activation in a red cell. The Journal of membrane biology 88:1-13.

Le Roy C, Wrana JL (2005) Clathrin- and non-clathrin-mediated endocytic regulation of cell signalling. Nat Rev Mol Cell Biol 6:112-126.

Lev S, Moreno H, Martinez R, Canoll P, Peles E, Musacchio JM, Plowman GD, Rudy B, Schlessinger J (1995) Protein tyrosine kinase PYK2 involved in Ca(2+)-induced regulation of ion channel and MAP kinase functions. Nature 376:737-745.

Li H, Tornberg J, Kaila K, Airaksinen MS, Rivera C (2002) Patterns of cation-chloride cotransporter expression during embryonic rodent CNS development. The European journal of neuroscience 16:2358-2370.

Li H, Khirug S, Cai C, Ludwig A, Blaesse P, Kolikova J, Afzalov R, Coleman SK, Lauri S, Airaksinen MS, Keinanen K, Khiroug L, Saarma M, Kaila K, Rivera C (2007) KCC2 Interacts with the Dendritic Cytoskeleton to Promote Spine Development. Neuron 56:1019-1033.

Liedtke CM, Wang X, Smallwood ND (2005) Role for protein phosphatase 2A in the regulation of Calu-3 epithelial Na+-K+-2Cl-, type 1 co-transport function. The Journal of biological chemistry 280:25491-25498.

Lowenstein DH, Alldredge BK (1998) Status epilepticus. N Engl J Med 338:970-976.

Ludwig A, Li H, Saarma M, Kaila K, Rivera C (2003) Developmental up-regulation of KCC2 in the absence of GABAergic and glutamatergic transmission. The European journal of neuroscience 18:3199-3206.

Macek TA, Schaffhauser H, Conn PJ (1999) Activation of PKC disrupts presynaptic inhibition by group II and group III metabotropic glutamate receptors and uncouples the receptor from GTP-binding proteins. Ann N Y Acad Sci 868:554-557.

Madison DV, Malenka RC, Nicoll RA (1991) Mechanisms underlying long-term potentiation of synaptic transmission. Annu Rev Neurosci 14:379-397.

Mahajan VB, Pai KS, Lau A, Cunningham DD (2000) Creatine kinase, an ATP-generating enzyme, is required for thrombin receptor signaling to the cytoskeleton. Proceedings of the National Academy of Sciences of the United States of America 97:12062-12067.

Malinow R, Schulman H, Tsien RW (1989) Inhibition of postsynaptic PKC or CaMKII blocks induction but not expression of LTP. Science 245:862-866.

McDonald BJ, Moss SJ (1994) Differential phosphorylation of intracellular domains of gamma-aminobutyric acid type A receptor subunits by calcium/calmodulin type 2-dependent protein kinase and cGMP-dependent protein kinase. The Journal of biological chemistry 269:18111-18117.

McDonald BJ, Moss SJ (1997) Conserved phosphorylation of the intracellular domains of GABA(A) receptor beta2 and beta3 subunits by cAMP-dependent protein kinase, cGMP-dependent protein kinase protein kinase C and Ca2+/calmodulin type II-dependent protein kinase. Neuropharmacology 36:1377-1385.

McDonald BJ, Amato A, Connolly CN, Benke D, Moss SJ, Smart TG (1998) Adjacent phosphorylation sites on GABAA receptor beta subunits determine regulation by cAMP-dependent protein kinase. Nature neuroscience 1:23-28.

Mercado A, Broumand V, Zandi-Nejad K, Enck AH, Mount DB (2006) A C-terminal domain in KCC2 confers constitutive K+-Cl- cotransport. The Journal of biological chemistry 281:1016-1026.

Molinaro G, Battaglia G, Riozzi B, Storto M, Fucile S, Eusebi F, Nicoletti F, Bruno V (2007) GABAergic drugs become neurotoxic in cortical neurons pre-exposed to brain-derived neurotrophic factor. Mol Cell Neurosci.

Morgado C, Pinto-Ribeiro F, Tavares I (2008) Diabetes affects the expression of GABA and potassium chloride cotransporter in the spinal cord: A study in streptozotocin diabetic rats. Neuroscience letters.

Morishita R, Ueda H, Ito H, Takasaki J, Nagata K, Asano T (2007) Involvement of Gq/11 in both integrin signal-dependent and -independent pathways regulating endothelin-induced neural progenitor proliferation. Neuroscience research 59:205-214.

Moss SJ, Smart TG (1996) Modulation of amino acid-gated ion channels by protein phosphorylation. International review of neurobiology 39:1-52.

Moss SJ, Doherty CA, Huganir RL (1992) Identification of the cAMP-dependent protein kinase and protein kinase C phosphorylation sites within the major intracellular domains of the beta 1, gamma 2S, and gamma 2L subunits of the gamma-aminobutyric acid type A receptor. The Journal of biological chemistry 267:14470-14476.

Moss SJ, Blackstone CD, Huganir RL (1993) Phosphorylation of recombinant non-NMDA glutamate receptors on serine and tyrosine residues. Neurochemical research 18:105-110.

Moss SJ, Ravindran A, Mei L, Wang JB, Kofuji P, Huganir RL, Burt DR (1991) Characterization of recombinant GABAA receptors produced in transfected cells from murine alpha 1, beta 1, and gamma 2 subunit cDNAs. Neuroscience letters 123:265-268.

Mount DB, Delpire E, Gamba G, Hall AE, Poch E, Hoover RS, Hebert SC (1998) The electroneutral cation-chloride cotransporters. J Exp Biol 201:2091-2102.

Nakashima S (2002) Protein kinase C alpha (PKC alpha): regulation and biological function. Journal of biochemistry 132:669-675.

Ottensmeyer FP, Beniac DR, Luo RZ, Yip CC (2000) Mechanism of transmembrane signaling: insulin binding and the insulin receptor. Biochemistry 39:12103-12112.

Owen DJ, Collins BM, Evans PR (2004) Adaptors for clathrin coats: structure and function. Annu Rev Cell Dev Biol 20:153-191.

Owens DF, Boyce LH, Davis MB, Kriegstein AR (1996) Excitatory GABA responses in embryonic and neonatal cortical slices demonstrated by gramicidin perforated-patch recordings and calcium imaging. J Neurosci 16:6414-6423.

Pascale A, Amadio M, Govoni S, Battaini F (2007) The aging brain, a key target for the future: the protein kinase C involvement. Pharmacol Res 55:560-569.

Pathak HR, Weissinger F, Terunuma M, Carlson GC, Hsu FC, Moss SJ, Coulter DA (2007) Disrupted dentate granule cell chloride regulation enhances synaptic excitability during development of temporal lobe epilepsy. J Neurosci 27:14012-14022.

Payne JA (1997) Functional characterization of the neuronal-specific K-Cl cotransporter: implications for [K+]o regulation. The American journal of physiology 273:C1516-1525.

Payne JA, Stevenson TJ, Donaldson LF (1996) Molecular characterization of a putative K-Cl cotransporter in rat brain. A neuronal-specific isoform. The Journal of biological chemistry 271:16245-16252.

Porter NM, Twyman RE, Uhler MD, Macdonald RL (1990) Cyclic AMP-dependent protein kinase decreases GABAA receptor current in mouse spinal neurons. Neuron 5:789-796.

Rapallino MV, Cupello A, Hyden H (1993) The increase in Cl- permeation across the Deiters' neuron membrane by GABA on its cytoplasmic side is abolished by protein kinase C (PKC) activators. Cell Mol Neurobiol 13:547-558.

Raymond LA, Tingley WG, Blackstone CD, Roche KW, Huganir RL (1994) Glutamate receptor modulation by protein phosphorylation. Journal of physiology, Paris 88:181-192.

Reid KH, Guo SZ, Iyer VG (2000) Agents which block potassium-chloride cotransport prevent sound-triggered seizures in post-ischemic audiogenic seizure-prone rats. Brain Res 864:134-137.

Reid KH, Li GY, Payne RS, Schurr A, Cooper NG (2001) The mRNA level of the potassium-chloride cotransporter KCC2 covaries with seizure susceptibility in inferior colliculus of the post-ischemic audiogenic seizure-prone rat. Neuroscience letters 308:29-32.

Rivera C, Voipio J, Kaila K (2005) Two developmental switches in GABAergic signalling: the K+-Cl- cotransporter KCC2 and carbonic anhydrase CAVII. The Journal of physiology 562:27-36.

Rivera C, Voipio J, Payne JA, Ruusuvuori E, Lahtinen H, Lamsa K, Pirvola U, Saarma M, Kaila K (1999) The K+/Cl- co-transporter KCC2 renders GABA hyperpolarizing during neuronal maturation. Nature 397:251-255.

Rivera C, Voipio J, Thomas-Crusells J, Li H, Emri Z, Sipila S, Payne JA, Minichiello L, Saarma M, Kaila K (2004) Mechanism of activity-dependent downregulation of the neuron-specific K-Cl cotransporter KCC2. J Neurosci 24:4683-4691.

Rivera C, Li H, Thomas-Crusells J, Lahtinen H, Viitanen T, Nanobashvili A, Kokaia Z, Airaksinen MS, Voipio J, Kaila K, Saarma M (2002) BDNF-induced TrkB activation down-regulates the K+-Cl- cotransporter KCC2 and impairs neuronal Cl- extrusion. The Journal of cell biology 159:747-752.

Rogers MV, Buensuceso C, Montague F, Mahadevan L (1994) Vanadate stimulates differentiation and neurite outgrowth in rat pheochromocytoma PC12 cells and neurite extension in human neuroblastoma SH-SY5Y cells. Neuroscience 60:479-494.

Roskoski R, Jr. (2004) Src protein-tyrosine kinase structure and regulation. Biochemical and biophysical research communications 324:1155-1164.

Russell JM (2000) Sodium-potassium-chloride cotransport. Physiol Rev 80:211-276.

Sallinen R, Tornberg J, Putkiranta M, Horelli-Kuitunen N, Airaksinen MS, Wessman M (2001) Chromosomal localization of SLC12A5/Slc12a5, the human and mouse genes for the neuron-specific K(+)-Cl(-)

cotransporter (KCC2) defines a new region of conserved homology. Cytogenet Cell Genet 94:67-70.

Sato K, Betz H, Schloss P (1995) The recombinant GABA transporter GAT1 is downregulated upon activation of protein kinase C. FEBS Lett 375:99-102.

Sheng ZH, Westenbroek RE, Catterall WA (1998) Physical link and functional coupling of presynaptic calcium channels and the synaptic vesicle docking/fusion machinery. J Bioenerg Biomembr 30:335-345.

Shimizu-Okabe C, Okabe A, Kilb W, Sato K, Luhmann HJ, Fukuda A (2007) Changes in the expression of cation-Cl- cotransporters, NKCC1 and KCC2, during cortical malformation induced by neonatal freeze-lesion. Neuroscience research 59:288-295.

Shuntoh H, Taniyama K, Tanaka C (1989) Involvement of protein kinase C in the Ca2+-dependent vesicular release of GABA from central and enteric neurons of the guinea pig. Brain Res 483:384-388.

Smith CD, Carney JM, Starke-Reed PE, Oliver CN, Stadtman ER, Floyd RA, Markesbery WR (1991) Excess brain protein oxidation and enzyme dysfunction in normal aging and in Alzheimer disease. Proceedings of the National Academy of Sciences of the United States of America 88:10540-10543.

Song L, Mercado A, Vazquez N, Xie Q, Desai R, George AL, Jr., Gamba G, Mount DB (2002) Molecular, functional, and genomic characterization of human KCC2, the neuronal K-Cl cotransporter. Brain Res Mol Brain Res 103:91-105.

Song M, Messing RO (2005) Protein kinase C regulation of GABAA receptors. Cell Mol Life Sci 62:119-127.

Song P, Kaczmarek LK (2006) Modulation of Kv3.1b potassium channel phosphorylation in auditory neurons by conventional and novel protein kinase C isozymes. The Journal of biological chemistry 281:15582-15591.

Staley K (1994) The role of an inwardly rectifying chloride conductance in postsynaptic inhibition. Journal of neurophysiology 72:273-284.

Strange K, Singer TD, Morrison R, Delpire E (2000) Dependence of KCC2 K-Cl cotransporter activity on a conserved carboxy terminus tyrosine residue. American journal of physiology 279:C860-867.

Taniyama K, Saito N, Kose A, Matsuyama S, Nakayama S, Tanaka C (1990) Involvement of the gamma subtype of protein kinase C in GABA release from the cerebellum. Adv Second Messenger Phosphoprotein Res 24:399-404.

Thomas SM, Brugge JS (1997) Cellular functions regulated by Src family kinases. Annu Rev Cell Dev Biol 13:513-609.

Tornberg J, Voikar V, Savilahti H, Rauvala H, Airaksinen MS (2005) Behavioural phenotypes of hypomorphic KCC2-deficient mice. The European journal of neuroscience 21:1327-1337.

Treiman DM, Walton NY, Kendrick C (1990) A progressive sequence of electroencephalographic changes during generalized convulsive status epilepticus. Epilepsy Res 5:49-60.

Turner KM, Burgoyne RD, Morgan A (1999) Protein phosphorylation and the regulation of synaptic membrane traffic. Trends Neurosci 22:459-464.

Uvarov P, Pruunsild P, Timmusk T, Airaksinen MS (2005) Neuronal K+/Cl- co-transporter (KCC2) transgenes lacking neurone restrictive silencer element recapitulate CNS neurone-specific expression and developmental up-regulation of endogenous KCC2 gene. Journal of neurochemistry 95:1144-1155.

Uvarov P, Ludwig A, Markkanen M, Rivera C, Airaksinen MS (2006) Upregulation of the neuron-specific K+/Cl- cotransporter expression by transcription factor early growth response 4. J Neurosci 26:13463-13473.

Uvarov P, Ludwig A, Markkanen M, Pruunsild P, Kaila K, Delpire E, Timmusk T, Rivera C, Airaksinen MS (2007) A novel N-terminal isoform of the neuron-specific K-Cl cotransporter KCC2. The Journal of biological chemistry 282:30570-30576.

Vale C, Caminos E, Martinez-Galan JR, Juiz JM (2005) Expression and developmental regulation of the K+-Cl- cotransporter KCC2 in the cochlear nucleus. Hearing research 206:107-115.

Vardi N, Zhang LL, Payne JA, Sterling P (2000) Evidence that different cation chloride cotransporters in retinal neurons allow opposite responses to GABA. J Neurosci 20:7657-7663.

Vinay L, Jean-Xavier C (2008) Plasticity of spinal cord locomotor networks and contribution of cation-chloride cotransporters. Brain research reviews 57:103-110.

Vu TQ, Payne JA, Copenhagen DR (2000) Localization and developmental expression patterns of the neuronal K-Cl cotransporter (KCC2) in the rat retina. J Neurosci 20:1414-1423.

Wake H, Watanabe M, Moorhouse AJ, Kanematsu T, Horibe S, Matsukawa N, Asai K, Ojika K, Hirata M, Nabekura J (2007) Early changes in KCC2 phosphorylation in response to neuronal stress result in functional downregulation. J Neurosci 27:1642-1650.

Walz W (1989) Role of glial cells in the regulation of the brain ion microenvironment. Prog Neurobiol 33:309-333.

Wang C, Shimizu-Okabe C, Watanabe K, Okabe A, Matsuzaki H, Ogawa T, Mori N, Fukuda A, Sato K (2002) Developmental changes in KCC1, KCC2, and NKCC1 mRNA expressions in the rat brain. Brain research 139:59-66.

Wardle RA, Poo MM (2003) Brain-derived neurotrophic factor modulation of GABAergic synapses by postsynaptic regulation of chloride transport. J Neurosci 23:8722-8732.

Williams JR, Sharp JW, Kumari VG, Wilson M, Payne JA (1999) The neuron-specific K-Cl cotransporter, KCC2. Antibody development and initial characterization of the protein. The Journal of biological chemistry 274:12656-12664.

Woo NS, Lu J, England R, McClellan R, Dufour S, Mount DB, Deutch AY, Lovinger DM, Delpire E (2002) Hyperexcitability and epilepsy associated with disruption of the mouse neuronal-specific K-Cl cotransporter gene. Hippocampus 12:258-268.

Wu J, Ohta N, Zhao JL, Newton A (1999) A novel bacterial tyrosine kinase essential for cell division and differentiation. Proceedings of the National Academy of Sciences of the United States of America 96:13068-13073.

Xu ZQ, Lew JY, Harada K, Aman K, Goldstein M, Deutch A, Haycock JW, Hokfelt T (1998) Immunohistochemical studies on phosphorylation of tyrosine hydroxylase in central catecholamine neurons using site- and phosphorylation state-specific antibodies. Neuroscience 82:727-738.

End of the thesis